

**TID1 MEDIATES AGRIN AND MUSCLE SPECIFIC KINASE SIGNALING
AT THE NEUROMUSCULAR JUNCTION**

by

Jenny Johanna Linnoila

S.B., Computer Science, University of Chicago, 2000

Submitted to the Graduate Faculty of
the University of Pittsburgh School of Medicine in partial fulfillment
of the requirements for the degree of
Doctor of Philosophy

University of Pittsburgh

2007

UNIVERSITY OF PITTSBURGH

School of Medicine

This dissertation was presented

by

Jenny Johanna Linnoila

It was defended on

July 10, 2007

and approved by

Donald DeFranco, Ph.D.
Committee Chair
Professor of Pharmacology

Elias Aizenman, Ph.D.
Professor of Neurobiology

Daniel Altschuler, Ph.D.
Associate Professor of Pharmacology

Willi Halfter, Ph.D.
Associate Professor of Neurobiology

Guillermo Romero, Ph.D.
Associate Professor of Pharmacology

Zuo-Zhong Wang, Ph.D.
Dissertation Advisor
Adjunct Associate Professor of Pharmacology, University of Pittsburgh
Associate Professor of Cell and Neurobiology, University of Southern California
Keck School of Medicine

Copyright © by Jenny Johanna Linnoila

2007

TID1 MEDIATES AGRIN AND MUSCLE SPECIFIC KINASE SIGNALING AT THE NEUROMUSCULAR JUNCTION

Jenny Johanna Linnoila, Ph.D.

University of Pittsburgh, 2007

The neuromuscular junction (NMJ) has a structure that is optimized to relay signals from nerve to muscle. As part of its organizational scheme, certain muscular proteins, like nicotinic acetylcholine receptors (AChRs), are clustered preferentially at the NMJ. Clustering of AChRs at the NMJ is essential for efficient neurotransmission. The major factor which strengthens and sustains the NMJ localization of AChRs is the motoneuron-derived glycoprotein agrin. Agrin acts via a receptor complex that includes the muscle-specific receptor tyrosine kinase (RTK) MuSK. Although MuSK has been well characterized, the signaling pathway by which it mediates agrin-induced clustering of AChRs remains elusive. Understanding this process will provide insights for the treatment of a variety of muscle weakness disorders, such as myasthenia gravis and muscular dystrophy. For instance, some forms of myasthenia gravis are caused by autoantibodies directed against MuSK. Future therapies could be designed to circumvent dysfunctional portions of the clustering cascade. In addition, studying this pathway may reveal mechanisms important for the formation and maintenance of synapses.

A bacterial two-hybrid assay was used to screen a rat muscle cDNA library for binding partners of the cytoplasmic domain of mouse MuSK. The mammalian homologue of the *Drosophila* protein, *tumorous imaginal discs*, *tid1*, was identified as a specific MuSK binding protein. Interestingly, *tid1* has recently been shown to bind to and to modulate the signaling of

the ErbB2 and Trk families of RTKs. Biochemical assays confirmed that tid1 binds to MuSK. Tid1 was colocalized with AChR clusters in cultured myotubes and at rodent NMJs. Denervation dispersed tid1 and AChRs from the postsynaptic membrane of the NMJ. Overexpression of the N-terminal half of tid1 in myotubes induced aneural AChR clustering. Short hairpin RNA (shRNA)-mediated knockdown of tid1 inhibited spontaneous and agrin-induced AChR clustering in cultured myotubes and resulted in the disassembly of preformed NMJs in skeletal muscles of adult mice. Furthermore, the amplitudes of spontaneous miniature endplate potentials (MEPPs) and evoked endplate potentials (EPPs) were significantly reduced in muscles electroporated with tid1-targeted shRNA. These results implicate tid1 as a novel NMJ player and define a new class of molecules in the agrin/MuSK signaling cascade.

TABLE OF CONTENTS

PREFACE	XIII
1.0 INTRODUCTION	1
1.1 THE NEUROMUSCULAR JUNCTION: STRUCTURE AND FUNCTION	1
1.2 CLUSTERING OF AChRS IN THE POSTSYNAPTIC NMJ MEMBRANE	3
1.2.1 Evidence for the induction of AChR clustering by motoneurons.....	4
1.2.2 Motoneurons are not necessary for AChR clustering.....	7
1.2.3 Current theory on AChR clustering at the NMJ	9
1.3 GOALS OF THE DISSERTATION	12
1.3.1 Significance of the work	12
1.3.2 MuSK: a critical player in the agrin → AChR clustering pathway	14
1.3.3 Other postsynaptic players involved in AChR clustering.....	17
1.4 TID1: A NEW DIRECTION IN CELLULAR SIGNALING AT THE NMJ	20
1.4.1 Tid1 as a signaling molecule.....	23
1.4.2 Tid1: an important player in NMJ development and maintenance	24
2.0 EXPERIMENTAL PROCEDURES	25
2.1 MATERIALS	25
2.1.1 Reagents.....	25
2.1.2 Antibodies	26

2.2	BACTERIAL TWO-HYBRID SCREENS	27
2.3	cDNA CONSTRUCTS	27
2.4	CELL CULTURE, TRANSFECTION, AND LYSATE PREPARATION	28
2.4.1	C2C12 Cells	28
2.4.2	COS-7 Cells.....	29
2.5	SKELETAL MUSCLES	29
2.5.1	Denervation	29
2.5.2	Cryosectioning.....	30
2.5.3	Muscle Homogenization	30
2.6	IMMUNOPRECIPITATION	31
2.7	IMMUNOBLOTTING	31
2.8	IMMUNOFLUORESCENT STAINING.....	32
2.8.1	Slides	32
2.8.2	Cell Culture	33
2.9	QUANTIFICATION OF AChR CLUSTERS	33
2.10	RADIOLIGAND BINDING ASSAY	34
2.11	RNA INTERFERENCE	34
2.11.1	<i>In vitro</i>	34
2.11.1.1	Rescue	35
2.11.2	<i>In Vivo</i>	36
2.12	ELECTROPHYSIOLOGY	36
2.13	STATISTICAL ANALYSIS.....	37
3.0	RESULTS	38

3.1	IDENTIFICATION OF TID1 AS A MUSK-BINDING PROTEIN	38
3.2	CONFIRMATION OF TID1 AND MUSK BINDING.....	42
3.3	TID1 COLOCALIZES WITH AChRS ON THE POSTSYNAPTIC MEMBRANE OF THE NMJ	44
3.4	CHRONIC DENERVATION DISPERSES TID1 AND AChRS FROM THE NMJ.....	48
3.5	NEURAL AGRIN INDUCES CO-CLUSTERING OF TID1 AND AChRS IN C2C12 MYOTUBES	52
3.6	THE N-TERMINAL DOMAIN OF TID1 ENHANCES AChR CLUSTERING AND EXPRESSION.....	54
3.7	TID1 KNOCKDOWN BY SHORT HAIRPIN RNA INHIBITS AChR CLUSTERING IN MYOTUBES.....	58
3.8	ShRNA-MEDIATED TID1 KNOCKDOWN DISRUPTS THE STRUCTURE AND FUNCTION OF THE NMJ.....	71
4.0	DISCUSSION	77
4.1	SUMMARY OF FINDINGS	77
4.2	RELEVANT BACKGROUND	78
4.3	BINDING OF TID1 TO MUSK.....	80
4.4	AChR CLUSTERING ROLE OF TID1: LIKELY MEDIATED BY N- TERMINUS.....	83
4.5	TID1-DEFICIENT NMJS FUNCTIONALLY MIMIC MYASTHENIA GRAVIS	84

4.6 POTENTIAL MECHANISMS OF ACTION FOR TID1 IN REGULATING THE CLUSTERING OF AChRS AT THE NMJ	88
4.7 OTHER POTENTIAL ROLES FOR TID1 AT THE NMJ.....	90
4.8 MOLECULAR CHAPERONES AT SYNAPSES.....	92
4.9 FUTURE DIRECTIONS.....	96
BIBLIOGRAPHY	101

LIST OF TABLES

Table 1. MEPP and EPP properties at control and tid1 shRNA-treated NMJs.	76
---	----

LIST OF FIGURES

Figure 1. Structure of the neuromuscular junction.	2
Figure 2. Schematic diagram of agrin alternative splice sites.	5
Figure 3. Schematic diagram of the agrin → MuSK → AChR clustering cascade.....	13
Figure 4. Schematic diagram of the main domains and phosphorylation sites of MuSK.....	16
Figure 5. Schematic diagram of AChR clustering, mediated through cytoskeletal changes.	19
Figure 6. Schematic diagram of the bacterial two-hybrid system.	22
Figure 7. Validation results for bacterial two-hybrid screens	39
Figure 8. Bacterial two-hybrid screens identify tid1 short as a MuSK binding protein.	40
Figure 9. Specificity of the rabbit polyclonal antibody against tid1 short.	41
Figure 10. Tid1 short and MuSK co-immunoprecipitate one another from myotubes.....	43
Figure 11. MuSK co-immunoprecipitates tid1 short from rodent skeletal muscle.....	44
Figure 12. Tid1 and AChRs colocalize at innervated mouse NMJs.	46
Figure 13. Tid1 and AChRs remain colocalized at denervated mouse NMJs.....	47
Figure 14. Dispersal of tid1 from motor endplates in chronically denervated muscles.....	50
Figure 15. Quantification of tid1 and AChR cluster size in chronically-denervated muscle.....	51
Figure 16. Neural agrin induces tid1 and AChR co-clustering.	53
Figure 17. Schematic diagram of tid1 fragments utilized for exploring domain function.....	54
Figure 18. The N-terminal half of tid1 induces AChR clustering.	56

Figure 19. The N-terminal half of tid1 induces AChR clustering and expression.	57
Figure 20. The specificity of shRNA-mediated knockdown of tid1 in COS cells.	60
Figure 21. Tid1 shRNA knocks down the expression of exogenous tid1.	61
Figure 22. Inhibition of spontaneous and agrin-induced AChR clustering by shRNA-mediated tid1 knockdown in myotubes.	63
Figure 23. Time course of agrin-induced AChR clustering demonstrates tid1-shRNA-mediated inhibition.	65
Figure 24. Tid1 shRNA's effects on AChR clustering are specifically mediated by tid1 knockdown and tid1's effects on AChR clustering are dependent upon a functioning DnaJ domain.	66
Figure 25. Quantification of tid1 shRNA rescue, spontaneous clustering.	68
Figure 26. Quantification of tid1 shRNA rescue, agrin-induced clustering.	69
Figure 27. Tid1-targeted shRNA does not change surface expression of AChR.	70
Figure 28. Tid1 knockdown disrupts the structure and function of the mouse NMJ.	72
Figure 29. Greater degree of tid1 knockdown results in more disrupted NMJ structure.	74
Figure 30. Tid1 knockdown disrupts NMJ function.	75
Figure 31. Schematic representation of putative pathways through which tid1 may regulate AChR clustering.	90

PREFACE

There are a number of people whose support made this entire endeavor possible. These include my family, friends, coworkers, and colleagues, to name a few. First of all, I would like to thank my family (Ilona, Juuso, William, Robert, Christina, and the Vilens) for their undying support. Completing my Ph.D. required my relocation from Pittsburgh to Los Angeles halfway through my studies. It was a great help to have family close by on both coasts to aid in the transition. And although they are no longer with us, the spirits of both Dad and Mummi remained close to my heart, inspiring me and giving me strength throughout my Ph.D. years.

I would also like to thank Dr. Wang, whose close guidance throughout these past four years enabled me to develop skills to become a responsible, independent, and free-thinking scientist. Words cannot express my gratitude!! Along with Dr. Wang, my coworkers Ying Wang and Yun Yao gave me tremendous support and help. Numerous discussions with Ying helped me to refine my experiments and theories. Yun's technical expertise was invaluable and allowed my work to proceed smoothly, from the first day to the last.

My committee's input was also incredibly important. Drs. Aizenman, Altschuler, DeFranco, Halfter, and Romero kept me on track and provided novel insights into my work, particularly during our intense troubleshooting debates. I would especially like to thank Dr. Halfter, who provided lab space, support, and input during my transitional period and Dr. DeFranco, who remained my unwavering advocate throughout my studies.

The support provided by University of Southern California's Zilkha Neurogenetic Institute, University of Pittsburgh's Department of Pharmacology, and the M.D./Ph.D. program at the University of Pittsburgh was instrumental in keeping everything running smoothly behind the scenes. Included in my thanks are Jonah Chan, Doug Hardaway, Barbara Lockley, Dale Odano, Bill Singleton, and Alapakkam Sampath (at USC), Holly Gergely, Jim Kaczynski, Dr. Reynolds, Rich Smith, Pat Smith, and Jen Wong, (Pharmacology Department), Manjit Singh and Clayton Wiley (M.D./Ph.D. program), and Cindy Duffy of the Interdisciplinary Program.

There are too many friends to list them all here, but special thanks go out to the Batteys, Matthias Geisbauer, Michael Hezel, Jill Iger, Ted Lifset, Amol Mhatre, Adela Milano, Cyrus Mirakhor, Felton Newell, Dareth Newton, Ben Ng, Bridget O'Shea, Katariina Rantanen, the Shaners, the Streightiffs, Jerry Smith, Jamie Sutherland, Erick Tatro, and Rob Tomko. Thanks for pushing me on and for being there through the ups and downs. Thanks L. Le Pourhiet, G. Occhipinti, and J. Rausch, for reminding me to breathe during my writing!!

Of course, I would not have made it to this point to begin with without the excellent training and guidance I received at Bethesda Elementary, the Math, Science, and Computers Magnet Programs at Takoma Park Junior High and Blair High Schools (all in Maryland), the University of Chicago, the University of Cambridge, and the University of Pittsburgh. I am extremely thankful for the time, effort, and patience my teachers and professors (too numerous to name here) put into educating me and pushing me to challenge my limits, all while fostering a love for science and learning!! Additionally, my summers during college spent at the Laboratory of Diagnostic Radiology Research at the National Institutes of Health shaped my early career as a medically-minded researcher. Thanks especially to Henry Bryant, Jr., Joe Frank, John Ostuni, and Nancy Richert.

A number of abbreviations are used throughout this dissertation. The most common ones are as follows: acetylcholine (ACh), nicotinic acetylcholine receptor (AChR), evoked endplate potential (EPP), miniature endplate potential (MEPP), muscle specific kinase (MuSK), neuromuscular junction (NMJ), receptor tyrosine kinase (RTK), shRNA (short hairpin RNA), and tumorous imaginal discs (tid1).

1.0 INTRODUCTION

1.1 THE NEUROMUSCULAR JUNCTION: STRUCTURE AND FUNCTION

The neuromuscular junction (NMJ) is one of the most well-studied synapses. In fact, the nicotinic acetylcholine receptor (AChR), highly concentrated on the postsynaptic membrane of the NMJ, was the first neurotransmitter receptor to be isolated, purified, and characterized. This is due in large part to the facts that the electric organs of the *Torpedo* fish have billions of cholinergic synapses and that the AChR has an almost irreversible inhibitor, α -bungarotoxin (α -BTX), derived from the venom of *Bungarus* snakes (Changeux and Edelstein, 2005). Thus, there exists an abundant supply of the receptor and a reliable way to pull it out of tissue extracts. Studies of the NMJ are aided by its comparatively large size, its accessibility, and its relative simplicity, as compared to synapses of the central nervous system. Many aspects of NMJ structure and function are generalizable to other synapses, making it an ideal model for studying synaptic transmission. Understanding the complex process of neurotransmission is of great biomedical importance, as many psychiatric and neurologic conditions result from disruptions in this fundamental phenomenon.

The NMJ is a highly specialized structure that is responsible for mediating fast synaptic transmission from motoneurons to muscles (Burden, 2002). It is comprised of the presynaptic

motoneuron terminal and surrounding Schwann cells, the synaptic cleft, which includes the basal lamina, and the postsynaptic myofiber (Figure 1).

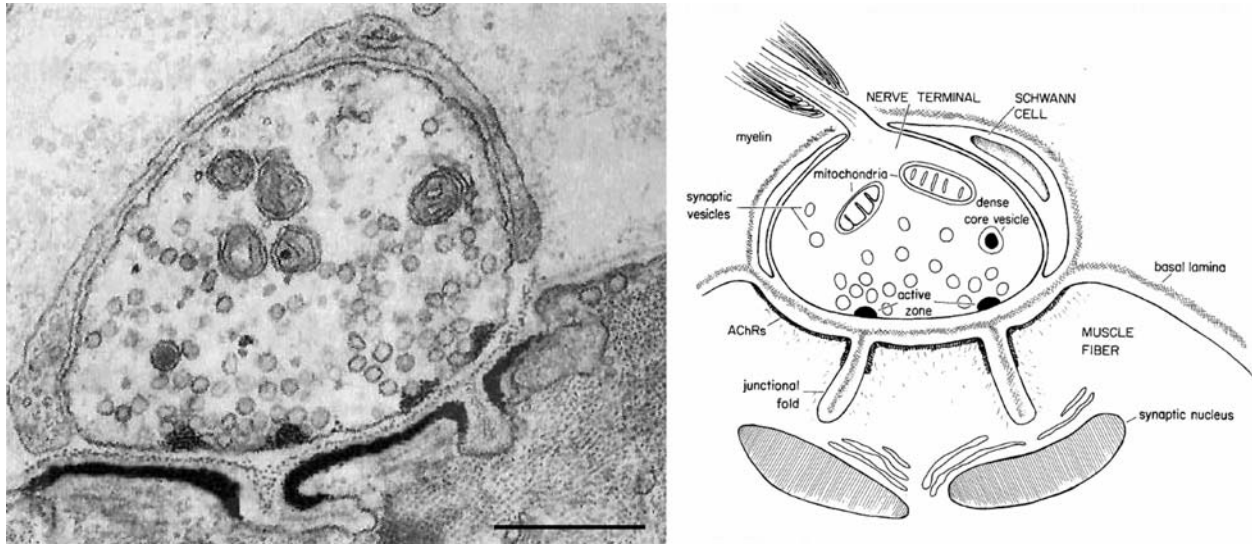


Figure 1. Structure of the neuromuscular junction.

A schematic diagram (right panel) demonstrates some of the key features of an electron micrograph (left panel) of the neuromuscular junction (NMJ). At this synapse, synaptic vesicles filled with the neurotransmitter acetylcholine are concentrated within the motoneuron terminal at active zones, across from the crests of postjunctional folds, which have a high density of nicotinic acetylcholine receptors (AChRs). The basal lamina, located in the synaptic cleft, serves to concentrate various factors such as acetylcholinesterase and agrin. Subsynaptic nuclei preferentially transcribe mRNAs for NMJ-specific proteins, such as AChRs. Scale bar = 0.5 μ m. Modified from Hall and Sanes, 1993.

Motoneurons synthesize the neurotransmitter acetylcholine (ACh), package it into synaptic vesicles, and, upon the arrival of an action potential and a subsequent influx of presynaptic calcium, release the vesicles from active zones, where they are concentrated. The vesicles fuse with the plasma membrane of the motoneuron nerve terminus, releasing their contents into the synaptic cleft. ACh binds to its receptor, the AChR, which is concentrated at the crests of the postjunctional folds of the myofiber membrane, at a ratio of two ACh molecules per AChR. The

entry of positively charged sodium ions through the central pore of the AChR results in a depolarization of the myofiber membrane potential, triggering the activation of voltage-gated sodium channels located at the troughs of the postjunctional folds. An action potential is then propagated through the myofiber, resulting in the eventual contraction of the motor unit, or all of the innervated myofibers associated with the branches of a particular motoneuron axon. ACh is hydrolyzed by acetylcholinesterase (AChE) in the synaptic cleft and its breakdown product, choline, is taken up by the motoneuron to be re-synthesized into ACh (Landowne, 2006). In this manner, a desire for movement is encoded as an electrical impulse which passes from the brain through the spinal cord, to the motoneuron, where it is briefly transformed into a chemical signal that triggers an action potential, resulting in the coordinated contraction of a muscle.

1.2 CLUSTERING OF AChRS IN THE POSTSYNAPTIC NMJ MEMBRANE

As seen above in Figure 1, the postsynaptic membrane of the NMJ is organized as a series of junctional folds, the crests of which directly appose the presynaptic active zones, in a central region of the muscle termed the endplate zone. As the result of a complex developmental program, several muscle proteins, such as the AChR and the receptor-associated muscle protein rapsyn, become highly concentrated at the endplate region, as opposed to being located elsewhere on the surface of the myofiber. This process is referred to as “clustering” (Glass et al., 1996) and it is critically important for efficient neuromuscular transmission. Clustering is a highly localized phenomenon. For instance, the endplate zone takes up only about 1% of the muscle cell surface area, yet the density of AChRs in this region is greater than 10,000 per μm^2 . In contrast, the extra-synaptic area of the muscle cell membrane has a density of receptors of less

than 10 per μm^2 (Arrowsmith, 2007). Clustering of AChRs at the NMJ is one example of how the structure of the NMJ is optimized for its primary role, neurotransmission.

1.2.1 Evidence for the induction of AChR clustering by motoneurons

Historically, it was believed that motoneurons are responsible for initiating AChR clustering at the NMJ. A number of lines of evidence lead to this conclusion. First, on cultured myotubes, prior to innervation, AChRs are spread diffusely throughout the muscle cell membrane. Upon innervation, AChRs cluster at neuromuscular synapses. Denervation results in the reversion of AChRs to their pre-innervation distribution. Studies of *Xenopus*, chick, and rodent neuron / myotube co-cultures revealed that motoneurons, as opposed to sensory or sympathetic neurons, are especially potent at inducing AChR clustering on the muscle cell surface (Dutton et al., 1995). As motoneurons grow over myotubes, they concentrate AChRs opposite to their points of contact. Other studies revealed that the basal lamina concentrates a factor that is responsible for AChR clustering: upon removing the motoneuron entirely from frog muscle, cutting the muscle away from the basal lamina, and allowing the muscle to regenerate, AChR clusters reform at their original sites (McMahan and Slater, 1984). This clustering factor was isolated and found to be the protein agrin.

Agrin is an approximately 200-kilodalton glycoprotein that is synthesized by different tissues, such as the brain, spinal cord, motoneurons, skeletal muscle, lungs, and kidneys (Rupp et al., 1991; Ruegg et al., 1992; Groffen et al., 1998). The different forms of agrin are alternatively spliced – there are three sites, named x, y, and z, in the C-terminus of agrin which contain either no insert or one or more residue inserts ranging in size between 3 and 19 amino acids (Ferns et

at inducing AChR clustering than agrin forms which lack this insert (Ferns et al., 1993). Indeed, the potency of agrin as a clustering factor can be attested to by the fact that as little as 0.5 nM of neural agrin added to cultured myotubes for a pulse of 5 minutes results in a maximal level of clustering identical to treatment with agrin for 8 hours (Mittaud et al., 2004). Agrin is synthesized by motoneurons and it is secreted into the synaptic cleft, where it binds to laminin in the basal lamina (Denzer et al., 1997). On the muscle cell membrane, agrin binds to and stimulates the phosphorylation of a receptor complex which includes the receptor tyrosine kinase (RTK) muscle specific kinase (MuSK, Valenzuela et al., 1995; Glass et al., 1996). Other muscle-specific factors are known to be necessary for the activity of agrin, as agrin does not bind directly to the isolated extracellular domain of MuSK, nor is the transfection of MuSK into fibroblasts sufficient to reconstitute MuSK phosphorylation. Rather, MuSK can only be activated by agrin in a differentiated myotube (Glass et al., 1996). Interestingly, agrin does not affect the transcription of AChR subunits or the NMJ-specific turnover of AChRs. Instead, agrin acts to induce the lateral movement of preformed AChRs and other components of the postsynaptic apparatus along the myofiber cell membrane (Wallace, 1989). It is believed that changes in the transcription of AChR subunits are regulated by neuregulin acting through ErbB RTKs (Carraway and Burden, 1995).

Mouse knockouts of agrin and MuSK were generated. These animals died at birth, unable to breathe. In the agrin knockout mice (Gautam et al., 1996), existing AChR clusters were smaller, less intensely stained, and located throughout the myotubes, as opposed to being restricted to the endplate region. Many myotubes had no AChR clusters, while others had multiple clusters, many of which were un-innervated. Thus, the usual ratio of 1 motoneuron branch terminal to 1 myotube fiber was disrupted. However, consistent with the fact that agrin

does not alter the transcription or turnover of AChR subunits, the total number of AChRs on the muscle cell surface remained largely unchanged. The muscles of the MuSK knockout mice were more dramatically disrupted (DeChiara et al., 1996). Unlike the agrin knockout mice, they demonstrated *no* evidence of NMJs – no AChR clusters were visible on the myofiber surface. However, the surface number of AChRs was normal, although transcription of the subunits was spread throughout the muscle. The phenotype of the agrin knockout led support to the “agrin hypothesis” (McMahan, 1990), that “agrin...is thought to be the neurally derived factor responsible for the initial clustering of...AChRs...at developing synapses” (Ferns et al., 1993). The phenotypic similarities between the agrin and MuSK knockout mice lead to the conclusion that agrin acts through a receptor complex which includes MuSK (Glass et al., 1996). Interestingly, the branching and arborization of the motoneuron terminals in these knockout mice were also in disarray, pointing to the idea that both agrin and MuSK regulate pre- and postsynaptic aspects of neuromuscular junction development.

1.2.2 Motoneurons are not necessary for AChR clustering

At the turn of the century, a few papers came out challenging the “agrin hypothesis” of AChR clustering. In these papers, the authors described experiments where motoneurons had been prevented from developing in mice, either via the expression of diphtheria toxin in motoneurons (Yang et al., 2001), or by the actual knocking out of motoneurons (Yang et al., 2000; Lin et al., 2001). According to the agrin hypothesis, if the motoneuron is not present, there should be no clustering of AChRs, as no neural agrin is being made and secreted into the basal laminar area. Instead, in mice lacking motoneurons, there *was clustering of AChRs* in the central region of skeletal muscles, the usual site of innervation and NMJ formation. During early

synaptogenesis (E14.5), the area of clustering was similar between knockout and wildtype control mice. By late synaptogenesis (E18.5), however, the pattern of clustering in the motoneuron knockout mice had changed little, whereas the area of clustering in the wildtype mice had narrowed considerably, such that the distribution of AChRs more closely apposed the nerve termini of the motoneuron. These papers demonstrated that the motoneuron, and thus agrin, is not necessary for the initiation of postsynaptic differentiation. Instead, muscle fibers are intrinsically able to cluster AChRs at the endplate region, in a broad “prepattern”. Moreover, these findings indicated that the process of AChR clustering is a dynamic one which evolves throughout embryogenesis. These observations prompted a reexamination of the role of agrin in normal synaptogenesis.

Lin et al. (2001) reexamined agrin knockout mice from the perspective of comparing early with late synaptogenesis. As was reported earlier, by the time of birth, agrin knockout mice die with poorly-formed NMJs that have no or few AChR clusters which are spread throughout the muscle fibers. However, the authors also studied agrin knockout mice during early synaptogenesis. Surprisingly, they found that at E14.5, agrin knockout mice do have a prepattern of clustered AChRs which closely resembles that of wildtype controls in location and size. Thus, as was seen in the motoneuron knockout mice, without agrin, muscle fibers are capable of clustering AChRs in the appropriate region. However, in contrast to the motoneuron knockout mice, the prepattern disappears by birth in agrin knockout mice. Thus, the motoneuron contains some other factor which disperses AChRs in the absence of agrin (Ferns and Carbonetto, 2001). Therefore, it appears that normal synaptogenesis involves a balancing of forces, some tending to disperse AChRs and others acting to cluster AChRs at the NMJ. Agrin’s

role seems to be “to strengthen synaptic contacts, to prevent dispersion of AChR clusters, and to control axon growth” (Witzemann, 2006).

1.2.3 Current theory on AChR clustering at the NMJ

What emerged from the motoneuron knockout studies was a recognition that the clustering process is dynamic, proceeding through phases from early to late synaptogenesis. As was demonstrated, muscle fibers produce a broad prepattern of AChRs in their central region prior to the arrival of motoneurons. Early in synaptogenesis, there exist AChR clusters which are not directly apposed by nerve terminals. In contrast, by birth, aneural AChR clusters have disappeared and remaining clusters are apposed by motoneuron branch termini (Witzemann, 2006). Thus, neuromuscular synaptogenesis proceeds through a refinement period, where aneural AChR clusters are dispersed by an agrin-independent factor and incorporated clusters are strengthened by agrin. Whereas the initial patterning of AChR clusters at the NMJ is determined by muscle fibers, refinement seems to be dependent upon motoneurons, for without them, the distribution of AChR clusters remains similar to that noted in early synaptogenesis.

Further confirmatory evidence for this theory has been provided by zebrafish studies. Zebrafish embryos are transparent and they develop outside of the mother. They are easily manipulatable with drugs and a knockdown technique which uses oligomers termed morpholinos to prevent the expression of target proteins (Nasevicius and Ekker, 2000). Their use as a model system for studying development and human diseases has exploded in the past few years (Driever et al., 1994; Hsu et al., 2007). In fact, a number of genetic mutants with defects specifically in neuromuscular synaptogenesis have been identified using this model system (Panzer et al., 2005). Another useful feature of zebrafish embryos is that it is relatively easy to

label particular cell types in them. Thus, by labeling the motoneurons and AChRs, neuromuscular synaptogenesis has been studied *in vivo*, in real time. Indeed, observation has confirmed the findings from the mouse knockout studies. Prior to the arrival of the motoneuron, a prepattern of AChR clusters appears. Some early aneural AChR clusters disappear as others are recruited towards the nascent synapse (Flanagan-Steet et al., 2005; Panzer et al., 2006).

Muscle fibers develop by the fusion of many embryonic muscle cells, termed myoblasts, into myotubes, which are eventually incorporated into muscle fibers. Thus, muscle fibers from a syncytium. Individual myofibers often contain hundreds of nuclei, most of which are found just underneath the cell membrane (Heffner and Balos, 2006). However, at the fully developed stage, it is only the subsynaptic nuclei, located directly beneath the NMJ, which transcribe AChR subunits (Brenner et al., 1990). During embryogenesis, fusion proceeds from the center of a muscle fiber to its outer limits. It is believed that the AChR cluster prepattern appears at the central endplate region of a muscle fiber because this area is older, or more mature, than the rest of the muscle fiber. Consequently, this area is the first to express MuSK and its associated proteins. MuSK is expressed at high levels in this region and similar to other RTKs, MuSK likely autophosphorylates itself, activating a positive feedback loop which leads to the expression of MuSK and AChR subunits. AChRs thus appear and cluster in the endplate region (Witzemann, 2006). Subsequently, the motoneuron grows into this area and secretes agrin. Existing clusters are strengthened by agrin, whereas extra-synaptic ones are dispersed. This theory also likely explains why spontaneous AChR clusters appear in cultured myotubes that are not exposed to agrin. The muscle cell membrane is not entirely homogenous throughout its length and certain areas, such as ones containing lipid rafts or scaffold complexes, may concentrate the many proteins that are necessary for AChR clustering to occur.

Evidence is mounting that the nerve-derived dispersal factor responsible for eliminating aneural AChR clusters is ACh itself. In 2002, Misgeld et al. described mice in which choline acetyltransferase (ChAT), the ACh-synthesizing enzyme, was mutated, resulting in a blockade of both spontaneous and evoked neurotransmission. In the mutant mice, AChRs cluster in a broader endplate band than usual, resembling those observed in the aneural muscles described by Yang et al. and Lin et al. (2001). These findings were confirmed by a second group which created independent ChAT-deficient mice (Brandon et al., 2003). This second group found that postsynaptic AChR clusters are increased in number and they occupy a broader area as compared to control animals. The band occupied by the clusters remains broad throughout development. Kummer et al. (2004) examined agrin and ChAT double mutant mice. AChR clusters are present in nerve/muscle contact points in these mice, just as they are present in the central zone of muscle in agrin/motoneuron double knockout mice. The authors hypothesized that ACh acts to disperse those AChR clusters that are not stabilized by agrin. Indeed, using a myotube culture system, they demonstrated that an ACh analogue disperses spontaneous AChR clusters, except in areas that are contacted by agrin tethered to heterologous cells. Further support for the idea that ACh is an AChR cluster dispersing agent comes from the zebrafish *twister* gain of function mutant, in which AChRs have a prolonged open time and excessive activity. In these mutants, AChRs do not cluster during initial synaptogenesis (Lefebvre et al., 2004). Whereas it has been proposed that electrical activity, as opposed to a motoneuron-derived factor, may be responsible for the dispersal of aneural AChR clusters, blockade of activity by tricaine (Panzer et al., 2004) has no effect upon the dispersal of clusters in developing zebrafish embryos. Together, these results point to the idea that the nerve-derived dispersal factor is likely to be ACh.

1.3 GOALS OF THE DISSERTATION

It is well accepted that agrin is essential for strengthening AChR clusters and for sustaining their localization at the NMJ. It is also known that agrin signals through a receptor complex on the muscle cell membrane which includes MuSK. Although MuSK itself is well characterized, the signaling pathway downstream of its activation by agrin, responsible for AChR clustering, remains poorly understood. *The overall goal of the research described in this dissertation is to elucidate the initial step(s) of the agrin → MuSK → AChR clustering cascade*, as highlighted in Figure 3.

1.3.1 Significance of the work

Uncovering the pathway responsible for AChR clustering will provide novel insights into molecular mechanisms underlying the assembly of postsynaptic protein complexes at the NMJ. Many diseases, such as myasthenia gravis and muscular dystrophy, are known to result from disruptions of the normal structure and function of the NMJ. Elucidating the steps of agrin-mediated signaling cascades at the NMJ is critical for better understanding the causes of and for designing more effective treatments for these debilitating conditions. For instance, some forms of myasthenia gravis are caused by autoantibodies directed against MuSK (Hoch et al., 2001). These antibodies induce the cross-linking of MuSK receptors, leading to their internalization from the muscle cell membrane. Neuromuscular transmission is adversely affected as NMJ AChRs decrease in number and muscle weakness ensues. Future therapies could be designed to circumvent this portion of the pathway by targeting proteins which are downstream of MuSK in the clustering cascade.

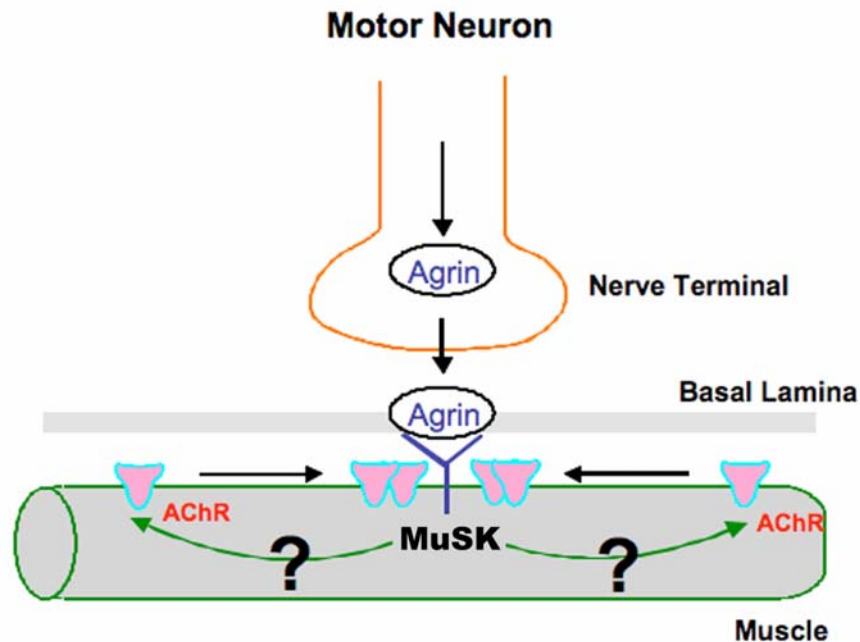


Figure 3. Schematic diagram of the agrin → MuSK → AChR clustering cascade

Motoneurons synthesize and secrete agrin into the basal lamina area, where it binds to laminin and α -dystroglycan. Agrin binds to a receptor complex in the muscle which includes the receptor tyrosine kinase muscle specific kinase (MuSK). Upon activation by agrin, MuSK is phosphorylated, activating a downstream signaling pathway, signified by ‘?’, which results in the eventual phosphorylation and translocation of AChRs to the NMJ region, a phenomenon known as “clustering”. The signaling cascade responsible for AChR clustering at the NMJ remains unclear. The main goal of the research detailed within this dissertation is to identify protein(s) immediately downstream of MuSK in the clustering pathway.

Defects in AChR clustering have also been linked to muscular dystrophy (MD). For instance, a type of MD known as Fukuyama-type congenital MD has been characterized by mutant α -dystroglycan, a major component of the dystrophin glycoprotein complex which links the extracellular matrix with the muscle cytoskeleton and is necessary for AChR cluster stabilization (Jacobson et al., 2001). Agrin is known to bind α -dystroglycan in addition to laminin in the basal lamina (Fallon and Hall, 1994). In addition, α -dystroglycan binds to AChRs via rapsyn (Noakes et al., 1993; Apel et al., 1995). In a mouse model of this disease, agrin and

laminin expression are decreased, as are their abilities to bind to α -dystroglycan. In addition, AChR clustering is impaired and the NMJs of these mice are fragmented (Saito et al., 2007). Better understanding the agrin/MuSK/AChR clustering cascade may provide insight into the structure, function, and regulation of the dystrophin complex. Furthermore, studying this signaling pathway may reveal basic principles and mechanisms that are applicable to the processes of synaptic development and maintenance in the central nervous system.

1.3.2 MuSK: a critical player in the agrin \rightarrow AChR clustering pathway

MuSK has been shown to be crucial for AChR clustering. Without MuSK, neither spontaneous, as that seen in the muscle prepattern, nor agrin-induced clustering of AChRs is possible (Herbst and Burden, 2000). Indeed, no AChR clusters are found in MuSK knockout mice (DeChiara et al., 1996). MuSK is essential not only for the initiation of AChR clustering embryonically, but also for the maintenance of NMJ structure throughout life. Removal of MuSK postnatally, either through a conditional knockout (Hesser et al., 2006) or through knockdown via small interfering (si)RNA (Kong et al., 2004), results in the dissolution of the NMJ. MuSK also has effects upon the presynaptic motoneuron and on postsynaptic gene transcription. In MuSK knockout mice, the branching pattern and arborization of motoneurons are disrupted. Motoneuron axons cover most of the muscle and motoneuron termini lack the usual level of arborization. Additionally, clustering of other NMJ-specific factors, such as rapsyn, utrophin, ErbB4, and AChE, is also abolished. Transcription of AChR subunits is spread throughout muscle fibers, as opposed to being concentrated at subsynaptic nuclei. This may be due to the fact that one of the regulators of subsynaptic transcription, ErbB4, is not clustered at the motor endplate without MuSK. In postnatal conditional MuSK knockout mice, AChRs

disappear and the motoneuron termini actually retract from the endplate region and begin to grow and branch excessively.

MuSK is a receptor tyrosine kinase (RTK) that is specific to skeletal muscles. It is expressed at high levels in fusing myotubes and after denervation, immobilization, or a blockage of electrical activity. In mature muscle, it is prominent only at the NMJ (Valenzuela et al., 1995). MuSK has a large extracellular domain with 4 immunoglobulin (Ig)-like regions, a transmembrane region, and an intracellular domain which contains a juxtamembrane region and a tyrosine kinase domain (Figure 4). The first Ig-like domain is needed for responsiveness to agrin and the fourth Ig-like domain is necessary for interaction with rapsyn (Strochlic et al., 2005). Additionally, the extracellular portion has 6 conserved cysteines and the cytoplasmic region of MuSK has 19 tyrosine residues, 6 of which are phosphorylated upon activation with agrin. The phosphorylated tyrosines include an NPXY motif, which is bound by proteins containing a phosphotyrosine binding (PTB) domain (Y553), and tyrosines within the kinase domain of MuSK (Y576, Y750, Y754, Y755, and Y812; Watty et al., 2000). MuSK phosphorylation activates a signaling cascade which results in the phosphorylation (within minutes) and eventual clustering (within hours) of AChRs (Wallace et al., 1991; Ferns et al., 1996; Glass et al., 1996). However, although it precedes clustering, phosphorylation of AChRs is not necessary for their clustering (Meyer and Wallace, 1998). Site-directed mutagenesis experiments have shown that tyrosine Y553, contained in the PTB domain target motif in the juxtamembrane region of MuSK, and others in the activation loop of the kinase domain (Y750 and Y754) are essential for AChR phosphorylation and clustering (Herbst and Burden, 2000). Thus, a functioning kinase domain is crucial for AChR clustering.

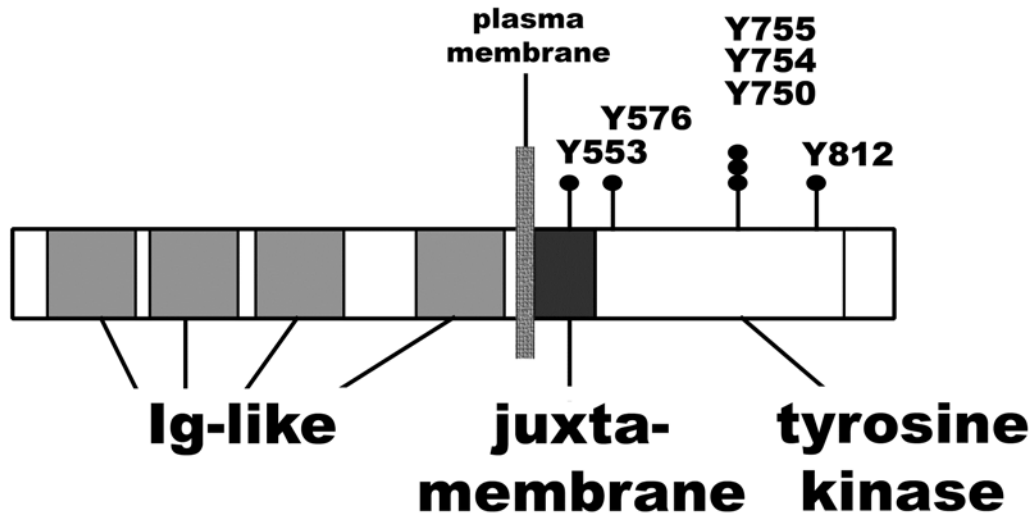


Figure 4. Schematic diagram of the main domains and phosphorylation sites of MuSK.

The extracellular domain of MuSK has 4 immunoglobulin (Ig)-like regions and 6 conserved cysteines (not pictured). The intracellular portion of MuSK has juxtamembrane and tyrosine kinase domains. 6 out of 19 intracellular tyrosine residues, Y553, Y576, Y750, Y754, Y755, and Y812, are phosphorylated upon stimulation with agrin. MuSK phosphorylation leads to the phosphorylation and clustering of AChRs. Tyrosines Y553, Y750, and Y754 are essential for AChR phosphorylation and clustering. Tyrosine Y553 is part of an NPXY motif, which is recognized and bound by proteins containing phosphotyrosine binding (PTB) domains, including Dok-7. The C-terminal tail of MuSK contains a VXX motif, bound by PDZ domain-containing proteins, such as the guanylate kinase MAGI-1c (not pictured). Modified from Herbst and Burden, 2000.

Although MuSK was discovered more than a decade ago, the precise mechanism by which it induces clustering of the AChR remains elusive. For instance, MuSK does not appear to signal through common MAP kinase or PI3 kinase pathways (Herbst and Burden, 2000). It does seem that agrin-induced clustering of AChRs is dependent upon tyrosine kinases (Wallace, 1994). Indeed, roles have been discovered for the tyrosine kinases src and abl (Mittaud, et al., 2001; Burden, 2002; Finn et al., 2003). Other aspects of MuSK signaling are poorly understood. However, evidence is building that MuSK acts as a complex signaling scaffold (Luo et al., 2003; Strohlic et al., 2005) at the NMJ. For instance, in addition to the NPXY motif in the

juxtamembrane region, the C-terminus of MuSK contains a VXY consensus motif, known to be bound by PDZ domain-containing proteins.

1.3.3 Other postsynaptic players involved in AChR clustering

Another skeletal muscle protein which has been shown to be indispensable for AChR clustering is rapsyn, for receptor associated protein at the synapse (Frail et al., 1988). Rapsyn was actually discovered due to its high affinity for the AChR. Early efforts to isolate and purify the AChR often detected the presence of a 43-kilodalton protein, later identified as rapsyn (Sobel et al., 1977; Neubig et al., 1979). Rapsyn knockout mice are similar to MuSK knockouts, in the sense that AChR clustering is entirely abolished and the growth and arborization of presynaptic axons are similarly disordered. However, in contrast to MuSK knockout mice, subsynaptic transcription of AChR subunits is preserved and MuSK accumulates normally at myofiber endplates (Gautum et al., 1995; Apel et al., 1997). Upon stimulation of rapsyn-deficient myotubes with agrin, MuSK is phosphorylated normally. However, AChR phosphorylation and subsequent clustering do not occur (Apel et al., 1997). The lack of AChR phosphorylation may be due to an absence of src family kinases, as src kinases are known to be associated with and activated by rapsyn (Mohamed and Swope, 1999; Mittaud et al., 2001). Additionally, the cytoskeletal dystrophin complex, with which AChRs are normally associated, is disrupted, indicating that rapsyn is also critical for organizing the postsynaptic cytoskeleton complex which likely stabilizes AChR clusters (Gautum et al., 1995). Therefore, rapsyn appears to be acting downstream of MuSK in the clustering cascade, likely just upstream of AChR clustering itself. Thus, the tail ends of the agrin signaling pathway appear to have been worked out – MuSK acts at the beginning of the cascade, directly downstream of agrin, whereas rapsyn is located at the

end of the clustering pathway, associated with the AChR. The challenge remains to fill in the intermediate details.

Some progress has been made in this regard. Recent studies have uncovered roles for Dishevelled (Dvl, Luo et al., 2002), the Rac/Rho and Cdc42 GTPases (Weston et al., 2000, 2003), as well as the PTB domain-containing muscle protein Dok-7 in mediating MuSK-dependent AChR clustering (Okada et al., 2006). Additionally, the dystroglycan complex (Jacobson et al., 2001), abl and src tyrosine kinases (Finn et al., 2003; Mittaud et al., 2001; Smith et al., 2001), the membrane associated guanylate kinase MAGI-1c (Strochlic et al., 2001), and geranylgeranyltransferase 1 (GGT, Luo et al., 2003) are thought to be involved in MuSK signaling at the NMJ. Some of these players are coming together to create an increasingly coherent picture of the clustering cascade (Figure 5). For instance, cytoskeletal changes are thought to be crucial for AChR clustering (Hoch et al., 1994). The small GTPases Rac1, RhoA, and Cdc42 have all been implicated as mediators of cytoskeletal changes (Hall, 1998) and they are known to be activated downstream of agrin (Weston et al., 2000, 2003). Dvl can be linked to Rac1/RhoA/Cdc42 activation through its interaction with the actin cytoskeleton regulator p21-activated kinase 1, or PAK1 (Luo et al., 2002). GGT inhibitors inhibit agrin-induced activation of Rac1, Cdc42, and PAK1 (Luo et al., 2003). If Dok-7 behaves as other members of the Dok family, namely Dok-1, it could be phosphorylated by abl kinase and it could mediate Rac1/RhoA/Cdc42 activation indirectly via interaction with RasGAP (Yamanashi and Baltimore, 1997), which is known to bind to the small GTPase activator p190 (Settleman et al., 1992). In addition, dystroglycan is known to be intimately connected with the muscle cell cytoskeleton (Henry and Campbell, 1996). However, other components of the MuSK receptor complex and

its downstream effectors remain to be determined. Additionally, a straightforward signaling pathway which incorporates known factors has yet to be proposed.

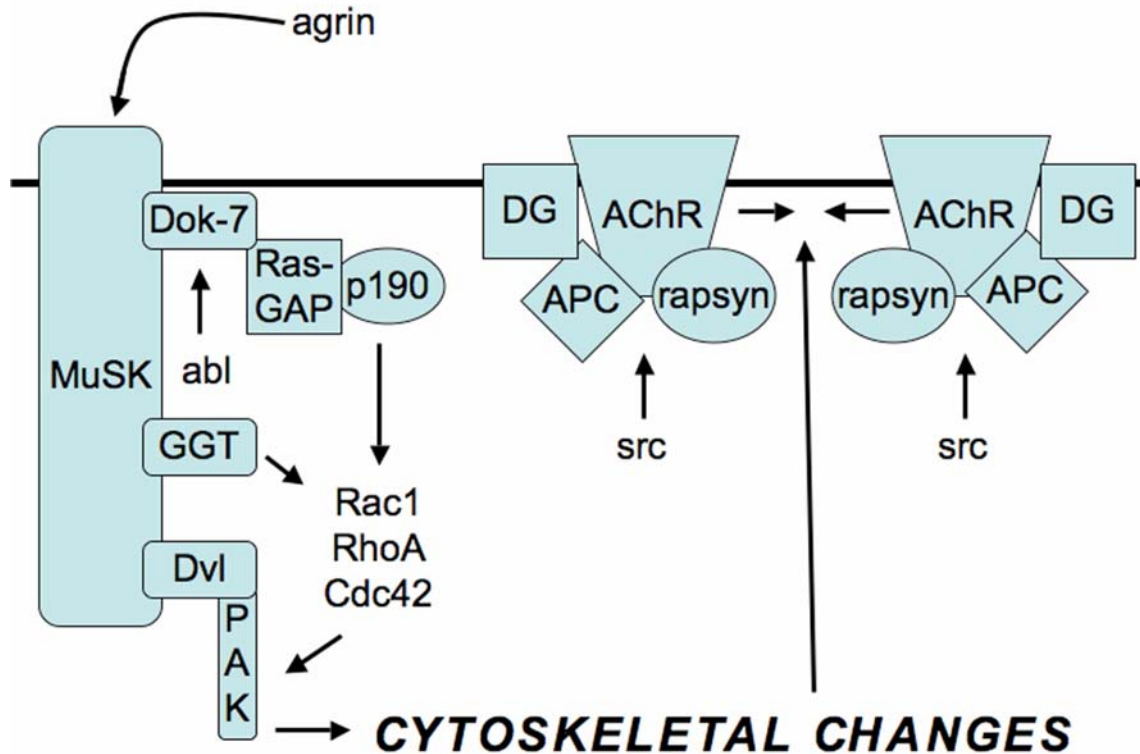


Figure 5. Schematic diagram of AChR clustering, mediated through cytoskeletal changes.

Pictured are components of the agrin/MuSK signaling pathway that have been linked to cytoskeletal changes, known to be essential for AChR clustering at the NMJ. Agrin activates the Rac1/RhoA/Cdc42 small GTPases, which are known to act through p-21-associated kinase (PAK1). Dishevelled (dvl) binds both MuSK and PAK1. Geranylgeranyltransferase1 (GGT) binds to MuSK. Inhibitors of GGT block agrin-induced activation of Rac1, Cdc42, and PAK1. Dok-7 binds to the NPXY motif of MuSK. If Dok-7 behaves like Dok-1, then it may be phosphorylated by an abl kinase and it may activate Rac1/RhoA/Cdc42 via RasGAP and p190. Additionally, the dystroglycan complex (DG), adenomatous polyposis coli (APC), rapsyn, and AChRs are all linked to the actin cytoskeleton. Src kinases bind to and are activated by rapsyn, leading to the phosphorylation of AChRs.

1.4 TID1: A NEW DIRECTION IN CELLULAR SIGNALING AT THE NMJ

The unusual nature of MuSK signaling has prevented a satisfactory resolution of the AChR clustering pathway since MuSK's discovery more than a decade ago. In order to address this problem, a new approach was needed. In an effort to clarify early steps of the AChR clustering cascade, I decided to use a bacterial-two hybrid assay to search for MuSK binding partners in skeletal muscle. Bacterial two-hybrid assays are based upon the principles of the better-known yeast two-hybrid assays used for discovering protein-protein interactions. However, as its name implies, a bacterial two-hybrid assay is carried out in bacteria. There are a number of advantages to performing protein-protein interaction screens in bacteria versus yeast. These include the facts that bacteria have no nuclei, so one does not need to rely on interacting proteins to get into the nucleus in order to observe an activation of the reporter construct, bacteria have less mammalian homologues than yeast, leading to less false positives, and they have a faster life cycle and are often easier to transform and manipulate than yeast, allowing for more rapid screening of large libraries of proteins. Together, these features allow for faster and more specific large-scale screens in bacterial two-hybrid assays as compared to yeast two-hybrid assays.

Stratagene (La Jolla, CA) sells both bacterial two-hybrid assay kits and an E19 rat skeletal muscle cDNA library. In the Stratagene BacterioMatch II system, "bait" cDNA is subcloned into the pBT vector and "target", or library, cDNA is subcloned into the pTRG vector. The bait cDNA is fused with the bacteriophage λ repressor protein λ cI, which is designed to bind to the λ operator sequence located just upstream of the promoter in the reporter construct. Target cDNA is fused with the N-terminal portion of the α subunit of RNA polymerase. Interaction between the bait and a target protein results in the recruitment of transcription machinery to the

reporter construct, which encodes the HIS3 enzyme and a streptomycin resistance gene. Translation of the reporter proteins allows for survival in a histidine-lacking (his-) and streptomycin-containing environment. Initial interactors are screened for by co-transforming reporter cells with the pBT and pTRG plasmids and looking for growth on his- plates which contain 3-amino-1,2,4-triazole to inhibit background levels of HIS3 activation. Positive clones are enriched and patched onto dual-selective plates which also contain streptomycin. The cDNA of interacting clones is isolated, purified, and verified by retransforming reporter cells with the bait and the isolated pTRG plasmids. Once positive interactors are confirmed, the cDNA is sequenced and identified using the BLAST algorithm (National Center for Biotechnology Information (NCBI), National Institutes of Health, Bethesda, MD). This process is outlined in Figure 6.

Knowing that the cytoplasmic domain of MuSK is essential for agrin-induced clustering of AChRs and that it is phosphorylated in response to agrin stimulation (Herbst and Burden, 2000), I used this part of mouse MuSK as bait in a bacterial two-hybrid assay which screened an E19 rat skeletal muscle cDNA library for MuSK binding partners. I identified the rat homologue of the *Drosophila* tumor suppressor, *tumorous imaginal discs* (tid1), a heat shock protein (hsp) 40 homologue, as a protein that specifically binds to the cytoplasmic domain of MuSK with high affinity.

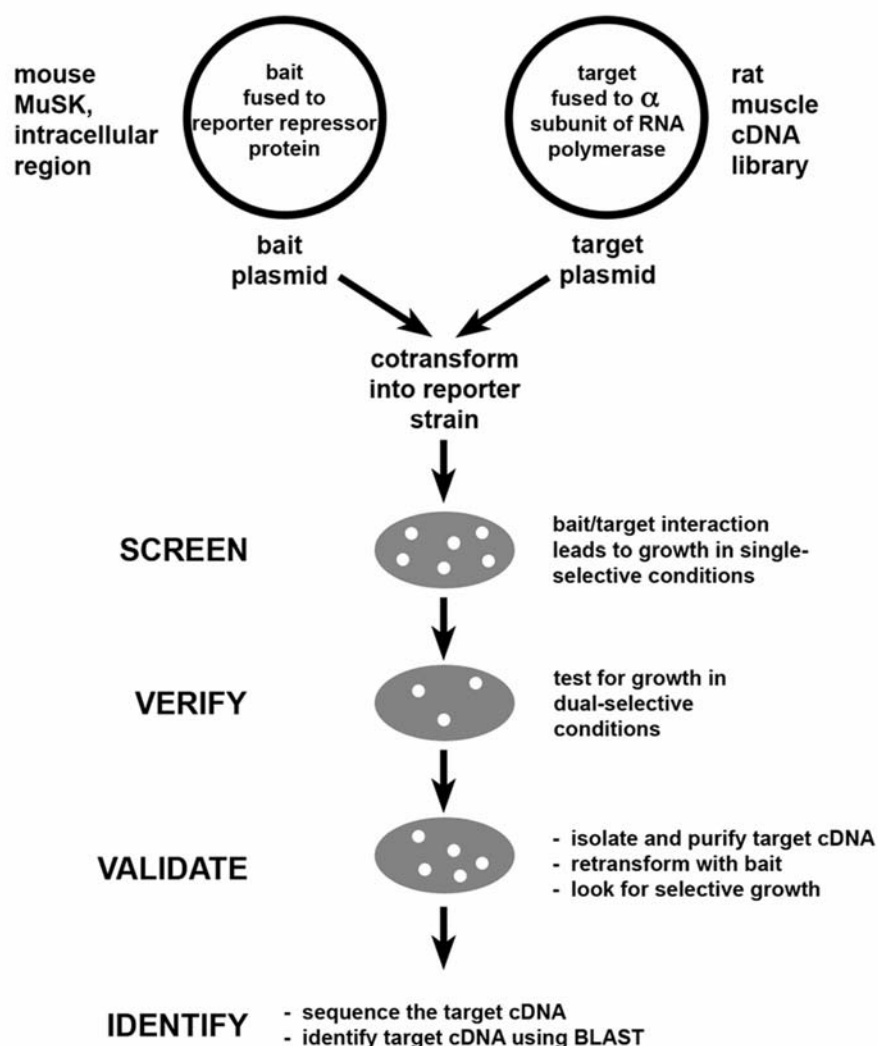


Figure 6. Schematic diagram of the bacterial two-hybrid system.

A bacterial two-hybrid assay was used to identify the MuSK-tid1 interaction. The cytoplasmic domain of MuSK (residues 515-869) was subcloned into the bait vector, pBT. A rat skeletal muscle cDNA library was subcloned into the target vector, pTRG. **SCREEN:** The bait and target plasmids were co-transformed into BacterioMatch II Validation Competent Reporter Cells and plated onto histidine-deficient plates containing 3-amino-1,2,4-triazole (3-AT). **VERIFY:** Putative clones identified in the initial screen were enriched and verified by growth on dual-selective plates with 3-AT and streptomycin. **VALIDATE:** Verified clones were validated by retransforming reporter cells with the pBT/MuSK construct and the isolated and purified pTRG plasmid. **IDENTIFY:** Validated clones were sequenced and interacting proteins were identified using the BLAST algorithm (NCBI, National Institutes of Health, Bethesda, MD). The screen was repeated using the juxtamembrane of MuSK (residues 515-692) as bait.

1.4.1 Tid1 as a signaling molecule

Tid56 was originally identified as a *Drosophila* tumor suppressor. Indeed, its mammalian homologue, *tid1*, has been found to decrease the malignancy (Kim et al., 2004) and mobility (Kim et al., 2005) of breast cancer cells and a tumor-associated mutation of *tid1* found in a glioma cell line sensitizes the cells to apoptosis (Trentin et al., 2004). Tid1 has also been shown to modulate cell senescence (Tarunina et al., 2004) and its two human isoforms were demonstrated to have opposite effects on apoptosis induced by exogenous stimuli (Syken et al., 1999). Tid1 is a hsp 40 homologue, known to bind to its co-chaperone, hsp70 (or heat shock cognate protein, hsc70). There is an increasing body of knowledge that implicates heat shock proteins in a variety of signaling pathways (Gaestel, 2006). Among these proteins, *tid1* is emerging as a molecule with previously unanticipated roles in cellular signaling, especially involving tyrosine phosphorylation. Tid1 interacts with the Jak family of protein-tyrosine kinases in lymphocytes (Sarkar, et al., 2001) and it is known to bind to the Ras-GTPase activating protein (Ras-GAP) (Trentin, et al., 2001). More recently, *tid1* has been shown to interact with and to mediate the signaling of the ErbB2 and Trk families of RTKs (Kim, et al., 2004; Liu, et al., 2005). Additionally, targeted deletion of the *tid1* gene results in the premature death of mouse embryos on day E7, suggesting the protein plays a critical role in early embryonic development (Lo, et al., 2004). The repeated discovery of *tid1* as a regulator of RTK signaling is especially interesting and relevant, as MuSK itself is a RTK.

1.4.2 Tid1: an important player in NMJ development and maintenance

The discovery of tid1 as a specific MuSK-binding protein led to the main hypothesis of the work detailed in this dissertation: *tid1 is a key mediator of agrin-induced clustering of nicotinic acetylcholine receptors at the neuromuscular junction.* After my identification of tid1 in the bacterial two-hybrid studies, I proceeded to show that tid1 is colocalized with AChR clusters in cultured C2C12 myotubes and on the postsynaptic membranes of mouse and rat NMJs. Upon prolonged denervation, tid1 immunostaining at the NMJ is diminished, with subsequent dispersal and disassembly of AChR clusters. Biochemical studies have demonstrated that endogenous tid1 is associated with MuSK in C2C12 myotubes and in rat muscles. Several lines of evidence suggest that tid1 is required for the formation of AChR clusters in cultured myotubes and that it is indispensable for the maintenance of NMJs in skeletal muscles. Overexpression of an N-terminal fragment of tid1 in C2C12 myotubes induces the formation of AChR clusters independently of neural agrin. In contrast, short hairpin RNA (shRNA)-mediated knockdown of tid1 inhibits spontaneous and agrin-induced AChR clustering in C2C12 myotubes. Furthermore, electroporation of tid1-targeted shRNA into adult mouse skeletal muscle results in the dispersal of AChR clusters from motor endplates and a reduction in the amplitudes of miniature endplate potentials (MEPPS) and evoked endplate potentials (EPPs) measured in the muscles. These results support the main hypothesis and strongly implicate tid1 as a novel player that regulates AChR clustering and maintenance, and thus synapse development, at the NMJ.

2.0 EXPERIMENTAL PROCEDURES

2.1 MATERIALS

2.1.1 Reagents

The bacterial two-hybrid screening kit and associated cells (BacterioMatch II Two-Hybrid System XR Plasmid cDNA Library Construction Kit (Cat. #200412)), BacterioMatch II Rat Skeletal Muscle cDNA Library (Cat. #982504), and the Quik-Change XL Site-Directed Mutagenesis Kit (Cat. #200516) were purchased from Stratagene (La Jolla, CA). Restriction enzymes for DNA subcloning were products of New England Biolabs (Ipswich, MA) and Invitrogen (Eugene, OR). Oligonucleotide primers were synthesized by Integrated DNA Technology (Coralville, IA). Protein A sepharose beads were obtained from Pharmacia Biotech (GE Healthcare, Piscataway, NJ). ¹²⁵I- α -bungarotoxin (α -BTX) was purchased from Perkin-Elmer (Boston, MA). Cell culture medium (Dulbecco's Modification of Eagle Medium (DMEM)) and supplements (penicillin/streptomycin and L-glutamine) were purchased from Mediatech (Herndon, VA). Fetal bovine serum and horse serum were from Equitech-Bio (Kerrville, TX). The Effectene transfection reagent (Cat. #301425) was purchased from Qiagen (Valencia, CA). Tissue Tek OCT cryosectioning medium was from Sakura Finetek U.S.A., Inc. (Torrance, CA). NuPAGE pre-cast gels and associated hardware and Western blotting reagents

were purchased from Invitrogen (Eugene, OR). The BCA protein assay kit was from Pierce Biotechnology, Inc. (Rockford, IL). All other chemicals, including the P3840 protease inhibitor cocktail and α -BTX were obtained from Sigma (St. Louis, MO). Neural and muscle agrin were produced as described by Ferns et al. (1992).

2.1.2 Antibodies

The tid1 short-specific polyclonal antibody was generated by immunizing a rabbit with a synthetic peptide corresponding to the last 20 residues in the C-terminus of mouse tid1 short (VEGTVNGVTHSTGKRSTGN) (Genemed Synthesis, San Francisco, CA). The antiserum was purified on an Affi-gel 10/15 immunoaffinity column (Bio-Rad Laboratories, Hercules, CA). The specificity of the antibody was confirmed by immunofluorescent staining and Western blotting (Figure 9). The rabbit anti-tid1 polyclonal antibody for immunostaining of the NMJ was a gift from Dr. Jiing-Dwan Lee (Department of Immunology, The Scripps Research Institute, La Jolla, CA). The rabbit anti-synaptophysin antibody was from Zymed (Invitrogen, Eugene, OR). The monoclonal antibodies mAb35 and 9E10 were obtained from Covance Research Products, Inc. (Berkeley, CA). Alexa Fluor 488- and 633-conjugated α -BTX as well as Alexa Fluor 488- and Alexa Fluor 633-conjugated goat anti-rabbit immunoglobulin G (IgG)s were purchased from Invitrogen (Carlsbad, CA). Alexa Fluor 680 goat anti-rabbit and anti-mouse IgG (H + L) antibodies were purchased from Molecular Probes (Invitrogen, Eugene, OR). Purified rabbit, goat, and mouse IgGs and Cy2 and Cy3-conjugated goat secondary antibodies were obtained from Jackson ImmunoResearch Laboratories, Inc. (West Grove, PA).

2.2 BACTERIAL TWO-HYBRID SCREENS

Bacterial two-hybrid screens were performed according to the manufacturer's protocols. The cytoplasmic domain of MuSK (amino-acid residues 515-869) was subcloned into the bait vector, pBT. The commercial rat skeletal muscle cDNA library was subcloned into the target vector, pTRG. The bait and target plasmids were co-transformed into BacterioMatch II Screening Reporter Competent Cells and plated onto histidine-deficient, single-selective plates containing 3-amino-1,2,4-triazole (3-AT), followed by enrichment and patching of clones onto dual-selective plates with 3-AT and streptomycin. Empty pBT and pTRG were used as negative controls and pBT-LGF2 and pTRG-gal11^P, provided by the manufacturer, were used as positive controls. Roughly 1×10^7 clones were screened, covering the rat muscle library. Target plasmids from verified interactions were subsequently isolated, purified, and retransformed along with pBT-MuSK into BacterioMatch II Validation Reporter Competent Cells. cDNAs of confirmed interactors in the target vector were sequenced and identified using the BLAST algorithm (The National Institutes of Health, Bethesda, MD). The process was repeated with the juxtamembrane domain (amino acids 515-692) of MuSK.

2.3 cDNA CONSTRUCTS

Full-length tid1 short (residues 1-453), tid1 short lacking the DnaJ domain (residues 151-453), tid1 short lacking the DnaJ and cysteine-rich domains (residues 304-453), the C-terminus of tid1 short (residues 428-453), and the N-terminal half of tid1 (residues 1-222) were amplified from a rat muscle cDNA library by Polymerase Chain Reaction (PCR) and subcloned into the

StuI site in the mammalian expression vector pCS2+MT. All constructs were confirmed by DNA sequencing. In addition, various pSIREN shRNA clones were created as detailed below.

2.4 CELL CULTURE, TRANSFECTION, AND LYSATE PREPARATION

2.4.1 C2C12 Cells

C2C12 myoblasts were grown in DMEM supplemented with 20% fetal bovine serum, 1% penicillin/streptomycin (5000 I.U./ml and 5000 $\mu\text{g}/\text{ml}$), and 1% L-glutamine (200 mM) at 37°C with 8% CO₂. Cells were passaged at 60-70% confluence. Cells were transfected at 50-60% confluence with Effectene according to the manufacturer's protocol. At ~95% confluence, myoblasts were switched to grow in fusion media (DMEM supplemented with 5% horse serum, 1% penicillin/streptomycin, and 1% L-glutamine). The fusion media was changed daily for ~72 h. For cell harvesting, myotubes were rinsed with Ca²⁺/Mg²⁺-free PBS, scraped off in Ca²⁺/Mg²⁺-free PBS with 1 mM sodium orthovanadate, and pelleted by centrifugation. The cells were resuspended in ice-cold extraction buffer (1% NP-40, 0.5% deoxycholic acid, 50 mM Tris-HCl pH 8.0, 50 mM NaCl, 5 mM EDTA, 50 mM NaF, 1 mM sodium orthovanadate) supplemented with a protease inhibitor cocktail (1%; Sigma catalog number P3840) and PMSF (4 mM). The extracts were rotated at 4°C for 30 min and then centrifuged at 20,800 x g at 4°C for 10 min to remove insoluble materials. The supernatants were subjected to a bicichoninic acid (BCA) assay, performed according to the manufacturer's specifications, normalized according to total protein amount, and either used for immunoblotting or immunoprecipitation studies, as detailed below.

2.4.2 COS-7 Cells

COS-7 cells were grown in DMEM supplemented with 10% fetal bovine serum, 1% penicillin/streptomycin (5000 I.U./ml and 5000 µg/ml), and 1% L-glutamine (200 mM) at 37°C with 5% CO₂. The cells were passaged at 100% confluence and they were transfected at 70-80% confluence with plasmid cDNAs by using an adenovirus-mediated DEAE-dextran method (Forsayeth and Garcia, 1994). Cells were harvested as detailed above for myotubes, except that a Triton-based extraction buffer (1.25% Triton X-100, 50 mM Tris-HCl pH 7.4, 50 mM NaCl, 1 mM EDTA, 1 mM EGTA) was used and the extracts were incubated on ice for 10 min instead of rotated at 4°C for 30 min.

2.5 SKELETAL MUSCLES

The use of animals was approved by and in compliance with the guidelines of the Institute Animal Care and Use Committee (IACUC) of University of Southern California.

2.5.1 Denervation

Adult C57/BL6 mice were anesthetized with sodium pentobarbital and the sciatic nerves of their right hindlimbs were exposed. A short segment (~5 mm) of the sciatic nerve was removed. The wound was sutured and the animal was returned to the animal facility. Eight days post-denervation, the soleus muscle was dissected out and cryosectioned as detailed below.

The soleus muscle from the left hindlimb was used as a control. Slices were immunostained as detailed below. The process was repeated at 7.5 weeks post-denervation.

2.5.2 Cryosectioning

Rodents were euthanized by anesthetic overdose. Fresh muscles were dissected out, suspended in OCT cryosectioning medium, and flash-frozen in dry ice-cooled isopentane as detailed by Wu et al. (1985). The frozen muscles were cryosectioned into 10 and 20 μm slices which were collected onto glass slides, with the knife set at -22°C and the sample cooled to -10°C .

2.5.3 Muscle Homogenization

Rodents were euthanized by anesthetic overdose. Fresh muscles were dissected out and minced with scissors while left on ice. The minced muscle was weighed and transferred to a glass douncer. Approximately 5 times (ml/g) the muscle weight of extraction buffer (1.25% Triton X-100, 50 mM Tris-HCl pH 7.4, 50 mM NaCl, 1 mM EDTA, 1 mM EGTA) supplemented with the protease inhibitors P3840 (1%) and PMSF (4 mM) was added to the douncer. The muscle was homogenized on ice. Briefly, the douncer was stroked vertically until the solution became cloudy with no large chunks of muscle remaining. The homogenized muscle was left on ice for 30 min. The samples were then cleared by centrifugation for 10 min at 20,800 g at 4°C . The supernatant was subjected to a BCA protein assay according to the manufacturer's protocol and used for immunoblotting or immunoprecipitation studies, as detailed below.

2.6 IMMUNOPRECIPITATION

Detergent extracts of myotubes, COS-7 cells, or skeletal muscles were incubated and rotated at 4°C with the appropriate antibodies (1:250 or 1:500) overnight. No antibody and species-appropriate purified IgGs were used as controls. Protein A Sepharose beads were added and the samples were rotated for 1 hour, after which time the samples were centrifuged at 500 g at 4°C for 5 min. The beads were washed with extraction buffer 3 times. Bound proteins were eluted by heating the beads at 95°C for 5 min in NuPAGE LDS Sample Buffer with NuPAGE Sample Reducing Agent diluted in extraction buffer. Samples were then immunoblotted as detailed below.

2.7 IMMUNOBLOTTING

Western blotting was carried out using standard methods. Briefly, proteins were separated on 4-12% NuPAGE Novex Bis-Tris Pre-Cast gels and electroblotted to nitrocellulose membranes using a Trans-Blot Semi-Dry Transfer Cell (Bio-Rad Laboratories, Hercules, CA). Membranes were blocked for 2 hours at room temperature in 5% milk in Tris-buffered saline (TBS: 20 mM Tris-HCl pH 7.4, 150 mM NaCl). The blots were probed with the indicated primary antibodies (at dilutions ranging from 1:100 for Anti-MuSK to 1:1000 for the other antibodies) diluted in blocking buffer plus 0.1% Tween-20 overnight at 4°C. Post-washing, the blots were then incubated for 1 hour at room temperature in the dark with Alexa Fluor 680 or 800 goat anti-rabbit or anti-mouse IgG (H + L) secondary antibodies diluted 1:40,000 in blocking buffer plus 0.1% Tween-20. Protein bands were revealed by scanning the membranes

on an Odyssey Infrared Imaging System (LI-COR, Lincoln, Nebraska). Some blots were stripped in stripping buffer (0.2 M glycine pH 2.5, 0.05% Tween-20) for 30 min at room temperature, washed, reblocked, and reprobbed with a different antibody. Band intensity was quantified by using ImageJ (National Institutes of Health, Bethesda, MD) software.

2.8 IMMUNOFLUORESCENT STAINING

2.8.1 Slides

Skeletal muscle cryosections were fixed in 4% paraformaldehyde for 5 min, washed with phosphate-buffered saline (PBS) 3 times, permeabilized with 0.3% Triton X-100 in PBS for 5 min, and blocked with 1% bovine serum albumin (BSA) in PBS for 30 min. The slices were stained with a rabbit anti-synaptophysin antibody, 1:1000, or a rabbit anti-tid1 antibody obtained from J.-D. Lee, 1:1000, in 1% BSA in PBS for at least 1 hour at room temperature. Purified rabbit IgG, 2 μ g / 100 μ l, preimmune serum from the rabbit that made the anti-tid1 antibody, 1:1000, and cold α -BTX, 1:500, were used as respective controls. After washing the slices three times with PBS, a secondary antibody mixture containing Alexa-488-conjugated α -BTX, 1:3000, and Cy3-conjugated goat anti-rabbit IgG, diluted 1:2000 in 1% BSA in PBS was added for at least 1 hour at room temperature. During this time, the slices were kept in the dark. The slices were then washed three times with PBS and mounted in a glycerol mixture (4% n-propyl gallate, 86% glycerol, and 10% PBS). The slices were viewed with a Nikon E600 upright epifluorescence microscope and photographed with a cooled CCD camera. Area of labeling was quantified using ImageJ (National Institutes of Health, Bethesda, MD) software.

2.8.2 Cell Culture

C2C12 myoblasts were grown in 35 mm culture dishes and differentiated into myotubes as described above. COS-7 cells were grown in 35 mm culture dishes as detailed in section 2.4.2. The media was removed and myotubes were fixed in 4% paraformaldehyde for 5 min. The cells were washed with PBS 3 times and were either blocked in 5% BSA in PBS (for DsRed and AChR visualization) or blocked and permeabilized in 5% BSA in 0.3% Triton X-100 in PBS (for anti-myc or anti-tid1 staining) for 20 min. They were then stained with the indicated antibodies in 5% BSA +/- 0.3% Triton X-100 in PBS overnight at 4° C. The concentrations used were as follows: rabbit anti-tid1 antibody obtained from J.-D. Lee, 1:1000, mouse anti-myc antibody (mAb9E10), 1:1000, and rat anti-AChR antibody (mAb35), 1:1000. Species-appropriate sera and preimmune sera were used as controls. The cells were washed 3 times with PBS. Alexa Fluor-conjugated α -BTX (Rhodamine and 633, 1:3000) and species-appropriate Cy2 or Cy3-conjugated secondary antibodies were added at a dilution of 1:1000 into 5% BSA +/- 0.3% Triton X-100 in PBS for 2 hours in the dark at room temperature. The cells were washed 3 times with PBS and left in fresh PBS for visualization. The cells were viewed either under an epifluorescence or under an Olympus Fluoview-1000 confocal microscope with 3 non-overlapping laser lines and were photographed with a cooled CCD camera.

2.9 QUANTIFICATION OF AChR CLUSTERS

Spontaneously and agrin-induced AChR clusters in C2C12 myotubes were quantified as described by Jacobson, et al. (1998). Briefly, myotubes were viewed at 400X with a Nikon E600

epifluorescent microscope. Ten random fields in each culture dish were chosen and for each myotube analyzed, the number of clusters greater than 2 μm in diameter was counted and divided by the area of the myotube segment (length of myotube (mm) X width of myotube (mm)). Results are expressed as the average number of clusters per mm^2 myotube surface area +/- standard error of the mean (S.E.M.) for each treatment group.

2.10 RADIOLIGAND BINDING ASSAY

Surface expression of AChRs was determined by incubating living C2C12 myotubes for 90 min with 5 nM ^{125}I - α -BTX in growth medium (Wang et al., 2003). Nonspecific binding was measured by pre-incubation with an excess amount of unlabeled α -BTX (500 nM). After washing the cells with PBS three times to remove the excess α -BTX, the bound ^{125}I - α -BTX was measured by solubilizing the cells in 0.2M NaOH and counting the radioactivity in a gamma counter.

2.11 RNA INTERFERENCE

2.11.1 *In vitro*

The design of a *tid1*-specific shRNA was aided by an online software package found at www.ambion.com. The sequence, which targets base pairs 347-361 of mouse *tid1* and is flanked by BamHI and HindIII overhangs, was GATCCAGATGATTATTACCAGATCTTCAAGAGA

GATCTGGTAATAATCATCTTTA (sense) and AGCTTAAAGATGATTATTACCAGATCTCTCTTGAAGATCTGGTAATAATCATCTG (antisense). The two oligonucleotides were annealed and subcloned into BamHI and HindIII sites in the RNAi vector, pSIREN-DNR-DsRed-Express (Clontech). Before the subcloning, the HindIII site, located immediately after the EcoRI site, was added to the vector by site-directed mutagenesis using the Quik-Change XL Site-Directed Mutagenesis Kit. A pSIREN vector containing a scrambled shRNA sequence was used as a control. The shRNA-containing plasmids were transfected into C2C12 myoblasts with Effectene. At ~24 h after transfection, the cells were switched to grow in fusion medium for another 72 hours. Myotubes were fixed in 2% paraformaldehyde and processed for immunofluorescent staining, as detailed above.

2.11.1.1 Rescue

For the rescue experiments, two nucleotides in the shRNA-targeted region of human *tid1* cDNA were changed by silent mutation. The final sequence of this region was AAGA**AGACTATTAT**CAGATA (silent mutations shown in bold). In addition to the mutations made, three other nucleotides (underlined) in this region of human *tid1* were also different from those in the mouse *tid1* cDNA. Thus, the human *tid1* sequence was not targeted by the mouse-specific shRNA. A *Sma*I site was added immediately before the DsRed sequence in the pSIREN vector by site-directed mutagenesis using the Quik-Change XL Site-Directed Mutagenesis Kit. cDNAs encoding human *tid1* short or the N-terminal domain of human *tid1* with the silent mutations, as well as the corresponding H121Q DnaJ domain mutants (provided by K. Munger), were subcloned into the *Sma*I site. As a result, human *tid1* (*htid1*) and DsRed were expressed as a fusion protein. The pSIREN construct used was that which contained the mouse *tid1* (*mtid1*)-

specific shRNA, described above. Thus, the rescue constructs co-expressed the htid1/DsRed fusion protein and the mtid1-specific shRNA.

2.11.2 *In Vivo*

In vivo RNA Interference was performed as described by Kong et al. (2004) and Sadasivam et al. (2005). Briefly, the pSIREN vector expressing mouse tid1-specific shRNA was injected into the TA muscles of four adult C57/BL6 mice (5 µg DNA in 30 µl 0.9% NaCl). A vector encoding the scrambled shRNA was injected into the muscles of three other mice as a control. Electroporation was performed on the hindlimbs immediately after DNA injection with an ECM 830 electroporator (BTX Inc., San Diego, CA). Eight pulses, each lasting for 20 ms, were applied at a frequency of 1 Hz and voltage of 200 V/cm. Six weeks after electroporation, the animals were perfused with 2% paraformaldehyde and the electroporated muscles were dissected and stained with Alexa Fluor 488-conjugated α -BTX (1:3000) and the rabbit anti-tid1 antibody (1:500) followed by an Alexa Fluor 633-conjugated goat anti-rabbit secondary antibody (1:1000). Fluorescent images were acquired by using an Olympus FluoView-1000 confocal microscope with three non-overlapping laser lines.

2.12 ELECTROPHYSIOLOGY

The soleus muscle and its neural branch were dissected from mice anaesthetized with sodium pentobarbital (65 mg/kg), pinned out in a Sylgard-coated Petri dish and continuously superfused with bubbled Krebs's solution (95% O₂ and 5% CO₂). To record full-size endplate

potentials (EPPs), muscle action potential and contraction was blocked by inclusion in the buffer of 2.5 mM m-conotoxin GIIIB (Alomone laboratories, Jerusalem, Israel). The miniature endplate potentials (MEPPs) and EPPs were recorded intracellularly with borosilicate glass electrodes filled with 3M KCl (10–15 M Ω resistance) at room temperature (20–22 $^{\circ}$ C) via an Axoclamp-2A amplifier (Axon Instruments, Union City, CA, USA). Impalement adjacent to an endplate was indicated by a fast EPP rise time of < 2 ms. To evoke an EPP, the nerve was stimulated supramaximally with a platinum wire suction electrode coupled to a pulse generator (A310 Accupulser and A360 stimulus isolator, WPI Inc., Sarasota, Florida). Upon impalement, a 30s period of equilibration was allowed before MEPP recordings were begun. The analog signal was converted to digital at 10 kHz sampling frequency using Digidata 1400 and acquired with the pClamp 10 program (Molecular Device, Union City, CA). Up to 30 MEPPs followed by up to 30 EPPs (stimulated at 1 Hz) were recorded per endplate for offline analysis later.

2.13 STATISTICAL ANALYSIS

For normalization of NMJ size data (Figure 15A), the following error calculation was used: if f and g are two independent means and f(e) and g(e) are their respective errors, then the error for f/g is $(f(e)*g - g(e)*f) / g^2$. Data was analyzed using Origin 6.0. Statistically-significant differences between two groups were determined by two-way Student's T-tests for independent populations. Differences between multiple groups were analyzed by one-way ANOVA. A p value less than 0.05 was considered statistically significant.

3.0 RESULTS

3.1 IDENTIFICATION OF TID1 AS A MUSK-BINDING PROTEIN

To identify proteins that may interact with MuSK, I carried out a bacterial two-hybrid screen using the cytoplasmic domain of mouse MuSK as bait and a cDNA library of day E19 rat skeletal muscle as target (Joung, et al., 2000; Also see Figure 6). *Tumorous imaginal discs* (tid1), a rat homologue of the *Drosophila* tumor suppressor tid56 and heat shock protein (hsp) 40, was the only molecule that was found in the screen to show a robust, specific, and reproducible interaction with MuSK. Both rat tid1 and mouse MuSK are highly homologous to their human counterparts. Tid1 appeared twice in the initial screen of $\sim 10^7$ cDNA clones using the entire cytoplasmic domain (amino acid residues 515-869) of MuSK as bait. The screen was also performed using the juxtamembrane region (residues 515-692) of the MuSK cytoplasmic domain, a segment that contains a tyrosine phosphorylation site required for agrin-induced AChR clustering (Herbst and Burden, 2000; Watty et al., 2000). With this shorter bait, overlapping clones of tid1 cDNA appeared six times in the assay, confirming the initial screening results that discovered tid1 as a MuSK-binding protein (Figure 7, Figure 8A). As can be seen from Figure 7, all of the isolated clones demonstrated strong growth on dual selective plates upon retransformation into reporter cells with the respective MuSK bait. Indeed, 3 clones grew even more robustly than the positive control pBT/pTRG pair.

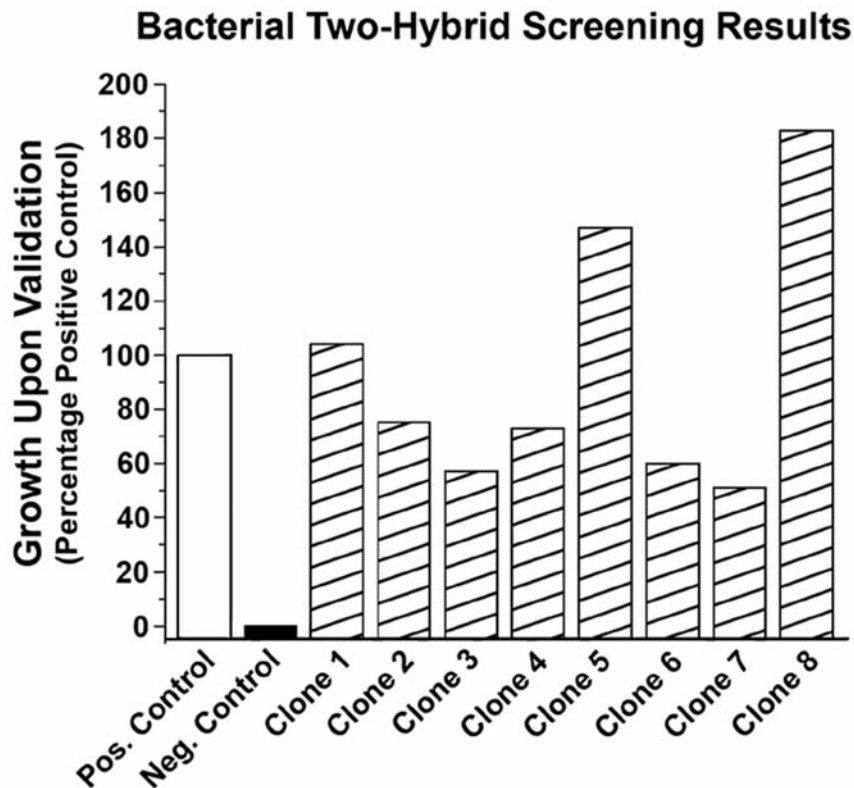
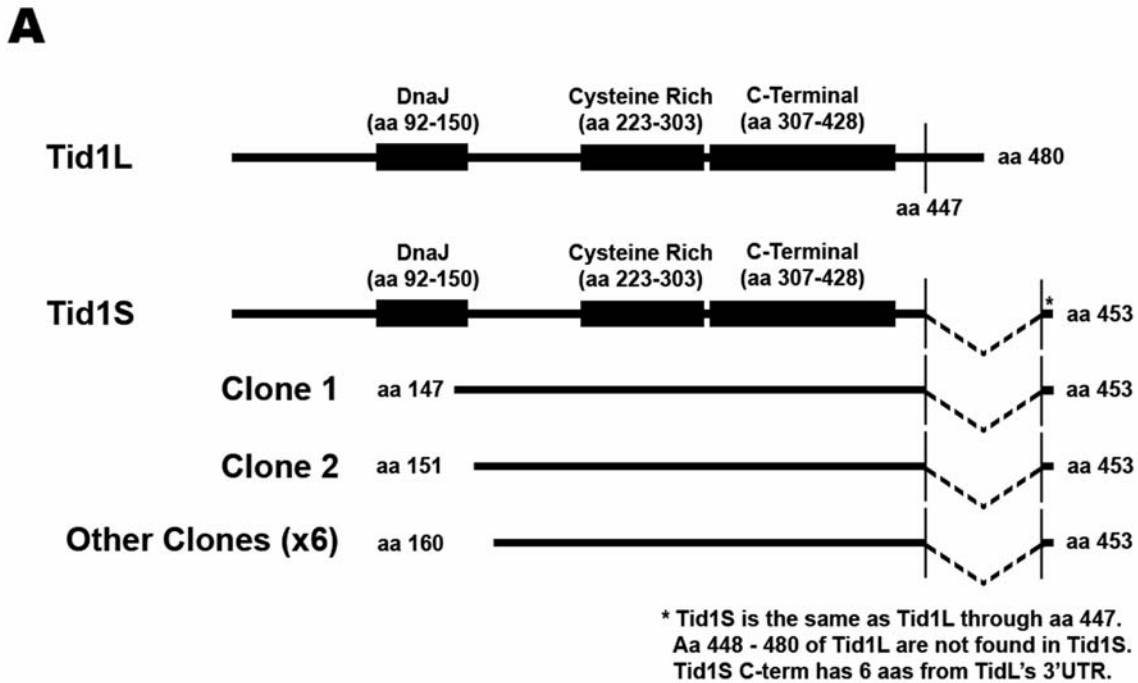


Figure 7. Validation results for bacterial two-hybrid screens

Results of the bacterial two-hybrid screening were validated by growth on dual selective plates and normalized against the number of colonies grown on positive control plates (pBT-LGF2 as bait and pTRG-gal11p as target). Empty pBT and pTRG were used as negative controls. Eight clones from the rat cDNA library were found to interact strongly with the MuSK bait, two (Clones 3, 4) with the full cytoplasmic region of MuSK (aa. 515-869) and six (Clones 1, 2, 5-8) with the juxtamembrane region of MuSK (aa. 515-692). The clones correspond with those pictured in Figure 8A.

Tid1 is known to have two alternatively spliced forms, “tid1 short” and “tid1 long”, which differ only in the last 33 amino acid residues at their C-termini (Syken et al., 1999; also see Figure 8A, B). Interestingly, the bacterial two-hybrid screens only pulled out the short isoform of tid1 as a MuSK-binding partner. None of the isolated clones were full-length tid1 short. Each of the validated clones contained the well-characterized cysteine rich and C-terminal

regions of tid1, although they lacked the DnaJ domain of tid1, known to be important for binding to tid1's co-chaperone, hsp70.



B

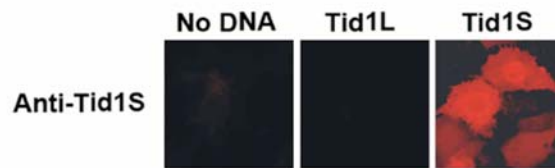


Figure 8. Bacterial two-hybrid screens identify tid1 short as a MuSK binding protein.

(A) Schematic representations of the full-length long and short isoforms of tid1 protein and the eight overlapping clones of tid1 short identified in the bacterial two-hybrid screens. The clone numbers correspond to those pictured in Figure 7. Clones 1 and 2 were isolated from the screen which used the juxtamembrane of MuSK (aa. 515-692) as bait. The others were isolated from both screens. (B) Alignment of amino acid residues in the C-termini of human tid1 long and tid1 short. Residues 1-447 of the two isoforms are identical (not shown). Modified from Syken et al., 1999.

Knowing that only tid1 short was identified as a MuSK binding protein, a tid1 short-specific polyclonal antibody was generated by immunizing a rabbit with a synthetic peptide corresponding to the last 20 residues in the C-terminus of mouse tid1 short. Mouse tid1 short was chosen as opposed to another species, as the main model systems used in this research were C2C12 myotubes, derived from embryonic mouse skeletal muscle, and C57/BL6 mice. The antibody was purified on an immunoaffinity column against the peptide and it was tested on transfected COS-7 cells, which express a low level of endogenous tid1 short and tid1 long. As is demonstrated in Figure 9, the antibody specifically and strongly recognizes tid1 short, both via immunostaining and immunoblotting.

A. Immunostaining



B. Immunoblotting

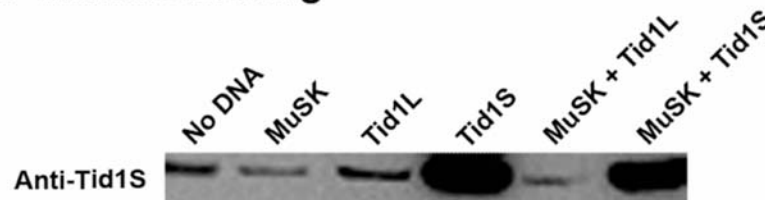


Figure 9. Specificity of the rabbit polyclonal antibody against tid1 short.

(A) The peptide antibody labels COS-7 cells transfected with a plasmid cDNA encoding human tid1 short (Tid1S) strongly. Labeling of endogenous tid1 in untransfected control cells (No DNA) or tid1 long-transfected cells (Tid1L) is not evident. (B) COS-7 cells were transfected with plasmid cDNAs as indicated. Detergent extracts of the cells were Western blotted and probed with the antibody. The antibody reveals a strong band in lanes loaded with lysates of COS-7 cells transfected with human tid1 short cDNA. COS-7 cells contain low levels of endogenous tid1 protein that can be detected as a faint band by the tid1 short-specific antibody.

3.2 CONFIRMATION OF TID1 AND MUSK BINDING

To determine whether MuSK interacts with tid1 in skeletal muscle cells, detergent-extracts of C2C12 myotubes were immunoprecipitated with a polyclonal antibody against MuSK (Sugiyama et al., 1997; Fuhrer et al., 1997). The precipitates were immunoblotted with a monoclonal antibody that recognizes both the short and long isoforms of tid1 (anti-pan tid1). A band of ~40 KDa, corresponding to tid1 short (453 residues), was detected on the immunoblots (Figure 10A, lane 3). This result is highly specific, as the band did not appear on the membrane when myotube extracts were immunoprecipitated with normal goat, rabbit, or mouse immunoglobulins (IgGs), or with Protein-A Sepharose beads in the absence of the primary antibody (Figure 10A, lanes 1, 6-8). Little, if any, long isoform of tid1 was detected in the precipitates that were pulled down by the anti-MuSK antibody (compare Figure 10A, lane 3, with lanes 2, 4, and 5, which were immunoprecipitated with antibodies against tid1 long, tid1 short, and pan tid1, respectively). To confirm the data, another experiment was carried out in which a polyclonal antibody specific for the short form of tid1 (Figure 9) was used for immunoprecipitation and the MuSK antibody was then employed for immunoblotting. As illustrated in Figure 10B, MuSK was immunoprecipitated by the tid1 short-specific antibody (lane 2), but not by Protein-A Sepharose beads (lane 3) or normal rabbit IgGs (lane 4). Thus, MuSK and tid1 short immunoprecipitate one another from C2C12 myotube lysates.

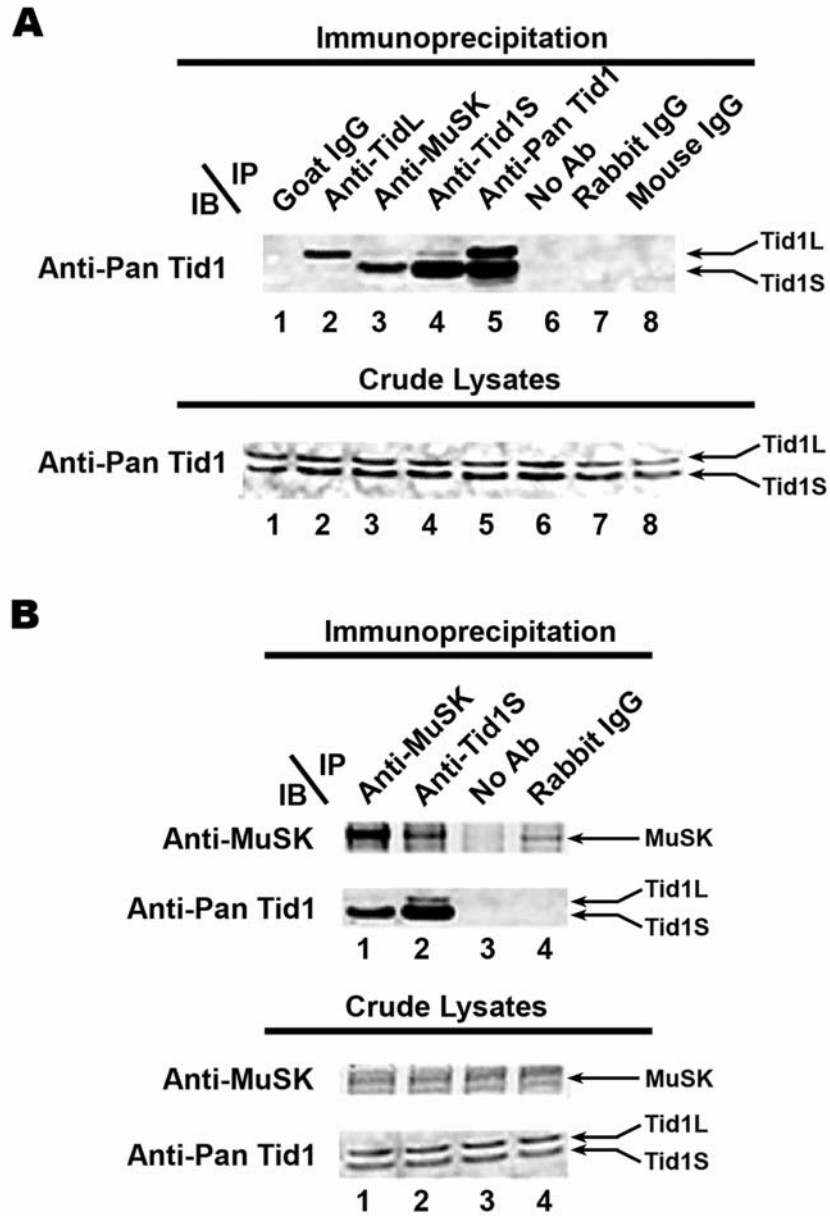


Figure 10. Tid1 short and MuSK co-immunoprecipitate one another from myotubes.

(A) Top panel: Lysates of C2C12 myotubes were immunoprecipitated (IP) with specific antibodies as indicated (lanes 2 – 5), Protein-A Sepharose beads without an antibody (lane 6), or control IgGs (lanes 1 and 7-8). mAb RS-13 (Anti-Pan Tid1), a mouse anti-tid1 antibody that recognizes both tid1 long and short, was used for immunoblotting (IB). Bottom panel: Crude lysates corresponding to each of the lanes in the top panel were immunoblotted with mAb RS-13 to show that tid1 protein was present in each of the samples. (B) Top panel: Lysates of C2C12 myotubes were immunoprecipitated (IP) with specific antibodies as indicated (lanes 1 and 2), Protein-A Sepharose beads without an antibody (lane 3), or purified rabbit IgGs (lane 4). A polyclonal antibody against MuSK or mAb RS-13 was used for immunoblotting. Bottom panel: Crude lysates corresponding to each of the lanes in the top panel were immunoblotted with Anti-MuSK or mAb RS-13 to show that approximately equal amounts of MuSK and tid1 proteins were present in each of the samples.

The “pull-down” assays were also performed with detergent extracts of the *tibialis anterior* (TA) muscle from adult rats. The MuSK-specific antibody resulted in a robust and specific co-precipitation of the short form of tid1 (Figure 11, lane 1). Thus, consistent with the results of the bacterial two-hybrid screens, biochemical studies unequivocally demonstrate that MuSK exclusively interacts with the short form of tid1 in myotubes and skeletal muscles.

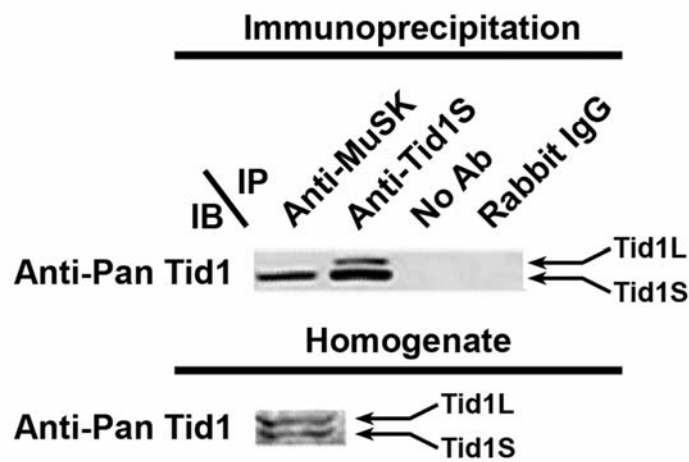


Figure 11. MuSK co-immunoprecipitates tid1 short from rodent skeletal muscle. Detergent extracts of adult rat tibialis anterior muscle were immunoprecipitated and immunoblotted as in Figure 10.

3.3 TID1 COLOCALIZES WITH AChRS ON THE POSTSYNAPTIC MEMBRANE OF THE NMJ

To examine the tissue distribution of tid1 in skeletal muscle, frozen sections of adult mouse soleus muscle were double-stained with Alexa Fluor 488-conjugated α -bungarotoxin (BTX) to label AChRs and with a tid1-specific polyclonal antibody followed by Cy3-conjugated

goat-anti-rabbit IgG to label tid1 (Figure 12, A-C). Some cryosections were stained with a polyclonal antibody against synaptophysin to reveal motor axons and Alexa Fluor 488-conjugated α -BTX to show AChRs (Figure 12, J-L). A striking colocalization of tid1 and AChRs was observed in the endplate region of normal mouse muscle (Figure 12, A-C). This pattern of tid1 distribution was consistently observed in the soleus muscles of animals ranging in age from E20 to P14 to 4 months (data not shown). The specificity of the immunofluorescent staining was confirmed by the lack of labeling of muscle sections reacted with a pre-immune serum or rabbit IgGs, or pre-incubated with unlabeled, “cold” α -BTX prior to staining with Alexa Fluor 488-conjugated α -BTX (Figure 12, D-I, M-R). To determine whether tid1 is localized to the presynaptic motoneuron or to the postsynaptic muscle fiber of the NMJ, the sciatic nerve, which innervates hindlimb muscles, of an adult mouse was transected and the nerve was allowed to degenerate for eight days. Cryosections were then prepared from denervated soleus muscles and incubated with antibodies against tid1, AChR, and synaptophysin. As illustrated in Figure 13 (a-c), the precise colocalization of tid1 and AChR was maintained in the muscle sections. In contrast, synaptophysin immunoreactivity was abolished, indicating that the presynaptic nerve termini had degenerated completely after sciatic nerve transection (Figure 13, j, m).

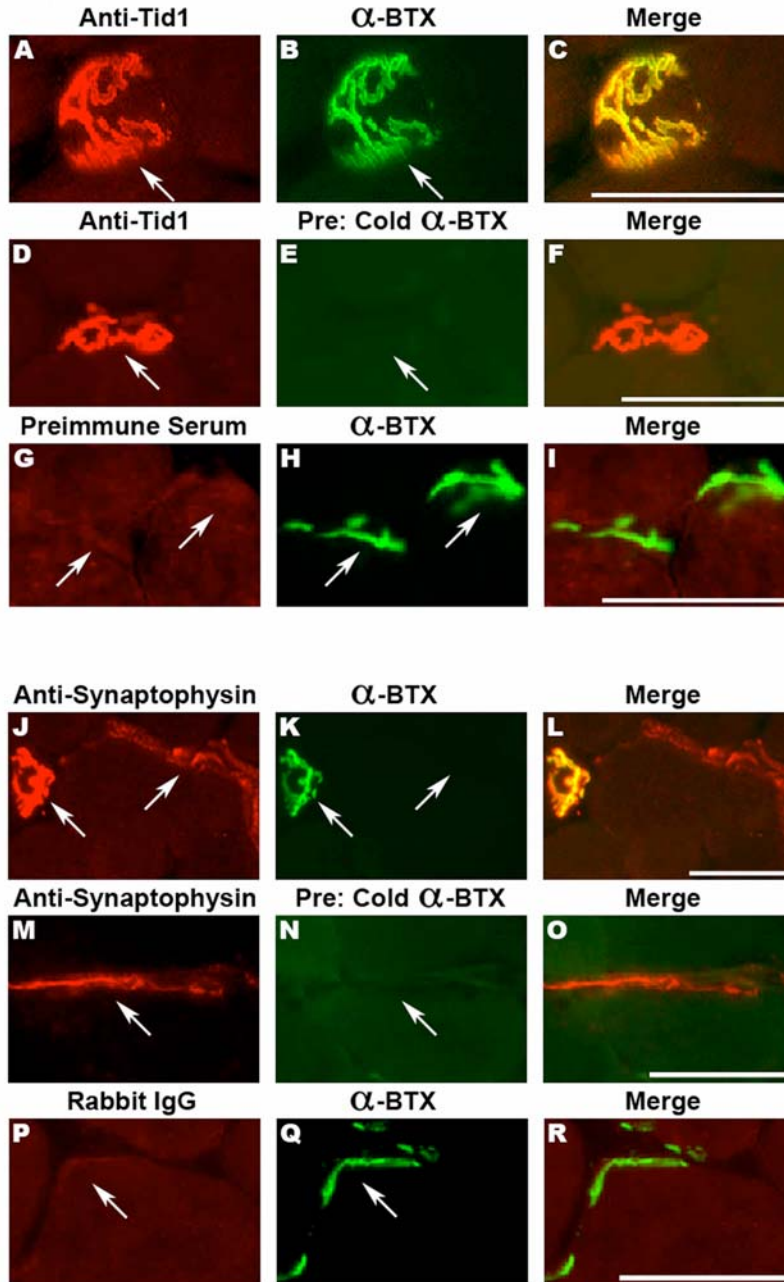


Figure 12. Tid1 and AChRs colocalize at innervated mouse NMJs.

The right sciatic nerve of an adult mouse was transected under anesthesia. Eight days after denervation, the contralateral (innervated) soleus muscle was dissected, cryosectioned, fixed and stained with a rabbit polyclonal antibody against tid1 (A, D), Alexa Fluor 488-conjugated α -BTX (B, H, K, Q), Alexa Fluor 488-conjugated α -BTX in the presence of excess unlabeled α -BTX (E, N), preimmune serum from the rabbit that was used to make the tid1 antibody (G) or rabbit IgGs (P). In J and M, a rabbit polyclonal antibody against synaptophysin was used to stain the motor axons. The red and green fluorescent channels were combined in C, F, I, L, O, R. Arrows highlight areas of interest. Scale bar = 25 μ m.

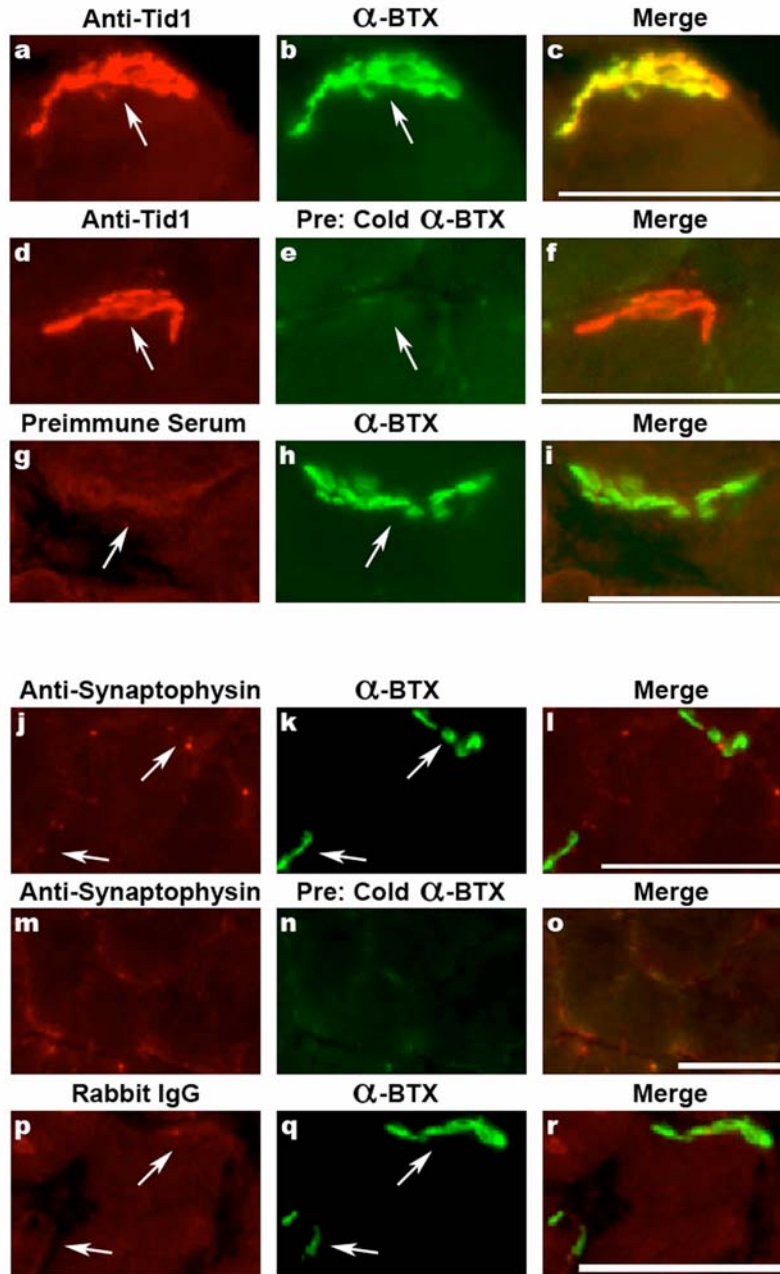


Figure 13. Tid1 and AChRs remain colocalized at denervated mouse NMJs.

The right sciatic nerve of an adult mouse was transected under anesthesia. Eight days after denervation, the ipsilateral (denervated) soleus muscle was dissected, cryosectioned, fixed and stained with a rabbit polyclonal antibody against tid1 (a, d), Alexa Fluor 488-conjugated α -BTX (b, h, k, q), Alexa Fluor 488-conjugated α -BTX in the presence of excess unlabeled α -BTX (e, n), preimmune serum from the rabbit that was used to make the tid1 antibody (g) or rabbit IgGs (p). In j and m, a rabbit polyclonal antibody against synaptophysin was used to stain the cryosections. The red and green fluorescent channels were combined in c, f, i, l, o, r. Arrows highlight areas of interest, especially the lack of synaptophysin labeling. Scale bar = 25 μ m.

Once again, the specificity of the staining was demonstrated by the lack of immunoreactivity when cryosections were incubated with pre-immune serum or rabbit IgG or pre-incubated with unlabelled α -BTX (Figure 13, d-i, m-r). Taken together, it is concluded that tid1 is confined primarily to the postsynaptic membrane of the mouse NMJ.

3.4 CHRONIC DENERVATION DISPERSES TID1 AND AChRS FROM THE NMJ

Long-term denervation causes disassembly of the postsynaptic apparatus at the NMJ, as reflected by the gradual loss of synaptic proteins from the endplate membrane. By 8 weeks post sciatic nerve transection, AChR binding sites at mouse motor endplates decrease by 60-70% (Frank et al., 1976). To investigate the role of innervation on tid1 localization, a short segment (~5 mm) of the main trunk of the sciatic nerve in the right hindlimb of an adult mouse was removed. Eight weeks later, cryosections of control (left leg) and denervated soleus muscles were prepared and immunostained with a mixture of the tid1 antibody and Alexa Fluor 488- α -BTX, or the synaptophysin antibody and Alexa Fluor 488- α -BTX (Figure 14, A-C). For semi-quantitative analysis, the stained sections were photographed, and the areas of individual AChR clusters were measured (Figure 15A).

In cross-sections of control muscle with intact innervation (Innervated), motor axons were readily visible by fluorescent staining of synaptophysin (Figure 14A, d). Intense immunofluorescence of tid1 was found and it was coextensive with AChR clusters, as defined by Alexa Fluor 488- α -BTX staining (Figure 14A ,a-c; Figure 15A). Semi-quantitative analysis

demonstrated that ~98% of the mean area of the AChR clusters was also positively stained by the anti-tid1 antibody (Figure 15, A, B). In sections of soleus muscles with sciatic nerve transection (Denervated), synaptophysin immunoreactivity was totally absent, indicating the motor axons had degenerated completely (Figure 14B, g). On the postsynaptic side of the NMJ, there was a significant reduction in the intensity of Alexa Fluor 488- α -BTX staining (Figure 14B, b, e, h). Moreover, the receptor clusters became fragmented with blurring edges. The mean size of individual AChR clusters decreased to 33% of that of the control muscle with innervation (Figure 15A, $p < 0.01$). In the denervated muscle, tid1 remained colocalized with the AChR. However, there was a significant reduction in the intensity of tid1 immunofluorescence (Figure 14B, a, d). The average size of individual clusters defined by tid1 staining decreased to 18% of that in the control muscle sections (Figure 15A, $p < 0.01$). The mean overlap of tid1 cluster size against that of AChR clusters dropped from 98% in control to 58% in denervated muscle (Figure 15B, $p < 0.01$). Hence, there was a more striking reduction in the size of tid1 clusters than in the size of receptor clusters. These data suggest that dispersal of tid1 from the NMJ preceded that of AChRs following denervation. Alternatively, tid1 may diffuse away from denervated endplates at a faster rate than AChRs.

In one animal, it was found that a minor branch of the sciatic nerve which was transected eight weeks prior had grown back to the soleus muscle and had re-innervated a small group of myofibers on the cross-sections (Reinnervated). In this region, synaptophysin immunoreactivity was restored. Similarly, tid1 and AChR staining also recovered to near-normal levels (Figure 14C; Figure 15).

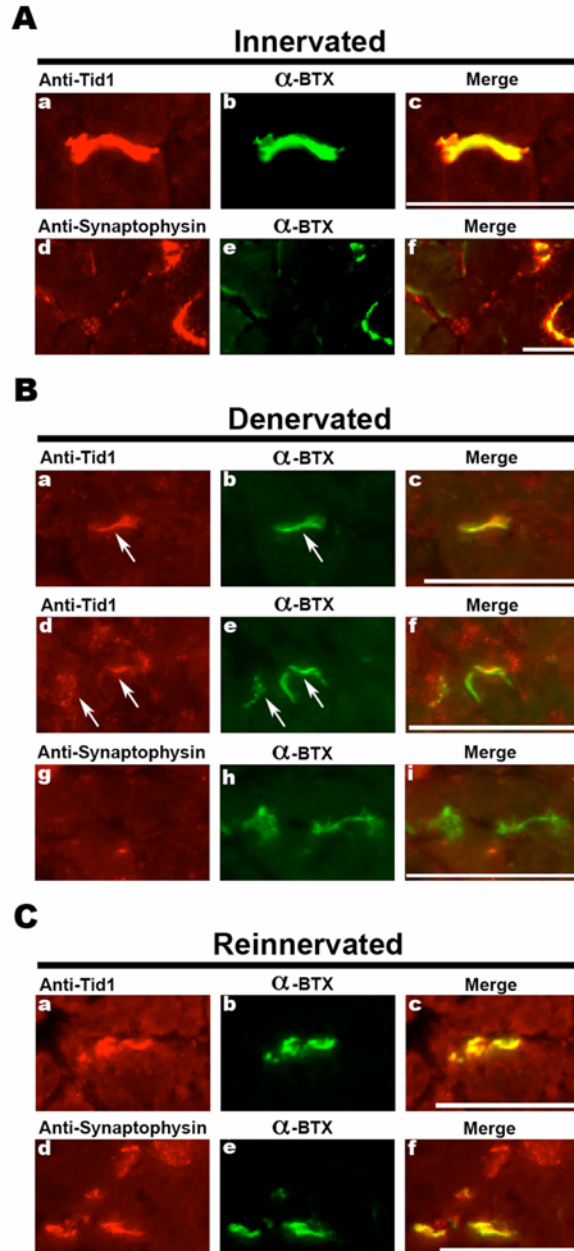


Figure 14. Dispersal of tid1 from motor endplates in chronically denervated muscles.

The right sciatic nerve of an adult mouse was transected under anesthesia. Seven and a half weeks after denervation, the ipsilateral (denervated) and contralateral (innervated) soleus muscles were dissected, cryosectioned, fixed, and stained with a rabbit polyclonal antibody against tid1 or a rabbit polyclonal antibody against synaptophysin, and Alexa Fluor 488-conjugated α -BTX. A TRITC-conjugated goat anti-rabbit IgG was used as a secondary antibody. (A) Tid1 (a) and AChRs (b) are colocalized in motor endplates on sections from the control muscle with normal innervation. Axonal terminals are clearly visible in sections stained with anti-synaptophysin (d). (B) In the denervated muscle, fluorescent staining of tid1 (a, d) and AChRs (b, e) is significantly reduced (arrows). Motor axons are absent in the sections as shown by the lack of anti-synaptophysin staining (g). (C) Staining of tid1, AChRs, and synaptophysin is restored in a small region of the muscle with re-innervation. Scale bar = 25 μ m in (A) – (C).

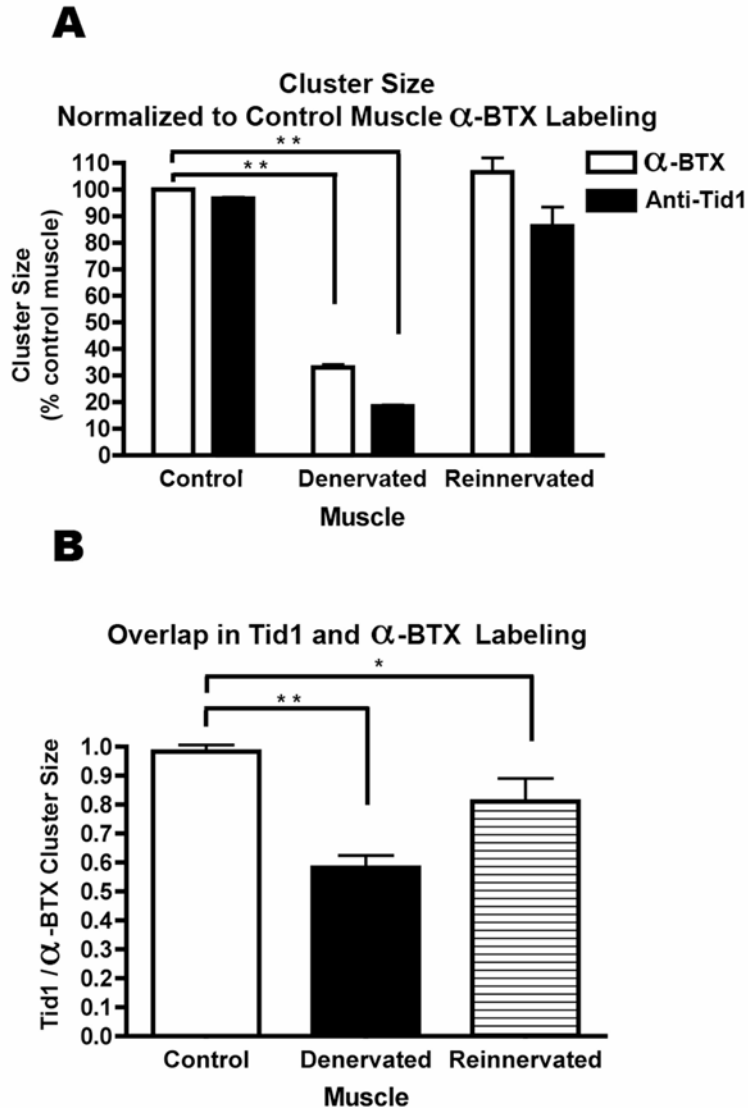


Figure 15. Quantification of *tid1* and AChR cluster size in chronically-denervated muscle. (A) A comparison of endplate size as defined by area of α -BTX or *tid1* staining in control, denervated, and reinnervated muscles. The size (area) of an individual endplate stained on the cross-sections was quantified by using NIH ImageJ software. The mean of each group was normalized to the mean area of α -BTX staining in control muscle. The error of this ratio was calculated as detailed in Experimental Procedures. (B) The ratio (overlap) of endplate size defined by anti-*tid1* stain against that defined by α -BTX stain. Data is expressed as mean \pm S.E.M. Data in (A) and (B) were analyzed by two-tailed Student's t-tests. *, $P < 0.01$; **, $P < 0.001$. $n = 24$ for control, 17 for denervated, and 9 for reinnervated groups, respectively.

3.5 NEURAL AGRIN INDUCES CO-CLUSTERING OF TID1 AND AChRS IN C2C12 MYOTUBES

In cultured myotubes, AChRs are normally distributed uniformly along the entire muscle cell surface. Co-culture with motor neurons, or treatment of myotubes with recombinant neural agrin, induces the aggregation of AChRs into high-density clusters resembling those on the postsynaptic membranes of NMJs (Christian et al., 1978; Ferns et al., 1992). We investigated whether tid1 on the surface of myotubes would redistribute like AChRs in response to agrin. In the absence of agrin, tid1 immunofluorescence was localized in the cytoplasm, mitochondria, and at the sparse spontaneous AChR clusters found on untreated myotubes (Figure 16A, a-c). However, in myotubes treated with recombinant neural agrin (CAg_{12,4,8}) (Ferns et al., 1992), tid1 was redistributed to the cell surface, where it co-aggregated robustly with AChRs (Figure 16A, g-i). In contrast, recombinant muscle agrin (CAg_{12,0,0}), an alternatively spliced isoform which has little AChR-clustering activity, failed to cause aggregation of tid1 above basal levels (Figure 16A, d-f). The specificities of tid1 and AChR staining in these experiments were demonstrated in Figure 16B by the complete absence of immunofluorescence in cultures that were incubated with a preimmune rabbit serum (control for anti-tid1) or with rat serum (control for anti-AChR). Thus, like the well-studied postsynaptic proteins rapsyn and MuSK, tid1 can redistribute and co-cluster with AChRs on the muscle cell membrane in response to stimulation by neural agrin.

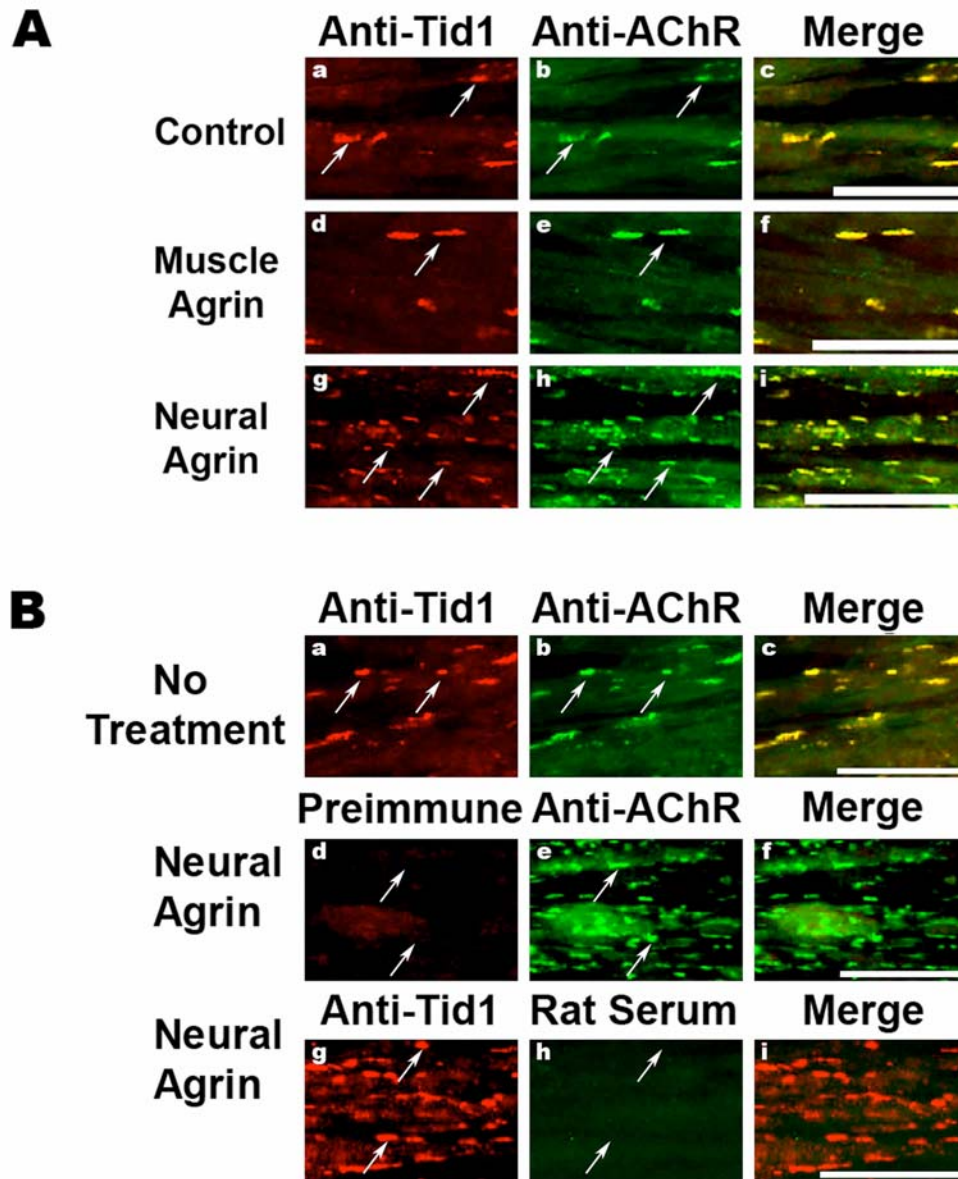


Figure 16. Neural agrin induces tid1 and AChR co-clustering.

(A) C2C12 myotubes were incubated with control conditioned medium, muscle agrin, or neural agrin for 4 h, fixed, and double-stained with a rabbit polyclonal antibody against tid1 and mAb35, a rat monoclonal antibody against AChR. Cy3-conjugated goat anti-rabbit and Cy2-conjugated goat anti-rat IgGs were used as secondary antibodies. Scale bar = 25 μ m. Arrows highlight AChR clusters. (B) C2C12 myotubes were incubated with or without neural agrin for 4 h and stained as in (A) for a-c. A preimmune rabbit serum (d) and normal rat serum (h) were used as negative controls for tid1 and AChR staining, respectively.

3.6 THE N-TERMINAL DOMAIN OF TID1 ENHANCES AChR CLUSTERING AND EXPRESSION

The protein sequence of *tid1* contains three well-characterized domains: a DnaJ domain (aa. 92–150), a cysteine-rich region (aa. 223–303), and a C-terminal domain (aa. 307–428, Figure 17). To examine the role of these domains in AChR clustering, a set of truncated fragments of the short form of rat *tid1* that lacked some or all of these domains was created (Figure 17). An epitope tag consisting of 6 copies of the c-myc sequence was fused in-frame to the N-terminus of each of the truncated fragments.

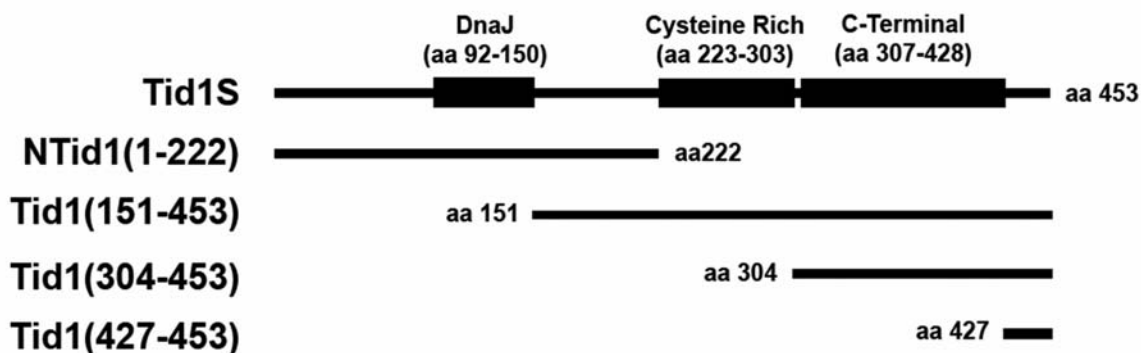


Figure 17. Schematic diagram of *tid1* fragments utilized for exploring domain function. Schematic diagram of the full-length and four truncated fragments of rat *tid1* short used for studies into the role(s) of the various domains of *tid1* in AChR clustering.

Plasmid cDNAs encoding the tagged constructs were each introduced into C2C12 myoblasts by transient transfection. Three to four days post-transfection, either a control conditioned medium or a conditioned medium that contains neural agrin ($C_{12, 4, 8}$) was added to myotubes formed in the culture dish. After incubation for 4 h, the myotubes were fixed, permeabilized, and stained with an anti-myc antibody (9E10) to reveal the expressed *tid1* constructs and with Rhodamine- α -BTX to label AChRs. As shown in Figure 18, neither the full-length *tid1* short (Tid1S), nor any of the constructs that lack the DnaJ domain, had a significant effect on the number and size of spontaneous AChR clusters and on the formation of AChR clusters in response to stimulation by agrin. In contrast, the N-terminal half of *tid1* (NTid1(1–222)), which contains the DnaJ domain, induced robust clustering of AChRs independently of agrin stimulation (Figure 18, VII-IX; Figure 19A). Thus, the N-terminal half of *tid1*, which contains the DnaJ domain, is capable of inducing AChR clustering in the absence of other parts of the protein. However, the clusters induced by the transfection of NTid1(1-222) were relatively smaller than those induced by neural agrin. They were similar to receptor micro-clusters that usually form in the early phase of AChR clustering following agrin stimulation (Weston et al., 2003).

Stimulation with neural agrin resulted in the formation of numerous AChR clusters in sham transfected C2C12 myotubes (Figure 18, i-iii). Transfection with NTid1(1-222) led to a slight, but statistically significant ($p < 0.05$), increase in the number of agrin-induced clusters on the myotube surface (Figure 19A). In addition, there was also an increase in the size of receptor clusters in cells that expressed NTid1(1-222) (data not shown). Transfection with the full-length *tid1* short or other truncated fragments, however, did not exert a detectable effect on AChR clustering induced by neural agrin.

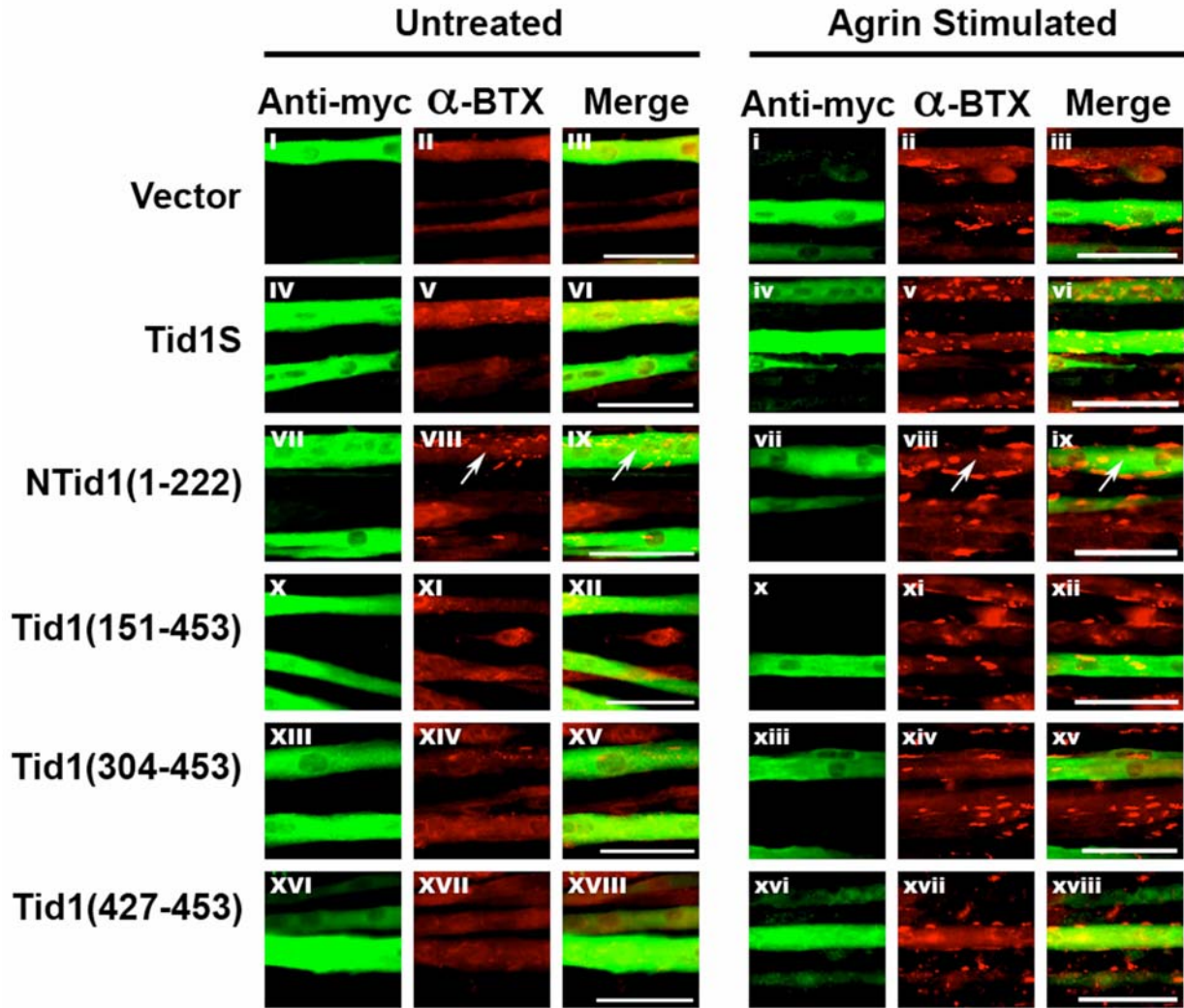


Figure 18. The N-terminal half of *tid1* induces AChR clustering.

C2C12 myoblasts were transfected with the control plasmid pCS2+MT, which expresses only 6 myc tags (Vector), or each of the plasmid cDNAs encoding myc-tagged full-length *tid1* short (Tid1S), the myc-tagged N-terminal half of *tid1* (NTid1(1-222)), or various myc-tagged C-terminal fragments of *tid1* short. At ~72 h after transfection, myotubes were either left untreated or treated with neural agrin for 4 h. They were then fixed and double-stained with Rhodamine-conjugated α -BTX and the anti-myc antibody mAb9E10 followed by FITC-conjugated goat anti-mouse IgG. Arrows highlight some of the cells transfected by *tid1* constructs. Scale bar = 100 μ m.

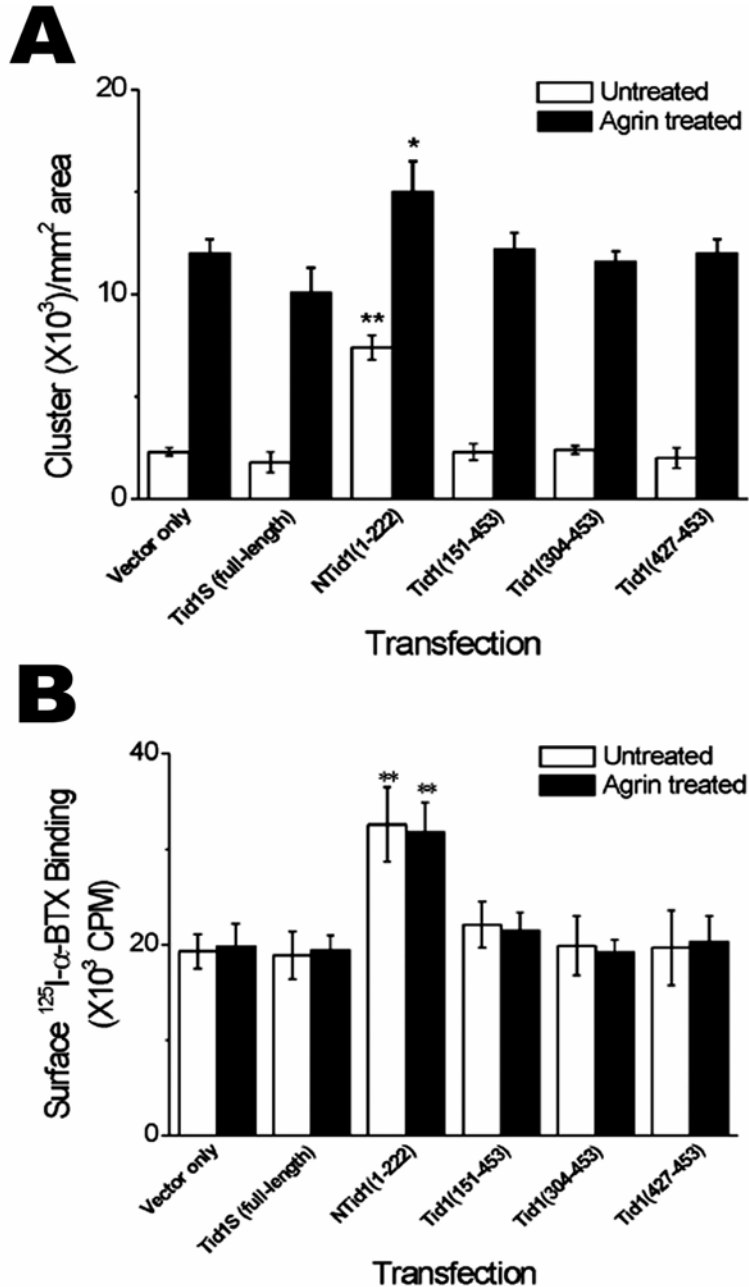


Figure 19. The N-terminal half of *tid1* induces AChR clustering and expression.

(A) A semi-quantitative analysis of the effects of the full-length and truncated fragments of *tid1* short on the number of spontaneous and agrin-induced AChR clusters on cultured myotubes. (B) The levels of AChR protein expressed on the surface of myotubes transfected with *tid1* short and various truncated fragments were determined by an ¹²⁵I-α-BTX binding assay. All data in (A) and (B) are expressed as mean ± S.E.M. Each data point represents results from four independent experiments. *, 0.01 < P < 0.05; **, P < 0.01.

The concomitant changes in the number and size of agrin-induced AChR clusters suggested that the N-terminal domain of *tid1* may have a potent effect on the expression of receptor protein in the myotubes. In support of this assumption, a radioligand-binding assay with iodinated α -bungarotoxin (^{125}I - α -BTX) revealed a striking increase in the levels of surface AChRs in myotubes expressing NTid1(1-222), independent of stimulation by neural agrin (Figure 19B). In contrast, overexpression of other truncated fragments that lack the DnaJ domain, or with full-length *tid1* short, had little effect on the overall levels of toxin-binding sites measured on the myotube surface. Based on these results, it is concluded that the N-terminal half of *tid1* confers AChR-clustering activity and promotes receptor subunit expression in cultured muscle cells.

3.7 TID1 KNOCKDOWN BY SHORT HAIRPIN RNA INHIBITS AChR CLUSTERING IN MYOTUBES

It was shown in Figure 16 that C2C12 myotubes contain detectable levels of endogenous *tid1* and that agrin stimulation induces co-aggregation of the protein with AChRs on the cell surface. To address whether muscle *tid1* is required for AChR clustering, an RNA interference (RNAi) approach was used to inhibit mouse *tid1* expression by using a short hairpin RNA (shRNA) targeted towards a specific region of the DnaJ domain. Expression of the shRNA was under the control of a U6 promoter in the plasmid vector pSIREN (Clontech, Mountain View, CA). The plasmid vector contained an additional promoter (CMV), which drove the co-expression of DsRed, a red fluorescent protein marker.

In preliminary experiments, the efficiency of the shRNA vector was tested by transfecting it into COS-7 cells. COS-7 cells do express endogenous *tid1*, however, its cDNA differs from that of mouse *tid1* by a few base pairs (bp) in the shRNA-targeting region. In contrast, rat *tid1* differs by mouse *tid1* in this area by only 1 bp. Thus, the mouse *tid1*-targeted shRNA plasmid was co-transfected along with a plasmid cDNA encoding myc-tagged full-length rat *tid1* short into COS-7 cells. An adenovirus-mediated DEAE dextran method was used to transfect the cells with either control (scrambled, Scr) or *tid1*-targeted shRNA subcloned into the DsRed-encoding pSIREN vector. Parallel dishes were also transfected with myc-tagged full-length rat *tid1* short (myc-*tid1*s), in a 5:1 (weight) ratio of shRNA to rat *tid1* short, to mimic shRNA-mediated knockdown of endogenous *tid1* protein. This transfection method resulted in a transfection efficiency of ~40-50%, regardless of whether shRNA only or shRNA and myc-*tid1*s were transfected together into the cells. The cells were then fixed, permeabilized, and stained using a mouse monoclonal antibody against the myc tag.

As is illustrated in Figure 20A, cells co-transfected with scrambled shRNA and myc-tagged *tid1* short show strong DsRed (g) and myc immunostaining (h). However, myc staining is dramatically reduced when cells are co-transfected with mouse *tid1*-targeted shRNA and myc-tagged rat *tid1* short (k, arrow). The decrease in exogenous *tid1* expression appears to be dose-dependent: cells expressing a lower level of *tid1*-targeted shRNA (m) express a higher level of myc-tagged *tid1* (compare n to k), although the level of expression, as judged by the intensity of fluorescence, is still lower than that observed in scrambled shRNA-transfected cells (compare n to h). Detergent extracts of transfected COS-cells were subjected to immunoblotting. Figure 20B clearly demonstrates that mouse *tid1*-specific shRNA knocks down the level of exogenous rat *tid1* short (compares lanes 2 and 4).

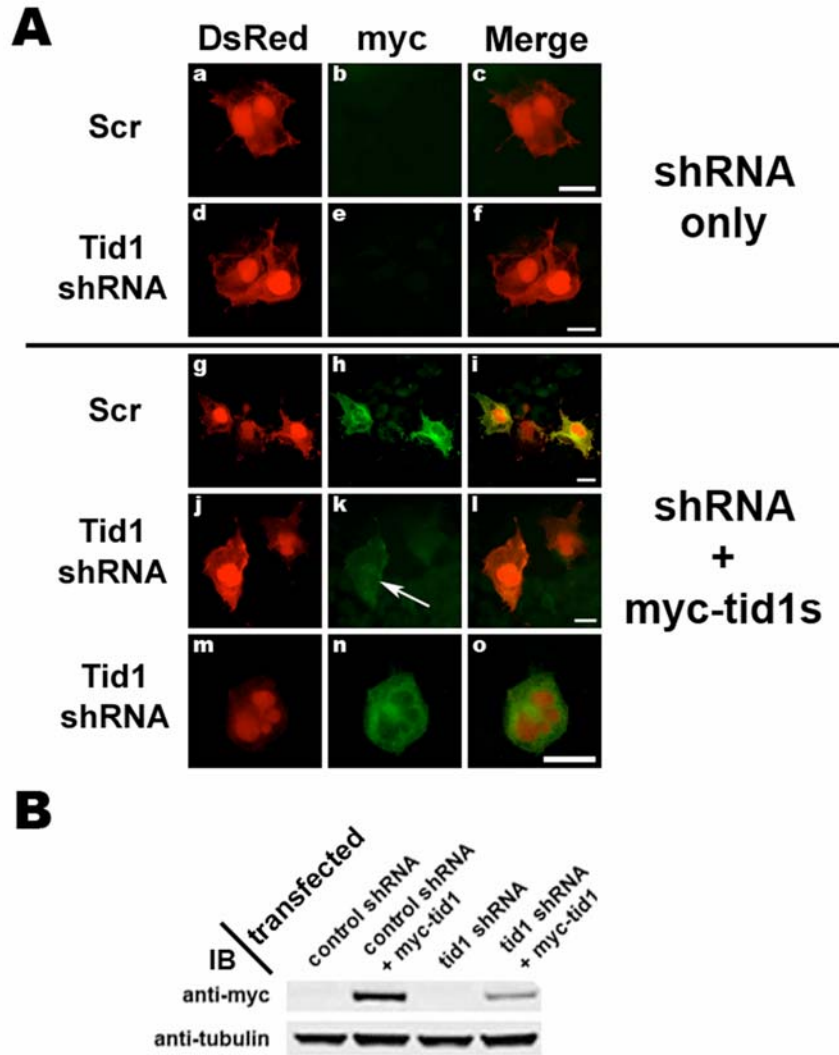


Figure 20. The specificity of shRNA-mediated knockdown of tid1 in COS cells.

(A) Cells were fixed, permeabilized, and stained with mAb9E10 against the myc tag followed by Cy2-conjugated goat anti-mouse IgG. All images were acquired by using a CCD camera with the same exposure settings. shRNA-only transfected cells (*top panels*) clearly express DsRed (a, d) and they are not stained by the anti-myc antibody (b, e). Cells co-transfected with the scrambled shRNA and myc-tagged rat tid1 short show strong DsRed (g) and myc immunostaining (h). However, the myc staining was reduced (arrow) when cells were co-transfected with mouse tid1-targetted shRNA and myc-tagged rat tid1 short (j – l). The decrease in exogenous tid1 expression appears to be tid1-shRNA dose-dependent (m-o). Scale bar = 10 μ m. (B) Detergent extracts of the cells were immunoblotted with the anti-myc antibody mAb9E10. The blot was stripped and reprobed with an anti- α/β tubulin antibody as a loading control. The intensity of each of the bands on the blot was quantified by using NIH ImageJ software and normalized to that of tubulin staining. This representative blot shows that co-transfection with tid1-specific shRNA results in a 46% reduction in the expression of myc-tagged tid1 short. The experiment was repeated a total of 3 times and the average shRNA-mediated reduction in exogenous tid1 expression was 55%.

Thus, both immunofluorescent staining and immunoblotting showed that the *tid1*-targeted shRNA resulted in a striking reduction in the expression of *tid1* short protein.

Knowing that the efficiency of transfection was less than 100% and that not all myc-tagged *tid1*-transfected cells were co-transfected with *tid1*-targeted shRNA, it was decided to quantify *tid1* knock down on a cell-by-cell basis (Figure 21). Comparing the DsRed fluorescence intensity between scrambled shRNA and *tid1*-targeted shRNA transfected cells, one sees that their distributions are relatively similar. However, comparing the intensity of myc fluorescence between scrambled shRNA and *tid1*-targeted shRNA transfected cells, one sees that the distribution of myc fluorescence intensity is highly skewed towards lower values for the *tid1*-targeted shRNA transfected cells as compared to the scrambled shRNA-transfected cells.

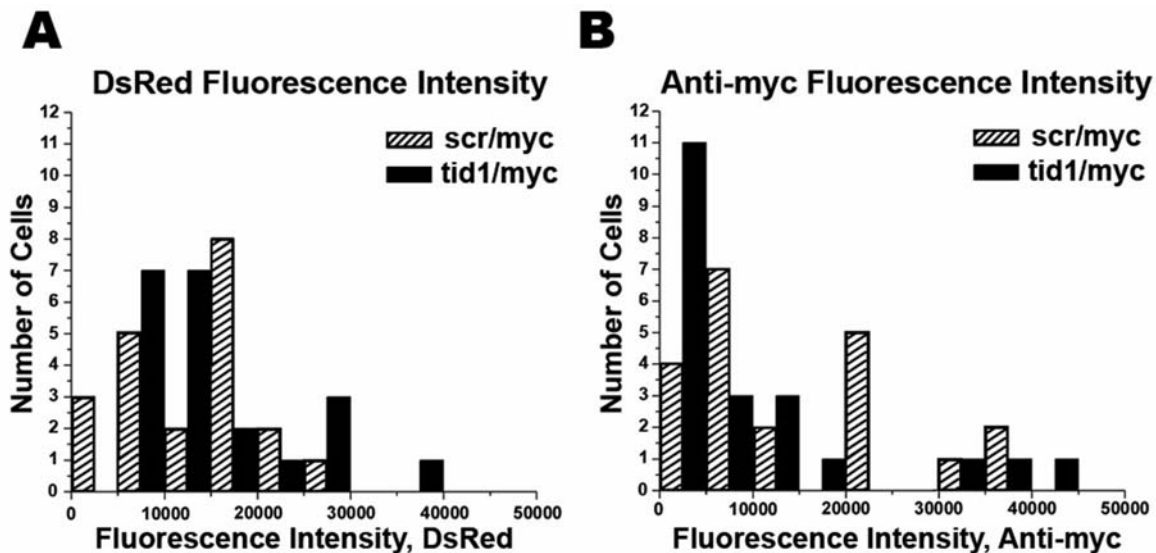


Figure 21. Tid1 shRNA knocks down the expression of exogenous *tid1*.

ImageJ software was used to measure the relative intensities of DsRed and myc fluorescence in cells co-transfected with scrambled shRNA and myc-tagged *tid1* short (*scr/myc*), and in cells co-transfected with *tid1*-targeted shRNA and myc-tagged *tid1* short (*tid1/myc*). Histograms were then constructed of the number of cells grouped by fluorescence intensity. $n = 21$ for each group.

Thus, the mouse *tid1*-targetted shRNA reduces the fluorescence intensity, and therefore the expression, of myc-tagged rat *tid1* short.

C2C12 mouse myoblasts were transfected with the plasmid vector encoding *tid1*-specific shRNA, or with a vector that expresses a scrambled shRNA as control. The cells were then switched to grow and differentiate in fusion medium. At 3 days post-transfection, moderate to high levels of the red fluorescent protein DsRed were readily visible in ~30% of myotubes formed in the culture dish, suggesting that the plasmid vectors were successfully transfected and that they were functionally active in these cells. The myotube cultures were incubated with neural agrin for 20 min and then switched back to agrin-free fusion media for 4.66 h. After brief fixation, the cells were double-stained with a polyclonal antibody against *tid1* followed by Alexa Fluor 633-conjugated goat anti-rabbit IgG and with Alexa Fluor 488-conjugated α -BTX.

Transfection with the scrambled control shRNA had little effect on AChR clustering in myotubes treated with the short pulse of agrin, nor did it change the level and localization of *tid1* in the cells (Figure 22A, a-d). In contrast, overexpression of the *tid1*-targetted shRNA potently blocked agrin-induced AChR clustering (Figure 22A, e-h). The inhibitory effect of shRNA correlated well with the reduction in immunofluorescent *tid1* staining in the cells. Hence, myotubes that retained relatively high levels of *tid1* were able to form a few AChR clusters in response to agrin stimulation (Figure 22A, i-l). However, the clusters were usually small and less bright than those found in untransfected or in control shRNA-transfected myotubes. Conversely, myotubes that had little or no *tid1* staining usually failed to form any visible receptor clusters.

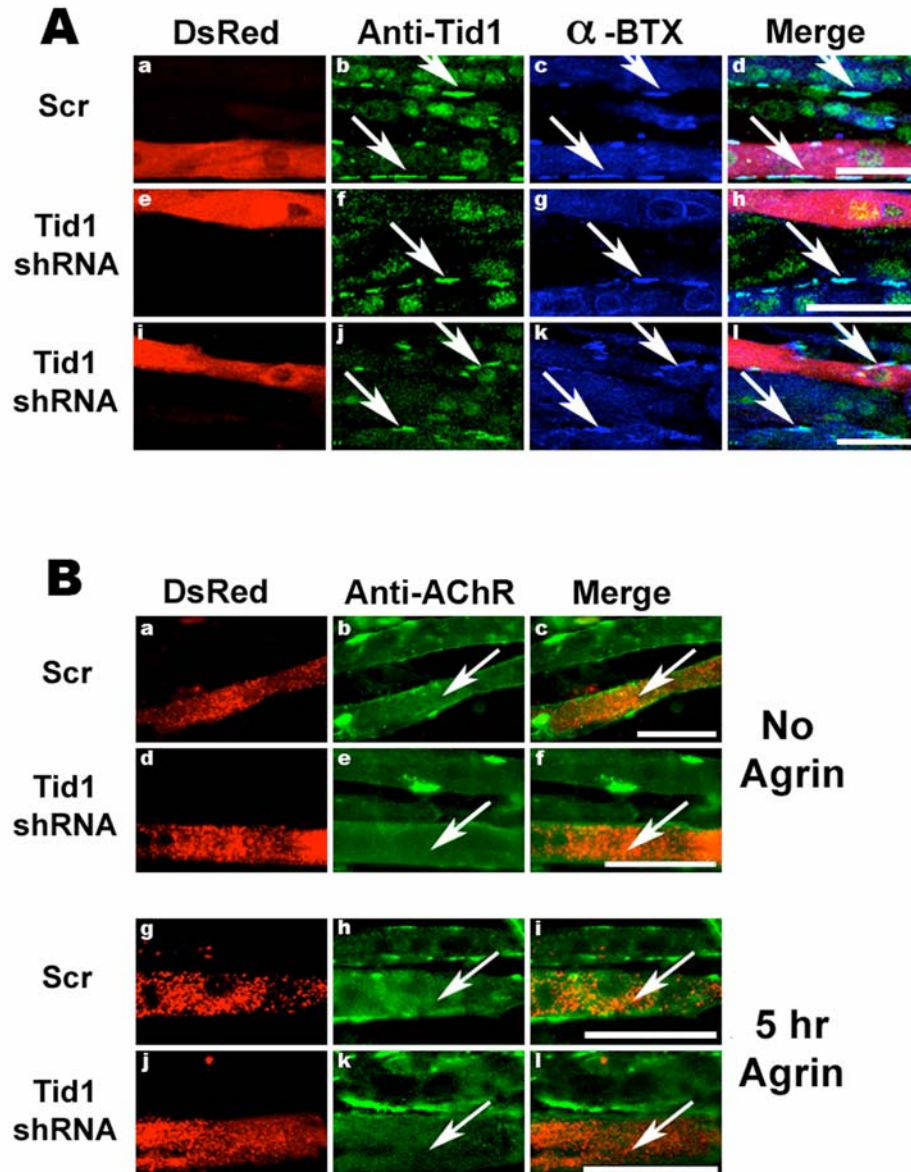


Figure 22. Inhibition of spontaneous and agrin-induced AChR clustering by shRNA-mediated *tid1* knockdown in myotubes.

C2C12 myoblasts were transfected with a pSIREN vector encoding the scrambled control (Scr) or *tid1*-targeted short hairpin RNA (shRNA). Scale bar = 25 μ m for (A) and (B). (A) At ~72 h post transfection, myotubes were incubated with fusion medium containing neural agrin for 20 min followed by fusion medium without agrin for 4.66 h. The cells were briefly fixed and stained with a rabbit antibody against *tid1* followed by an FITC-conjugated goat anti-rabbit IgG as well as Alexa Fluor 633-conjugated α -BTX. Transfected myotubes express the red fluorescent protein marker, DsRed. Arrows highlight AChR clusters. (B) Myotubes were left untreated (*top panels*), or incubated with neural agrin continuously for 5 h (*bottom panels*). They were then fixed and stained with mAb35 followed by Cy2-conjugated goat anti-rat IgG to label AChRs. Arrows highlight transfected myotubes.

The *tid1*-specific shRNA was highly effective in knocking down *tid1* expression and in preventing AChR clustering in cultured myotubes. It not only blocked AChR clustering induced by a short pulse of agrin (20 min), but it also suppressed the formation of AChR clusters caused by prolonged agrin stimulation (5 h) (Figure 22B, j-l). The time course of AChR cluster formation in the continuous presence of neural agrin was measured in untransfected, scrambled shRNA, and *tid1* shRNA-transfected myotubes. Consistent with a previous report (Ferns et al., 1996), in untransfected control myotubes, AChR clusters began to form after 2 h of agrin treatment and peaked in number at 4-6 h. Cluster number then declined slightly after 8 h of agrin stimulation. In the *tid1*-targeted shRNA-transfected myotubes, however, the number of AChR clusters measured at each time point of agrin stimulation was significantly reduced ($p < 0.01$), as compared to untransfected and scrambled shRNA-transfected myotubes (Figure 23). In addition to a potent effect on agrin-induced receptor clustering, the *tid1* shRNA also caused a significant reduction in the number of spontaneous AChR clusters that were occasionally seen on the surface of myotubes in the absence of agrin (Figure 22B, d-f; Figure 23; Figure 25).

A major concern with the knockdown approach was whether the phenotypes observed were caused by inhibition of the specific target (*tid1*), or by interference of the shRNA with the expression of unrelated genes (“off target” effects). To address this issue, a “rescue” experiment was carried out by co-expressing a cDNA that encodes human *tid1* short along with the *tid1*-targeted shRNA. Selected nucleotides were silently mutated in the shRNA-targeted region of the human *tid1* cDNA, in order to ensure that its expression is not affected by the mouse *tid1*-specific shRNA (see Experimental Procedures). Myoblasts were co-transfected with the constructs and treated with agrin as described for Figure 22A and stained as in Figure 22B.

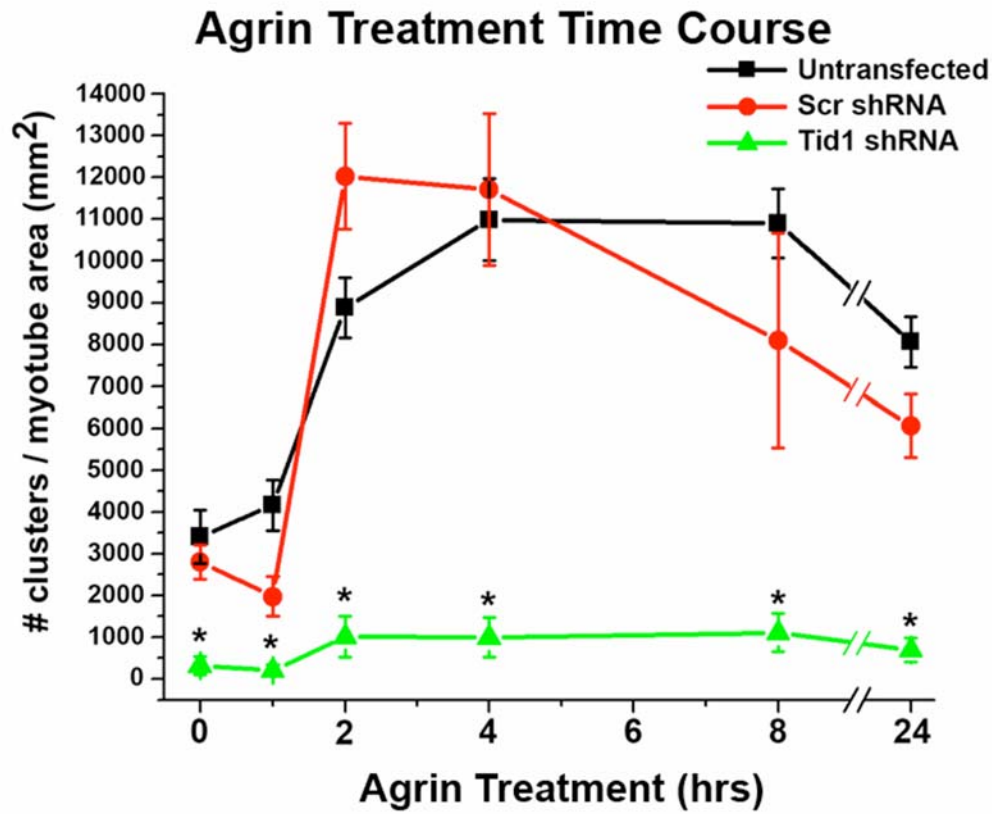


Figure 23. Time course of agrin-induced AChR clustering demonstrates tid1-shRNA-mediated inhibition.

Myotubes transfected with the scrambled control or tid1-targetted shRNA were incubated with neural agrin for 0, 2, 4, 8, or 24 h, respectively. The cells were fixed and stained as in Figure 22B. Data are expressed as mean \pm S.E.M. *, $P < 0.01$, Student's t-tests comparing values between scrambled and tid1-targetted shRNA-transfected myotubes. $n = 10$ for scr and tid1-shRNA transfected cells and $n = 20$ for untransfected myotubes for each time point.

As illustrated in Figure 24(a-c), co-expression of the mouse tid1-targetted shRNA with the full-length human tid1 short (hTid1S) successfully rescued the AChR clustering activity of C2C12 myotubes in response to agrin. This finding thus confirms that the inhibitory effect of shRNA on AChR clustering was mediated specifically by interference with tid1 expression in the mouse-derived C2C12 myotubes. In Figure 18, it was demonstrated that the N-terminus of rat tid1 (aa. 1–222), which contains the DnaJ domain, was sufficient to induce receptor clustering

when transfected alone into myotubes. Similarly, it was found that co-transfection of cDNA encoding the same N-terminal portion of human *tid1* (N-hTid1) was also highly effective in rescuing AChR clustering from inhibition by the mouse *tid1*- specific shRNA (Figure 24, d-f).

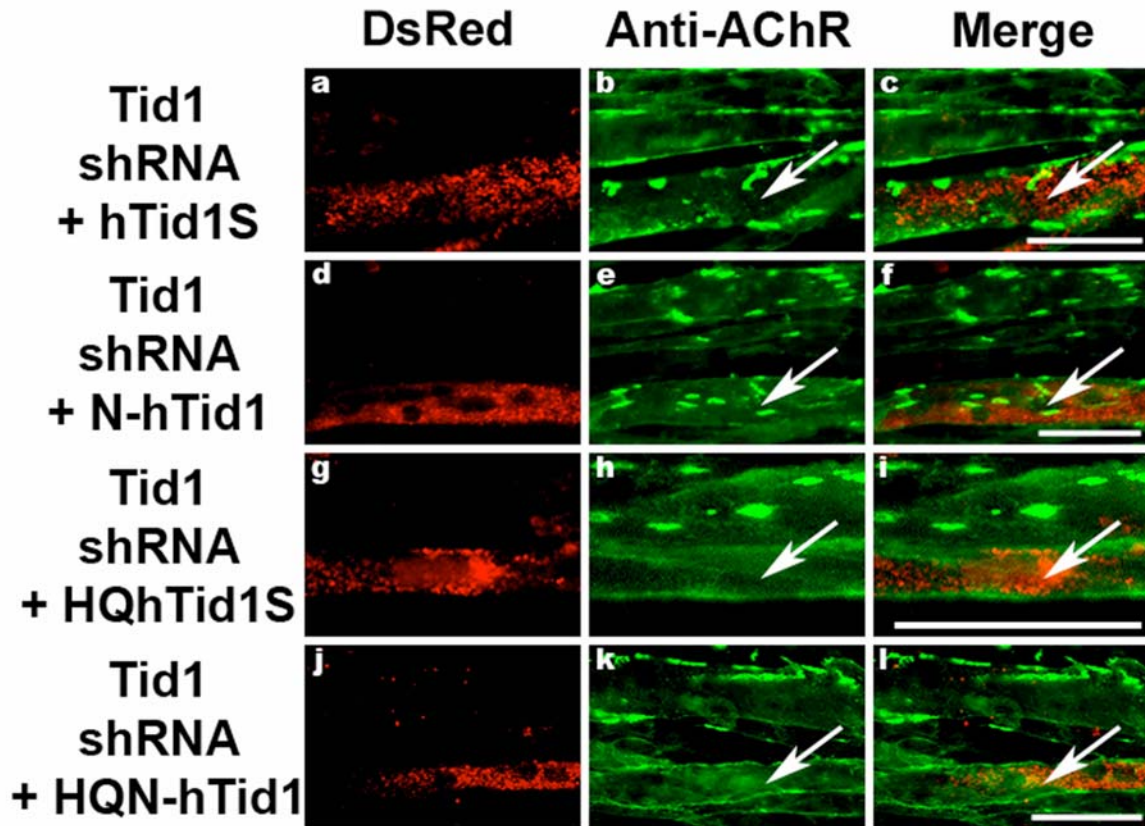


Figure 24. *Tid1* shRNA's effects on AChR clustering are specifically mediated by *tid1* knockdown and *tid1*'s effects on AChR clustering are dependent upon a functioning DnaJ domain.

Myotubes were treated as in Figure 22A and stained as in Figure 22B. Co-expression of silently-mutated full-length and the N-terminal domain of human *tid1* rescues AChR clustering from interference by mouse *tid1*-targeted shRNA (a–f). Mutation of the hsp70 activation site (H121Q) in the human *tid1* construct diminishes the rescuing effect (g–l). Arrows highlight transfected myotubes.

To assess the role of the DnaJ domain of *tid1* in the “rescue” experiments, a cDNA of human *tid1* with a mutation in a key residue (H121Q) in the region was obtained (Syken et al., 1999). The H121Q mutation allows *tid1* to bind to its co-chaperone, hsp70, but it prevents *tid1* from activating hsp70. The cDNA was used as a template to make silently-mutated human *tid1* constructs identical to hTid1S and N-hTid1, aside from the H121Q mutation. As shown in Figure 24, g-l, neither of the H121Q mutant constructs was able to rescue the shRNA-mediated inhibition of AChR clustering in response to stimulation by agrin. These data suggest that the effect of *tid1* on AChR clustering is likely dependent upon its ability to activate its co-chaperone hsp70.

The results of the rescue experiments using the wild-type hTid1S and N-hTid1 as well as the two H121Q mutants were semi-quantified and are summarized in Figure 25 and Figure 26. In each experiment (spontaneous (Figure 25) and agrin-induced (Figure 26) clustering), the *tid1*-targeted shRNA significantly inhibited and the H121Q mutants failed to rescue ($p < 0.001$) AChR clustering, as compared to the scrambled control shRNA. Without agrin treatment (Figure 25), the N-terminal half of human *tid1* short successfully rescued AChR clustering and full-length human *tid1* short also increased the observed level of clustering versus *tid1*-shRNA alone. With agrin treatment (Figure 26), full-length human *tid1* short fully restored AChR clustering and the N-terminal half of human *tid1* increased clustering above the levels observed with shRNA-mediated knockdown of *tid1* or the failed rescues of the H121Q mutants.

Radioligand binding assays with ^{125}I - α -BTX revealed that myotubes transfected with the scrambled or *tid1* shRNA expressed similar levels of surface AChR proteins as untransfected and sham controls (Figure 27).

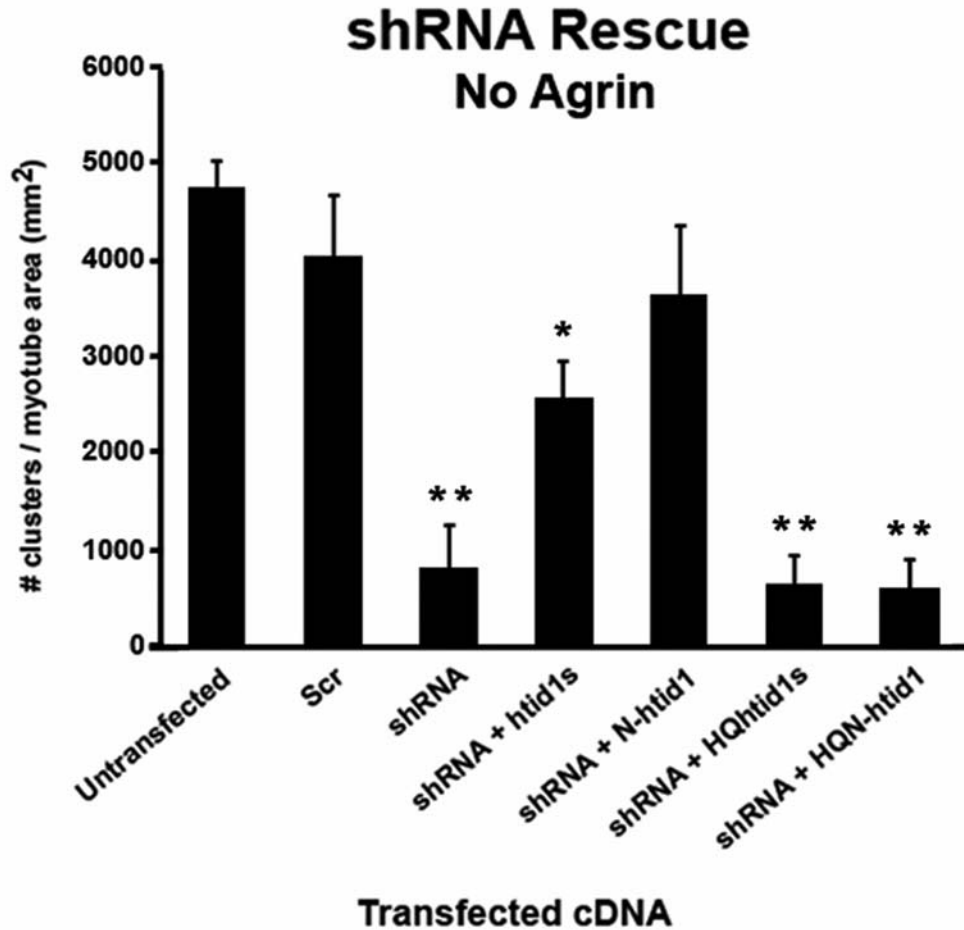


Figure 25. Quantification of tid1 shRNA rescue, spontaneous clustering.

The effects of various shRNA constructs on the formation of spontaneous AChR clusters in myotubes. Data are expressed as mean \pm S.E.M. *, $0.01 < P < 0.05$; **, $P < 0.001$. Student's t-tests were performed comparing values between scrambled and the various tid1-targeted shRNA-transfected myotubes. $n = 120$ for untransfected myotubes and $n = 20$ for every other group. shRNA = tid1-specific shRNA.

shRNA Rescue Agrin Treatment

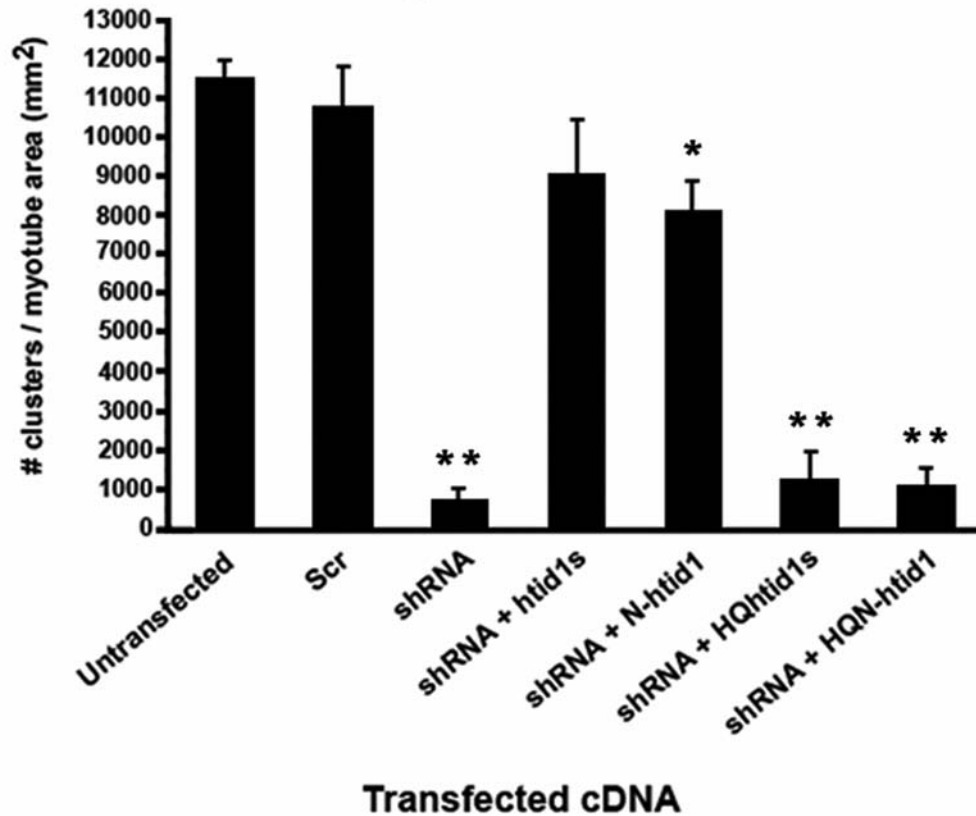


Figure 26. Quantification of *tid1* shRNA rescue, agrin-induced clustering.

The effects of various shRNA constructs on the formation of agrin-induced AChR clusters in myotubes. Data are expressed as mean \pm S.E.M. *, $0.01 < P < 0.05$; **, $P < 0.001$. Student's t-tests were performed comparing values between scrambled and the various *tid1*-targeted shRNA-transfected myotubes. $n = 120$ for untransfected myotubes and $n = 20$ for every other group. shRNA = *tid1*-specific shRNA.

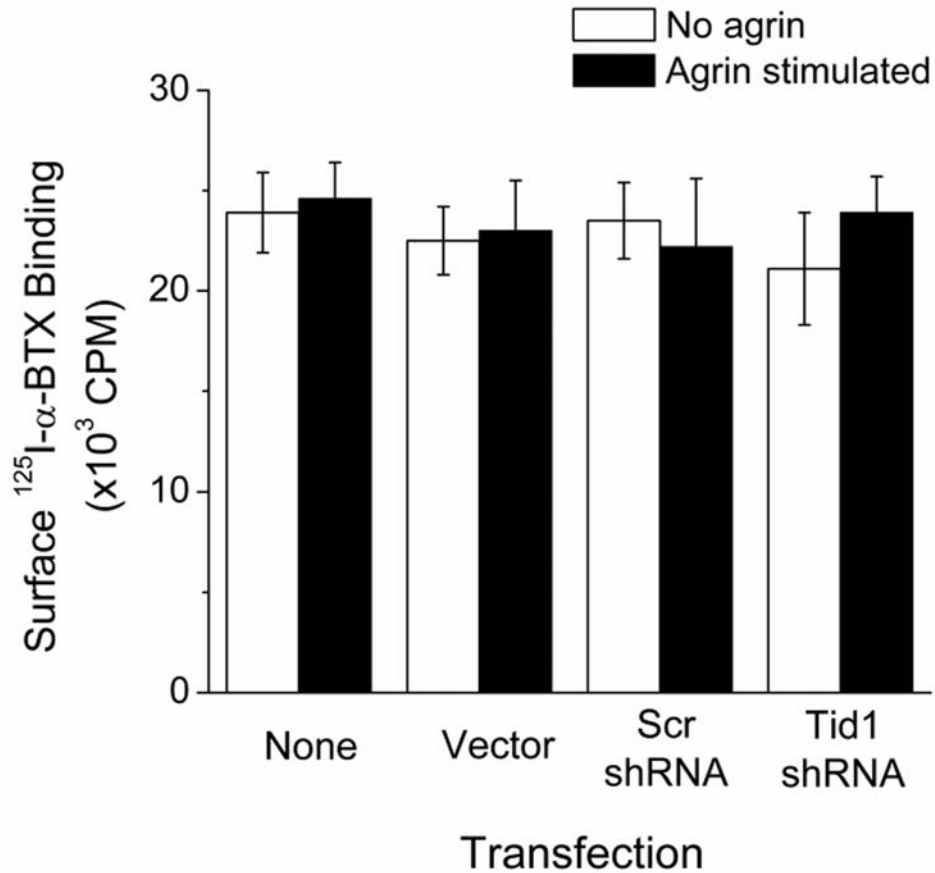


Figure 27. Tid1-targeted shRNA does not change surface expression of AChR.

C2C12 myoblasts were transfected with the control plasmid pSIREN (vector), a plasmid encoding the control scrambled (scr) shRNA, or tid1-specific shRNA. At ~72 h after transfection, myotubes were either left untreated or treated with neural agrin for 4 h. The levels of AChR protein expressed on the cell surface were determined by ¹²⁵I-α-BTX binding assays. The data are expressed as mean±S.E.M. Each data point represents results from four independent experiments. *, 0.01 < P < 0.05; **, P < 0.01.

3.8 ShRNA-MEDIATED TID1 KNOCKDOWN DISRUPTS THE STRUCTURE AND FUNCTION OF THE NMJ

Results derived from experiments using C2C12 myotubes suggest that *tid1* plays a role in the formation of AChR clusters. It is unclear, however, whether *tid1* is required for the maintenance of AChR clusters that have already been formed in an adult NMJ. To address this question, electroporation was used to introduce the *tid1*-specific shRNA into the TA muscles of living adult mice. A scrambled shRNA was electroporated into the same muscle of another group of age-matched mice to serve as negative controls. The plasmids containing the shRNAs also co-expressed the fluorescent marker DsRed. Five and a half weeks after the electroporation, animals were anaesthetized, perfused with fixative, and the TA muscles were collected. The muscles were teased apart into fascicles of 1-5 fibers and stained with Alexa Fluor 488-conjugated α -BTX and an anti-*tid1* antibody followed by an Alexa Fluor 633-conjugated secondary antibody. The triple labeled samples were examined under an Olympus FluoView 1000 confocal microscope with three non-overlapping laser lines (excitation wavelengths 488 nm for Alexa Fluor 488, 543 nm for DsRed, and 633 nm for Alexa Fluor 633, respectively). Transfected myofibers were easily identified by the expression of DsRed.

In untransfected muscles or muscles that expressed the scrambled control shRNA, a single AChR cluster was invariably visualized in the central region of each myofiber. The cluster appeared as a brightly stained, large continuous structure in a “pretzel-like” shape with sharp boundaries (~40 μ m in diameter). *Tid1* immunofluorescence was colocalized with the receptor cluster at the NMJ (Figure 28, a-h). In contrast, overexpression of the *tid1*-targeted shRNA by electroporation caused mild to severe disruption of AChR clusters depending on the

degree of reduction in *tid1* expression. In fibers that showed a slight decrease in *tid1* staining, the individual receptor cluster was broken into several large fragments that remained at the NJM (Figure 28, i-l). In more severe cases where *tid1* staining was considerably reduced, AChR clusters fragmented into many (> 20) small and discontinuous structures (~2-5 μm in diameter). These structures had round, ovoid, or irregular shapes and were less intensely stained by Alexa Fluor 488- α -BTX than the large intact receptor clusters in normal control muscles (Figure 28, m-t).

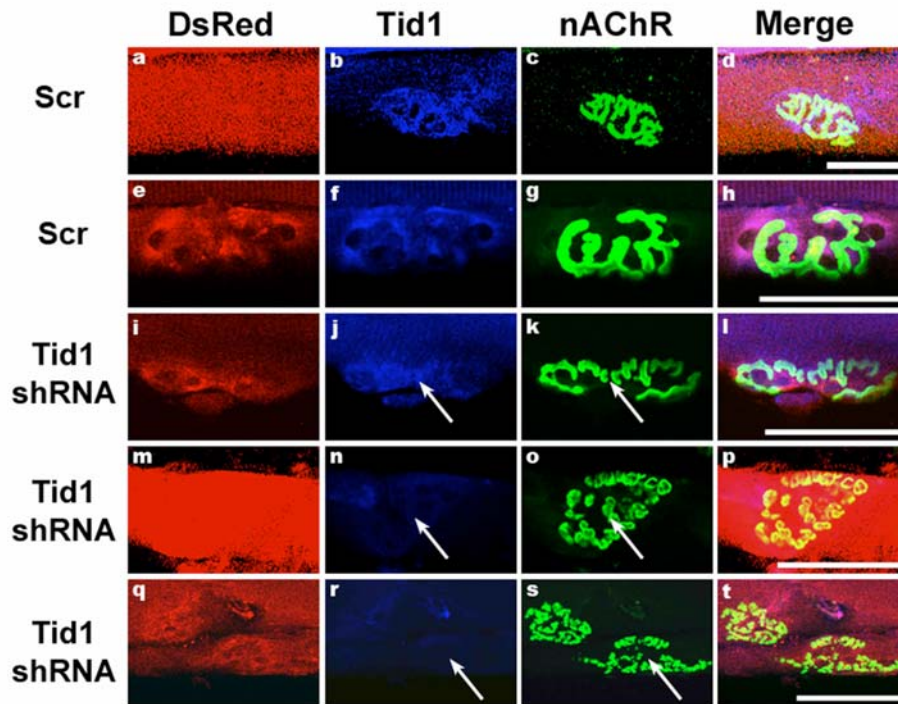


Figure 28. Tid1 knockdown disrupts the structure and function of the mouse NMJ.

TA muscles of adult mice were injected with 5 μg of pSIREN plasmid encoding either control (scrambled, Scr) or *tid1*-targetted shRNA and electroporated. 5.5 weeks later, the animals were perfused with fixative and the muscles were dissected and stained with Alexa Fluor 488-conjugated α -BTX and a rabbit polyclonal antibody against *tid1*, followed by an Alexa Fluor 633-conjugated goat anti-rabbit IgG. Transfected myotubes express DsRed. Arrows highlight decreased *tid1* staining (mild: j, moderate: n, and severe: r) and the resulting NMJs (k, o, s). Scale bar = 50 μm .

In the most severe cases where *tid1* immunostaining was completely absent, the NMJ was massively disorganized. α -BTX staining revealed numerous small spots (\sim 1-2 μ m in diameter) that were weakly stained and whose boundaries were poorly defined. These structures scattered over an area that was larger than the size of a normal AChR cluster, indicating that they were diffusing away from the endplate region of the NMJ (Figure 29A, b, e, h). At 10 weeks after electroporation, a few myofibers in the soleus muscle still maintained a high level of expression of the shRNAs. In fibers expressing *tid1*-targeted shRNA, Alexa Fluor 488- α -BTX staining showed that the receptor clusters were largely degraded. Only a few residual fragments were observed and they were weakly stained, small, and irregularly shaped (Figure 29B, d-f). Taken together, these results demonstrate that *tid1* is required for maintaining the normal structure of AChR clusters in the motor endplates of adult animals.

To explore whether shRNA-mediated *tid1* knockdown affects synaptic transmission at the NMJ, the amplitudes of endplate potentials (EPPs) and miniature endplate potentials (MEPPs) were measured in the skeletal muscles of mice at 5 weeks post-electroporation. Examples of the intracellular recordings from muscles are shown in Figure 30 (A and B) and the results are summarized in Table 1. It was observed that the resting membrane potentials (RMP) of myofibers transfected with the scrambled control and *tid1*-specific shRNAs were not different from those recorded in normal untransfected muscles. There was also little change in the frequency of MEPPs recorded from myofibers electroporated with the shRNAs, suggesting that *tid1* knockdown did not alter the release of ACh from presynaptic terminals. However, the mean amplitude of MEPPs was reduced in fibers expressing the *tid1*-specific shRNA. On average, there was an approximately 40% reduction in the MEPP size. This change could not be attributed

to differences in the placement of the recording electrode relative to the endplate, as the mean rise times of the synaptic potentials (t_{10-90}) were virtually identical (Table 1).

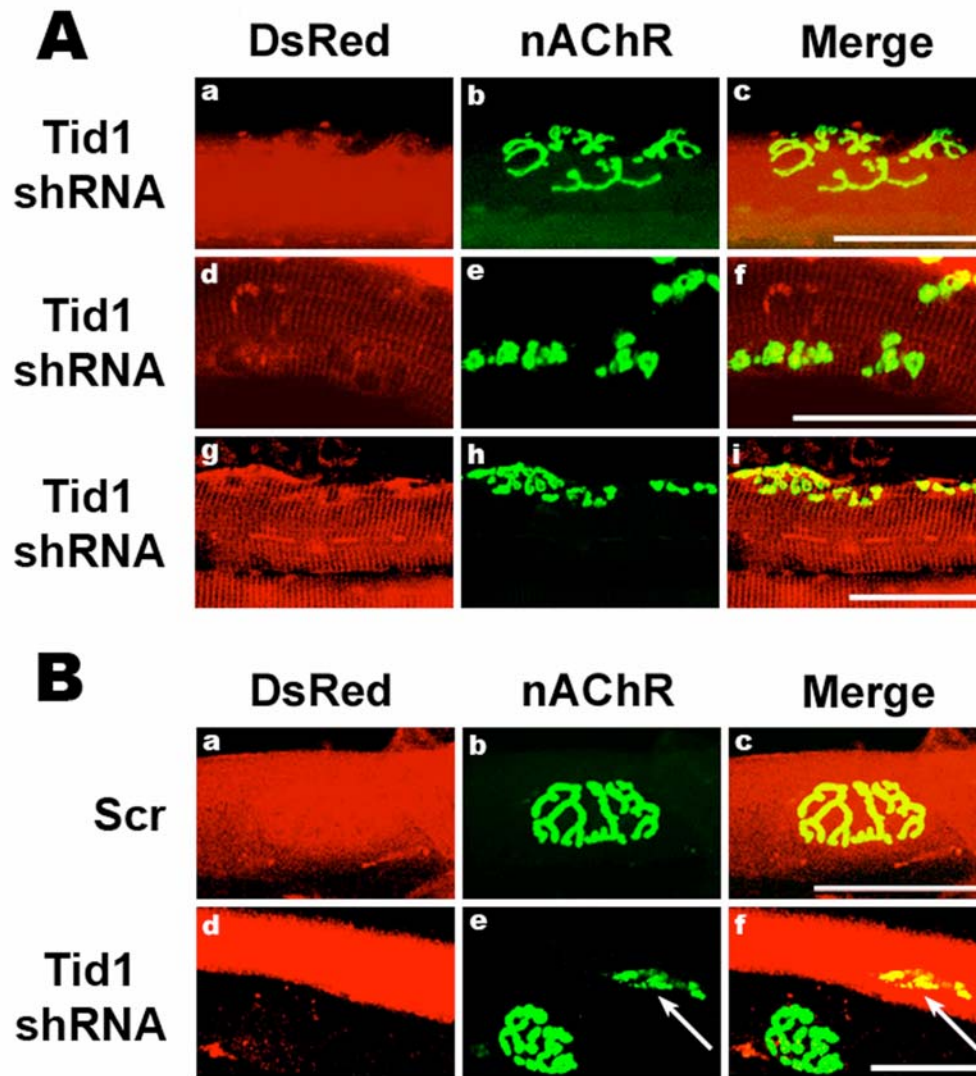


Figure 29. Greater degree of *tid1* knockdown results in more disrupted NMJ structure.

(A) Some muscles were electroporated with a higher dose (12 μ g) of *tid1*-specific shRNA. They were perfused with fixative, dissected, and stained with Alexa Fluor 488-conjugated α -BTX. Transfected myotubes express DsRed. (B) Other muscles were examined 10 weeks after electroporation with 5 μ g of shRNA cDNA. They were processed as detailed for A. Scale bar = 50 μ m for (A) and (B).

Full size EPPs were measured after blocking muscle action potentials and contraction with 2.5 μ M m-conotoxin GIIIB. At endplates of myofibers expressing the tid1-specific shRNA, the mean evoked EPP response was significantly reduced (by ~50%). There was a slight decrease in the corrected quantal content, but the difference was not statistically significant from control myofibers. The markedly reduced amplitudes of MEPPs and EPPs suggest that there was a drastic decrease in the number of AChRs on the postsynaptic membranes of the NMJs. These data, together with the observed disruption in the morphology of AChR clusters, demonstrate unequivocally that tid1 is essential for the maintenance of postsynaptic structure and for normal synaptic transmission at mammalian NMJs.

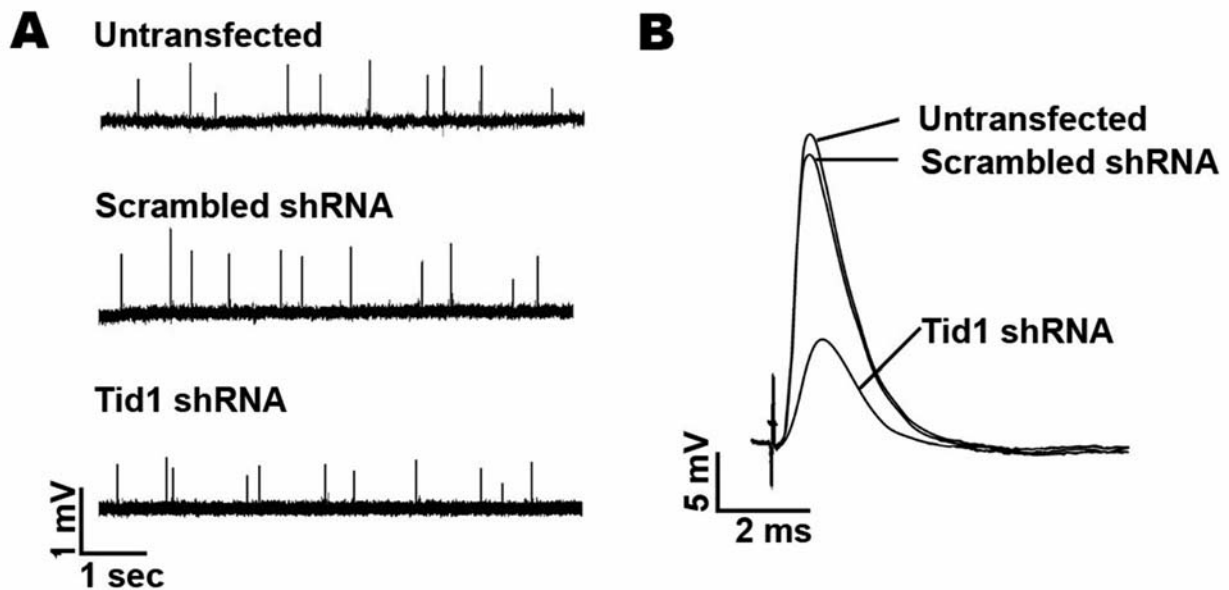


Figure 30. Tid1 knockdown disrupts NMJ function.

Spontaneous miniature endplate potentials (MEPPs, A) and nerve stimulation-evoked endplate potentials (EPPs, B) were recorded from control and shRNA-transfected myofibers at 5 weeks after electroporation.

Table 1. MEPP and EPP properties at control and tid1 shRNA-treated NMJs.

	Untransfected	Scrambled shRNA	Tid1 shRNA
RMP (mV)	-74.3 ± 0.9	-73.9 ± 0.6	-74.1 ± 0.8
MEPP rise time (ms)	0.86 ± 0.11	0.86 ± 0.08	0.87 ± 0.12
MEPP Amplitude (mV)	0.80 ± 0.04	0.79 ± 0.04	0.45 ± 0.02 *
MEPP frequency (s ⁻¹)	1.4 ± 0.09	1.5 ± 0.06	1.4 ± 0.07
EPP rise time (ms)	0.79 ± 0.03	0.77 ± 0.02	0.82 ± 0.05
EPP amplitude (mV)	25.3 ± 0.12	26.1 ± 0.09	13.7 ± 0.04 **
QC (Corrected)	64.8 ± 0.7	65.1 ± 0.6	62.19 ± 1.2

The values in the table are the means ± S.E.M. for 30 endplates from each group (three animals). The rise time was calculated as the time taken for the EPP or MEPP to rise from 10% to 90% of its full amplitude. QC, quantal content. *, 0.01 < P < 0.05 and **, P < 0.01 by One-Way ANOVA.

4.0 DISCUSSION

4.1 SUMMARY OF FINDINGS

Bacterial two-hybrid screens discovered a strong interaction between MuSK and a mammalian homologue (tid1) of the drosophila tumor suppressor, tid56. Immunoprecipitation and immunoblotting experiments confirmed that the protein-protein interaction also occurs in transfected COS cells, C2C12 myotubes and skeletal muscles. Immunofluorescent staining of rat and mouse skeletal muscle revealed that tid1 is localized on the postsynaptic membranes of normal NMJs, colocalized and coextensive with AChRs, from the ages of embryonic synapse formation to adulthood. Chronic denervation induces dispersal of tid1 from the NMJ, apparently slightly before the breakdown and disappearance of AChR clusters. Based on these novel findings, it is postulated that tid1 is a new member of a relatively long list of proteins that constitute the postsynaptic apparatus of the NMJ. In addition to the AChR and MuSK, other well-known molecules on this list include rapsyn, utrophin, dystroglycan, dystrobrevin, and ErbB2/ErbB4. A series of studies using C2C12 myotubes and mouse skeletal muscles provided compelling evidence demonstrating that tid1 is critical to the formation and maintenance of AChR clusters at the NMJ. First, C2C12 myotubes contain endogenous tid1 in their cytoplasm, which co-aggregates with AChRs to form high-density clusters on the plasma membrane in response to stimulation by recombinant neural agrin. Overexpression of the N-terminal half of

tid1 in C2C12 myotubes increases the number of spontaneous receptor clusters in the absence of agrin. On the contrary, knocking down tid1 expression in myotubes by RNA interference blocks the formation of agrin-induced AChR clusters. Finally, inhibition of tid1 expression *in vivo* by RNA interference causes severe disruption of preformed AChR clusters and leads to a striking reduction of synaptic transmission at NMJs. Taken together, it is concluded that tid1 is a novel player at the NMJ that is required for the formation, development, and maintenance of normal synaptic structure and function.

4.2 RELEVANT BACKGROUND

Clustering of AChRs in embryonic muscles during early development is critically dependent on the motoneuron-derived factor, agrin. Activation of MuSK by neural agrin is known to be the first step of a complex signaling program that eventually leads to the aggregation and maintenance of AChRs at the NMJ (Glass et al., 1996). While the events occurring in muscle subsequent to MuSK activation are poorly understood, several molecules have been found to interact with MuSK and are thought to mediate or modulate agrin signaling through MuSK. Among these are the muscle proteins dystroglycan (Jacobson et al, 2001), Dishevelled (Luo et al., 2002), the abl tyrosine kinases (Finn et al., 2003), the membrane associated guanylate kinase MAGI-1c (Strochlic et al., 2001) and geranylgeranyltransferase 1 (GGT, Luo et al., 2003). Particularly worth noting is a recent report which identified Dok-7, a phosphotyrosine binding (PTB) domain-containing protein, as a MuSK binding partner in muscle. Dok-7 is thought to act as an adaptor and a positive effector that links MuSK to other molecules in the downstream signaling pathway (Okada et al., 2006; Beeson et al., 2006). The

discovery of *tid1* at the NMJ has further increased the complexity of this expanding list of potential downstream effectors for MuSK. Like other receptor tyrosine kinases, MuSK is thought to form the core of a protein complex that may diverge into multiple signaling pathways. In fact, several recent studies have shown that MuSK may act as a scaffold to recruit multiple muscle proteins to initiate the formation and to maintain the stability of AChR clusters at the NMJ (Luo et al., 2003; Strochlic et al., 2005).

Tid1 was identified as a mammalian homologue of the *Drosophila* tumor suppressor, *tumorous imaginal discs 56* (*tid56*), a member of the DnaJ protein family and a homologue of heat shock protein 40 (*hsp40*). *Tid56* was first identified in a mutagenesis screen looking for lethal recessive tumor mutations affecting *Drosophila* larvae. Homozygous mutation of *tid56* results in the malignant growth of imaginal discs cells (precursors to the adult head, thorax, appendages, and genitalia), which causes the death of mutant larvae before progression onto the pupal stage. If the tumorous tissue is implanted into ready-to-pupariate wild type larvae, the larvae do not differentiate. Implantation of tumorous tissue into wild type adult flies results in undifferentiated, malignant, and lethal tumorous growth (Gateff, 1978; Gateff and Mechler, 1989; Kurzik-Dumke et al., 1995; Kurzik-Dumke et al., 1992). Interestingly, the wild type *l(2)tid⁺* (*tid56*) gene is *not* heat shock inducible (Kurzik-Dumke et al., 1995). Whereas DnaJ proteins are emerging as the largest of all chaperone families (Cheetham and Caplan, 1998), *tid* is thus far the only tumor suppressor identified in the DnaJ family (Lo, et al., 2004). Homozygous mice with a deletion in the *tid1* gene die prematurely (E6.5), suggesting that the protein product is also critical for early mammalian embryonic development (Lo et al., 2004). Other studies have found that *tid1* can regulate mitochondrial function, especially with regards to cell survival and apoptosis (Syken et al., 1999), and also signaling by receptor tyrosine kinases

(RTKs) including ErbB2 (Kim et al., 2004) and the Trk family (Liu et al., 2005). Additionally, tid1 is known to mediate Jak kinase signaling (Sarkar et al., 2001) and it binds to the Ras-GTPase activating protein (Ras-GAP, Trentin et al., 2001). Thus, tid1 is emerging as an important signaling molecule in many diverse cellular processes.

4.3 BINDING OF TID1 TO MUSK

Tid1 has two alternatively spliced isoforms, tid1 long and tid1 short. In the bacterial two-hybrid experiments, the short form of tid1 was found to be the sole target that bound to the MuSK bait. It was also confirmed that MuSK interacts only with tid1 short, not tid1 long, in C2C12 myotubes and rodent muscles. Both isoforms of tid1 contain three prominent domains: a DnaJ domain (aa. 92-150), a cysteine rich region (aa.223-303), and a unique C-terminal domain (aa.307-428) (Figure 8A). Because the two differ only in the last 33 residues of the polypeptide chains, protein sequences near the C-terminus of tid1 short are thus most likely to be involved in the interaction with MuSK. Indeed, all of the clones isolated from the two-hybrid screens contained the full C-terminus of tid1 short (Figure 8A). Interestingly, the C-terminal region of tid1 has also been shown to mediate the binding of tid1 to other RTKs in neural and non-neural cells (Kim et al., 2004; Liu et al., 2005).

However, if one examines tid1 short in comparison to tid1 long, it becomes evident that the minimal binding domain which is specific to tid1 short is only 6 amino acids long. Moreover, the tid1 short-specific polyclonal antibody which was created is targeted towards the last 20 amino acids of tid1 short, which includes this 6 amino acid stretch. Based on this information, 3 important questions arise: 1) how is it that the tid1 short-specific antibody does

not prevent binding between MuSK and tid1 short, 2) how is the binding tid1 short specific, and 3) how is it that MuSK/tid1 binding is tid1 short specific, yet the N-terminal half of tid1 alone has an effect on clustering?

First, examining the coimmunoprecipitation data, one sees from Figure 11 that with whole muscle homogenates, the pull down succeeded in only one direction – the anti-MuSK antibody was able to pull down MuSK and tid1 short, which was detected by a pan tid1 antibody. However, the tid1 short antibody was not able to pull down both MuSK and tid1 short. As for C2C12 myotube lysates, demonstrated in Figure 10, whereas the anti-MuSK antibody clearly pulls down both MuSK and tid1 short, the tid1 short-specific antibody is much less successful at pulling down MuSK along with tid1 short. The MuSK band is considerably weaker, with higher background. Such results indicate that the tid1 short antibody may indeed be interfering with the binding of MuSK to tid1 short. This is especially true of the whole muscle homogenate results, where co-immunoprecipitation with the tid1 short antibody was not successful. The low level of MuSK that is pulled down by the tid1 short antibody from the C2C12 myotube lysates could reflect the fact that the tid1 short antibody is polyclonal and thus some antibodies may bind to tid1 short slightly upstream of the MuSK binding site. This, however, is an unlikely explanation, as antibodies are relatively large and the antibodies may still allosterically hinder the binding of MuSK to tid1 short.

Alternatively, tid1 could have a second binding site to MuSK, most likely in its N-terminal region. The tid1 short antibody could bind to tid1 in the C-terminus, leaving the N-terminus available to bind to MuSK. Indeed, it has been demonstrated that both the N-terminal and C-terminal portions of tid1 bind to the human papillomavirus type E17 oncoprotein (Schilling et al., 1998). The existence of such a binding site could also explain why the N-

terminal half of tid1 alone is able to target itself to the plasma membrane and to induce AChR clustering without the C-terminus. Another possibility is that tid1 exists as a dimer. While the tid1 short antibody could bind one monomer of tid1, the other could bind to MuSK. Along these lines, it remains unclear whether MuSK binds to tid1 directly or indirectly in skeletal muscle cells. Direct *in vitro* binding studies have been hampered by the difficulty in obtaining soluble tid1 proteins amenable to biochemical analysis. Tid1 short could actually be binding to another protein or to a multiprotein complex which binds to MuSK. For instance, Dok-7 has recently been shown to bind to MuSK and to mediate its downstream signaling. A homologue of Dok-7, Dok-1, is known to bind to Ras-GAP, which binds to tid1 (Trentin et al., 2001). Therefore, Dok-7 may localize RasGAP to the neuromuscular junction and RasGAP may in turn bind to tid1, allowing it to interact with MuSK-associated proteins (Figure 31). Thus, the tid1 short antibody could bind to tid1 without affecting its indirect binding with MuSK.

The next question raised is how the binding of MuSK to tid1 is tid1 short specific. The terminal 6 amino acids of tid1 short could act as a targeting signal to specifically direct it to the plasma membrane to mediate AChR clustering. Alternatively, the C-terminus of tid1 long could contain a signal which targets it to another cellular location, away from the plasma membrane. The longer C-terminus of tid long could also bind to a protein or multiple proteins which could prevent it from binding to the same proteins that tid1 short binds to (or which act in a different location in the cell). Alternatively, the different C-termini of tid1 short and tid1 long could take on dissimilar spatial conformations which account for differences in their binding partners. Along the lines of tid1 potentially having N-terminal and C-terminal binding sites for MuSK, tid1 short could actually take on the appearance of Ouroboros, or a “snake biting its own tail”. It could be this structure which binds to MuSK, at the N/C-terminal junction. The C-terminal

portion of tid1 short could potentially contain an auto-inhibitory domain which keeps the system turned off until a signal allows for activation of the N-terminal half of tid1 and subsequent AChR clustering. Tid1 long may be incapable of taking on this conformation. The N-terminal half of tid1, lacking this auto-inhibitory domain, yet still containing a MuSK-binding site, may thus be well-suited to induce AChR clustering independently of agrin, as was seen upon transfecting this portion of tid1 into C2C12 muscle cells.

In the bacterial two-hybrid assays, it was found that the juxtamembrane region (residues 515-692) of the cytoplasmic domain of MuSK interacted potently with tid1 short in the absence of other parts of MuSK. This region contains a tyrosine phosphorylation site that is required for agrin-induced AChR clustering (Herbst and Burden, 2000; Watty et al., 2000). However, the finding that tid1 interacts with MuSK in bacteria and in myotubes without agrin treatment suggests that phosphorylation of MuSK may not be required for the protein-protein interaction to occur. In fact, what may be important is the oligomerization of MuSK, rather than its phosphorylation, per se. It may be the agrin-induced oligomerization of MuSK which brings together numerous tid1 molecules and activates the AChR clustering pathway. Nevertheless, the possibility that tyrosine phosphorylation may change the binding affinity of MuSK to tid1 cannot be excluded.

4.4 AChR CLUSTERING ROLE OF TID1: LIKELY MEDIATED BY N-TERMINUS

Transfection of cDNA encoding the C-terminal domain alone into myotubes did not cause a significant change in the number of spontaneous AChR clusters, nor did it lead to the formation of massive AChR clusters following stimulation by agrin. Hence, while the C-

terminal domain is likely involved in mediating tid1 interaction with MuSK, it is not active in inducing AChR clustering in the absence of other parts of tid1. In contrast, transfection with cDNA encoding the N-terminal half of rat tid1 induced robust clustering of AChRs in myotubes, even in the absence of agrin. Moreover, co-expression of the N-terminal half of human tid1 efficiently rescued AChR clustering from potent inhibition by shRNA-mediated knockdown of tid1. Thus, the N-terminal sequence of tid1 is intrinsically active and sufficient to induce AChR clustering. This region of the protein contains a DnaJ domain, which has been shown to mediate interaction with and activation of heat shock protein 70 (hsp70), a co-chaperone of tid1. When histidine 121 of the tid1 DnaJ domain is mutated (H121Q), tid1 is still able to bind hsp70. However, it is no longer able to stimulate its ATPase activity (Syken et al., 1999). In the present study, it was found that the H121Q mutation disrupts the ability of the tid1 N-terminus to rescue C2C12 myotubes from clustering inhibition by RNA interference. These data therefore suggest that the DnaJ domain may regulate AChR clustering by mediating the activation of hsp70 by tid1. Interestingly, the H121Q mutation also interferes with tid1's ability to down-regulate the ErbB2 receptor in breast cancer cells in which it is overexpressed (Kim et al., 2004). Thus, it appears that activation of hsp70 by the DnaJ domain of tid1 is an important component of tid1-mediated RTK signaling.

4.5 TID1-DEFICIENT NMJS FUNCTIONALLY MIMIC MYASTHENIA GRAVIS

Knocking down tid1 protein expression in the muscles of adult mice produces an interesting electrophysiological picture. Examining Table 1, one sees that whereas the resting membrane potential, miniature endplate potential (MEPP) and evoked endplate potential (EPP)

rise times, MEPP frequency, and quantal content remain unchanged between untransfected muscles and those transfected with scrambled or *tid1*-targeted shRNA, the amplitudes of both MEPPs and EPPs are reduced. Thus, the release of ACh from the presynaptic motoneuron terminal remains unchanged, both in terms of the frequency of spontaneous release and the quantal content, or number of vesicles which are released in response to a nerve impulse. Additionally, the inherent speed of the muscle fiber's response to ACh binding at AChRs (depolarization of the membrane potential), reflected in the mean rise time for both MEPPs and EPPs, is unaltered. However, the magnitude of the muscle fiber's response to both spontaneously and nerve-released ACh is decreased in *tid1*-shRNA transfected muscles. Although both MEPP and EPP mean amplitudes are reduced, it is evident that the mean EPP amplitude remains approximately 30 times that of the mean MEPP amplitude, same as for control muscles. Additionally, the reduced EPP amplitude is still greater than the mean MEPP amplitude for control muscles.

Prima facie, the reduced MEPP amplitude in *tid1*-shRNA transfected muscles is difficult to reconcile with theory. For instance, both MEPPs and EPPs arise from the same active area of vesicular release on the motoneuron terminus. Whereas MEPPs represent the release of a single quantum, EPPs are the summation of multiple quanta. If the mean EPP amplitude in *tid1*-shRNA transfected muscles is still greater than the average control MEPP amplitude, then there should be enough receptors on the muscle cell surface to have a normal sized MEPP. In other words, one would not expect to see a decrease in the MEPP amplitude in the *tid1*-shRNA transfected muscles. If there are not enough receptors present on the muscle cell membrane to accommodate spontaneous release, it is hard to imagine that there are enough to produce a larger response to nerve-induced ACh release.

However, the electrophysiologic profile of muscle in which *tid1* has been knocked down closely mirrors that which is classically associated with myasthenia gravis (MG). MG is an autoimmune disease where antibodies attack patient AChRs and, in rarer cases, MuSK. The result is a progressive and fatigable muscle weakness disorder that is worsened with exertion or physiologic stressors. Postsynaptically, the number of AChRs is reduced to around 11-30% of normal and the structure of the postsynaptic membrane is greatly simplified, with sparse and shallow postjunctional folds (Drachman, 1981). Electrophysiologically, both the average MEPP and EPP amplitudes are decreased. However, the mean EPP amplitude remains larger than the average control or MG MEPP amplitude. This is true in human MG patients (Lindstrom et al., 1976), when the serum of human MG patients is injected into rodents (Toyka et al., 1975), or when MG is experimentally induced in rodents either passively, acutely, or chronically (Lindstrom et al., 1976). In contrast, there are a normal number of presynaptic ACh vesicles, and both the MEPP frequency and quantal content remain unchanged. In terms of the AChRs themselves, they have normal current flow and the opening times of their ion channels are unaltered (Drachman, 1981).

Reexamination of the theory helps to reconcile the electrophysiologic findings in MG (and *tid1* knockdown) with the anatomic picture. The magnitudes of MEPPs and EPPs both depend upon the number of interactions between ACh molecules and AChRs. At the normal NMJ, only a proportion of the released ACh molecules will interact with AChRs. Similarly, only a small fraction of the millions of AChRs at the NMJ will be activated at one time. If either the number of AChR molecules released or the number of AChRs is altered, the amplitudes of the MEPPs and/or EPPs will change accordingly. For instance, an α -cobra toxin, which binds to and inhibits AChRs, will decrease the measured MEPP and EPP amplitudes. A reduction in the total

number of postsynaptic AChRs at the NMJ will similarly decrease the number of interactions between ACh molecules and AChRs and thus the MEPP and EPP amplitudes will be decreased, as is seen in MG. Regardless of the number of ACh molecules present (MEPP versus EPP), there are still less AChRs available to interact with them. Consequently, both amplitudes are reduced. Using a cholinesterase inhibitor increases the EPP amplitude measured in MG muscle. This can be accounted for by an increase in the amount of available ACh and thus an increase in the number of interactions between ACh and AChRs (Drachman, 1981). Presynaptically in MG, the amount of ACh released remains normal. Even at a level of 20% of normal, the number of postsynaptic AChRs at the NMJ remains at least a couple magnitudes greater than the number of ACh molecules released from one vesicle. Consequently, EPPs, which represent the muscle fiber's response to the release of multiple quanta (essentially a flooding of the system with ACh molecules), are still greater in magnitude than MEPPs in MG.

The fact that the electrophysiologic characteristics of neuromuscular junctions in which *tid1* has been knocked down so closely resemble those found in myasthenia gravis emphasizes the importance of *tid1* at the NMJ and its potential link to muscle weakness disorders. Additionally, it gives a glimpse into the expected clinical picture upon depletion of *tid1*. It is possible that further characterization of patients with MG-like symptoms but with no circulating antibodies to AChRs or MuSK may reveal that these patients have a defect or mutation in *tid1*. The electrophysiologic profile seen in MG is not merely based upon an alteration in the number of AChRs at the NMJ. As mentioned above, the morphology of the NMJ is fundamentally altered. This is likely due to lymphocytic invasion and destruction of the postsynaptic membrane by macrophages and complement-mediated lysis (Lindstrom et al., 1976). During the acute phase of experimentally induced MG, segmental necrosis of the NMJ occurs and there is actually

splitting of the endplate from the muscle fiber. More complete studies are needed to fully characterize the *tid1*-deficient NMJ, both electrophysiologically and anatomically. Certainly, the gross NMJ morphology is altered by *tid1* knockdown. However, it is unclear exactly how the NMJ shape is changed and what modifications are taking place, dynamically speaking, at the NMJ.

4.6 POTENTIAL MECHANISMS OF ACTION FOR TID1 IN REGULATING THE CLUSTERING OF AChRS AT THE NMJ

The precise mechanism by which *tid1* regulates synapse formation at the NMJ remains largely unknown. However, based on data derived from the current studies and previously published research, it is postulated that *tid1* may act via several distinct pathways. First, it has previously been reported that the protein Adenomatous Polyposis Coli, APC, binds to the beta subunit of AChR in C2C12 myotubes and at the mouse NMJ, and that it may play a role in regulating the formation of AChR clusters (Wang et al., 2003). Interestingly, studies by others have demonstrated a direct interaction between *tid1* and APC (Polakis, 1997). Thus, *tid1* may link AChRs to the MuSK scaffold at the NMJ through a connection with APC (Figure 31, pathway A). Secondly, *tid1* may play a role in regulating the activity of small GTPases and the dynamics of the muscle cytoskeleton during NMJ development. Neural agrin has been shown to activate Rac1, Cdc42, and RhoA in muscle cells (Weston et al., 2000, 2003). Reorganization of the postsynaptic cytoskeleton subsequent to the activation of small GTPases is believed to be one of the final steps in the signaling cascade that leads to AChR clustering (Weston et al., 2000, 2003; Luo et al., 2002). Through the DnaJ domain, *tid1* can interact with and activate hsp70,

which has been shown to influence cytoskeletal dynamics directly (Liang and MacRae, 1997; Figure 31, pathway B). Tid1 is also known to bind to heat shock cognate protein 70 (hsc70) (Lu et al., 2006), which can negatively regulate the activation of Rac1, Cdc42, and RhoA by Dbl, a guanine nucleotide exchange factor (GEF, Kauppinen et al., 2005). Tid1 could signal Hsc70 to disengage from Dbl, thus releasing the latter to activate downstream Rho GTPases (Figure 31, pathway B). It has been proposed that interaction between tid1/hsp70 and RasGAP promotes the formation of a signaling complex which influences the fate of the cytoskeleton (Trentin et al., 2001). Indeed, in addition to binding to tid1 and Dok-1, RasGAP is also known to bind to p190 (Settleman et al., 1992), a Rho/Rac GTPase activating protein. Interaction between tid1 and RasGAP and subsequent activation of p190 could thus provide a mechanism for Rho GTPase activation downstream of MuSK (Figure 31, pathway C). If Dok-7 behaves as Dok-1 does, it could provide a link between MuSK activation, the involvement of abl kinases, and downstream stimulation of the Rac1/Cdc42/RhoA small GTPases. For instance, Dok-1 is known to be phosphorylated by abl kinases (Yamanashi and Baltimore, 1997). This phosphorylation better enables activation of RasGAP and subsequently p190 and the small GTPases. Finally, tid1 could be acting through a yet-unknown pathway (Figure 31, pathway D).

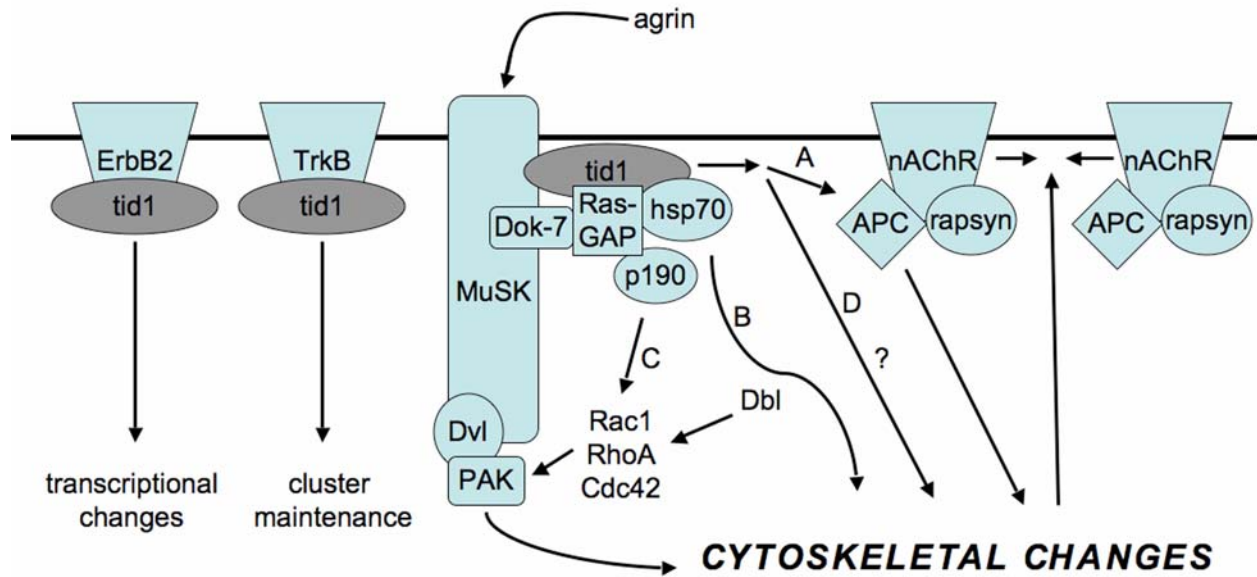


Figure 31. Schematic representation of putative pathways through which tid1 may regulate AChR clustering.

Tid1 may act downstream of MuSK through pathways A–D to cause reorganization of the postsynaptic cytoskeleton in muscle cells, an important step in AChR clustering. In addition, tid1 may interact with two other RTKs, ErbB2 and TrkB, at NMJ postsynaptic membranes. The ErbB2 pathway regulates subsynaptic transcription of genes encoding AChR subunits. TrkB has been shown to be required for the maintenance of AChR clusters.

4.7 OTHER POTENTIAL ROLES FOR TID1 AT THE NMJ

Tid1 may have additional roles at the NMJ other than the regulation of small GTPase activity and cytoskeletal reorganization. In non-muscle cells, tid1 interacts with the RTKs ErbB2 and TrkA and regulates their downstream signaling pathways (Kim et al., 2004; Liu et al., 2005). ErbB2 and TrkB, to which tid1 also binds, have been shown to be highly concentrated on the postsynaptic membranes of the NMJ (Jo et al., 1995; Gonzalez et al., 1999; Falls, 2003). ErbB2, together with ErbB4, acts as the receptor for motoneuron-derived neuregulin (ARIA), which regulates sub-synaptic gene transcription and the local insertion of AChRs at the NMJ

(Escher et al., 2005; Jaworski and Burden, 2006). In binding assays with ^{125}I - α -BTX as a radioligand, it was shown that overexpression of the N-terminal domain of *tid1* in C2C12 myotubes markedly enhanced the expression of AChRs on the cell surface. This finding is consistent with the notion that *tid1* may also be acting as a potential downstream effector of ErbB2 at the NMJ. MuSK has also been linked to the regulation of subsynaptic gene transcription. Some crosstalk has been demonstrated between MuSK and ErbB signaling (Strochlic et al., 2005). *Tid1* could thus be a potential mediator of such coordinated interaction between the two pathways. Additionally, the N-terminal portion of *tid1* contains the DnaJ domain, which traditionally interacts with hsp/c70 as an activator of chaperone-like activities, such as protein folding. The N-terminal half of *tid1* could thus be enhancing sub-synaptic protein synthesis by aiding in the folding of nascent polypeptides (Ohtsuka and Suzuki, 2000).

A role for TrkB in the maintenance of AChR localization at the NMJ has also been firmly established. Disruption of TrkB signaling by dominant negative inhibition or a reduction of TrkB expression in muscles of mutant mice (*TrkB^{+/-}*) results in a dispersal and gradual loss of AChRs from the NMJ (Gonzalez et al., 1999). Interestingly, the abnormalities in the morphology of AChR clusters seen in the TrkB mutant mice closely resemble those found at the NMJs in myofibers whose level of *tid1* has been reduced by RNA interference. Through a complex interplay with TrkB, ErbB and MuSK, *tid1* may help to unite these multiple RTK signaling programs and to coordinate the synaptic localization and expression of AChRs. An important question to be addressed in future studies is how and when these different pathways may converge during neuromuscular synapse development.

4.8 MOLECULAR CHAPERONES AT SYNAPSES

By identifying *tid1* as a novel player in the postsynaptic apparatus, the present studies build on the notion that molecular chaperones, or members of the heat shock protein (hsp) family, play important roles in regulating synaptic structure and function at the NMJ. This is an interesting development, as such activities are outside the realm of functions traditionally attributed to hsps. However, there is increasing evidence that hsps act as players in numerous cellular signaling pathways, in addition to their better-known roles in aiding protein folding and promoting cellular survival under stress (Gaestel, 2006). Indeed, *tid1* itself has been attributed with a number of signaling roles. As mentioned above, *tid1* is a member of the DnaJ protein family, which includes *hsp40*. DnaJ proteins comprise perhaps the largest group of chaperones known (Cheetham and Caplan, 1998). However, unlike other chaperone families, which are well conserved throughout evolution, the DnaJ family is comprised of a group of proteins with surprisingly diverse structures. Indeed, it is only the 70 amino acid J domain which is absolutely conserved in DnaJ proteins. The other regions in these proteins are extremely variable. As stated by Cheetham and Caplan, “DnaJ-like proteins are not all variations on a theme”. In fact, although they are all DnaJ proteins, *tid1*, *hsp40*, and another protein known as cysteine string protein are each in different sub-groupings of DnaJ proteins, due to their dissimilar domain structures. It has been proposed that the diverse DnaJ proteins serve to target the co-chaperone *hsp/c70* to particular cellular locations for site-specific functions. The lack of a standard DnaJ protein structure may account for the wide range of functions attributed to J domain-containing proteins, such as roles in protein folding, protein degradation, exo/endocytosis, viral infection, cell cycle control, and immortality control.

Tid1 is not the first DnaJ protein to be implicated in the regulation of synaptic structure and function. In fact, cysteine string protein, or csp, has previously been identified as a presynaptic protein that regulates synaptic growth, the evoked release of neurotransmitters, and the intra-terminal level of calcium (Bronk et al., 2005). Specifically, csp modulates presynaptic calcium channels (Mastrogiacomo et al., 1994), plays a direct role in exocytosis, and behaves as a use-dependent synaptic molecular chaperone. As a secretory vesicle protein, csp plays important roles in presynaptic neurotransmission and regulated exocytosis from non-neuronal cells. In adipocytes, csp is actually stably associated with the plasma membrane, as opposed to being a component of glucose transporter storage vesicles (Chamberlain et al., 2001). When csp is knocked out in mice and flies, there is progressive central nervous system neurodegeneration, paralysis, and premature lethality. In terms of the NMJ, a lack of csp leads to abnormal neurotransmitter release and calcium levels at the motoneuron termini, especially with temperature changes. Whereas progressive deterioration with age and temperature imply chaperone-like functions of csp, in-depth structure/function analyses of csp have revealed that the protein clearly has non-chaperone-like functions, including G-protein linked signaling and exocytosis (Bronk et al., 2005). Like tid1, csp has been linked with hsc70 activity through its J domain (Bai et al., 2007). Overall, csp has been hypothesized to have a mixture of chaperone-like and un-chaperone-like functions.

One must be cautious not to over-extrapolate functions from one DnaJ protein to another, on account of their varying structures. Indeed, it is becoming apparent that even tid1 long and tid1 short, both DnaJ proteins which differ only in their C-termini after 447 common amino acids, have strikingly diverse, if not opposing, functions. For instance, whereas tid1 short suppresses exogenously induced apoptosis, tid1 long enhances it (Syken et al., 1999).

Interestingly, csp has two forms, 1 and 2, which differ in the C-termini in a similar fashion to tid1 long and short. Namely, csp1 has an additional 34 amino acids at its C-terminus (tid1 long has 33), whereas csp2 has an additional 3 amino acids (tid1 short has 6). The two isoforms of csp are differentially regulated during development and the dissimilarities in their C-termini account for the selectivity in binding between csp1 and 2 and their respective partners (Chamberlain et al., 2001). For instance, whereas syntaxin 4 interacts exclusively with csp1, syntaxin 1A binds to both csp1 and 2, although with a higher affinity to csp2. However, csp remains an established example of a DnaJ protein that is associated with synapses and which has un-chaperone-like functions.

Similarly, hsp40 and hsp/c70 have also been localized to synapses of the central nervous system. Like tid1 at the NMJ, hsps 40 and 70 are found postsynaptically (Ohtsuka and Suzuki, 2000). While they certainly function to stabilize the folding of wild type and denatured proteins, especially in the face of harmful stimuli, it has been proposed that their presence at synapses could be essential for normal synaptic transmission in the absence of cellular stress. For example, it has been hypothesized that the chaperones may regulate protein-protein interactions mediated via specific domains, such as PDZ-like domains.

Considering what is known about its DnaJ protein homologues csp and hsp40, it is not surprising that tid1 does not appear to be acting in the traditional chaperone-capacity at the NMJ and that its function appears to be isoform-specific. Remember, the *Drosophila* homologue to tid1, tid56, is not heat shock inducible, and thus tid56 has not been classified as a hsp (Kurzik-Dumke et al., 1995). However, one cannot at this stage rule out the possibility that tid1 is somehow acting as a molecular chaperone to stabilize the conformation of a multiprotein complex that is essential for AChR clustering at the NMJ. Indeed, the reliance of tid1-mediated

AChR clustering on hsp/c70, a traditional molecular chaperone, points in this direction. Similarly, it has been proposed that csp functions at least partially as a chaperone that aids in the assembly of secretory vesicle proteins and protein complexes which modulate presynaptic calcium channels. It has been postulated that such activities need not be acute functions (Chamberlain et al., 2001), which could account for the involvement of these chaperone proteins in processes which are generally more stable than traditional chaperone-associated functions. This is especially true of AChR clustering, which is a relatively stable and long-term phenomenon that must be maintained throughout life. Like the DnaJ proteins csp and hsp40, it is probable that tid1 is actually performing a variety of functions at the NMJ, likely a combination of traditional chaperone-like and un-chaperone-like roles.

Interestingly, hsps are gaining importance in a number of neurological conditions, especially in the field of neurodegeneration. A number of diseases, such as Alzheimer's, Parkinson's, and Huntington's, are associated with large aggregates of misfolded proteins. A current theory behind this is the titrating out, or overwhelming, of hsps. Hsps are well known for their ability to aid proteins in folding. However, with their multiple cellular responsibilities, when confronted with stressors, hsps may reduce their protein folding activities in favor of actions which cope with altered environmental conditions, such as oxidative damage or inflammation, that more immediately threaten the overall wellbeing of the cell (Urbanics, 2000; Calabrese et al., 2004). For instance, it is well known that patients with myasthenia gravis (MG) demonstrate worsening symptoms upon exertion or on experiencing heat, stress, or illness from any type of infection (Hopkins, 1994). Such characteristics implicate the involvement of a hsp-like protein. These exacerbations could, in theory, be caused by tid1 temporarily suspending its non-chaperone-like actions at the NMJ in order to deal with the additional stressor(s) through

one of its other, hsp-like roles. MG patients already have decreased reserves and a reduced capacity for neurotransmission at the NMJ. A depletion of *tid1* from the NMJ could thus have dire consequences and could explain the worsening clinical picture that is observed. Therapeutic approaches which aim at overexpressing hsps are currently being explored as treatments for neurodegenerative conditions and ischemic injuries. Perhaps similar strategies need to be investigated for the treatment of diseases of the NMJ.

4.9 FUTURE DIRECTIONS

The current studies point to the idea that *tid1* regulates both the formation and maintenance of AChR clusters at the NMJ. However, while the evidence for *tid1*'s role in AChR cluster maintenance was gathered from both *in vitro* and *in vivo* studies, findings supporting *tid1*'s role in cluster formation were taken solely from *in vitro* experiments. The findings that 1) *tid1* knockdown prevents the formation of spontaneous and agrin-induced clusters and that 2) the N-terminal half of *tid1* induces AChR cluster formation in the absence of neural agrin in cultured myotubes do provide support for the notion that *tid1* plays a role in AChR cluster formation. However, the fact remains that this assertion has not been tested *in vivo*.

The hypothesis that *tid1* regulates AChR cluster formation needs to be further tested and confirmed. An indirect way to do this would be to examine *tid1* expression throughout development. It would be useful to examine where and when *tid1* transcripts are detected and when the protein is expressed. If, for instance, *tid1* transcripts are localized to the motor endplate during early neuromuscular synaptogenesis and if *tid1* is expressed just prior to the arrival of the motoneuron, then there is at least evidence that it is temporally and spatially

feasible that *tid1* is involved in AChR cluster formation. A more direct way to test whether *tid1* is required for the formation of AChR clusters is to knock it out entirely. A global knockout of *tid1* has been generated (Lo et al., 2004). Unfortunately, it is embryonic lethal, dying at E6.5, even before skeletal muscles have started to form, which usually occurs around E11-12. A conditional knockout would have to be generated specifically in skeletal muscle. This has already been done for cardiac muscle (Hayashi et al., 2006). Cardiac muscle in which *tid1* has been knocked out is highly abnormal, with a large degree of mitochondrial disruption. In fact, this conditional knockout has been proposed as a model for dilated cardiomyopathy.

Skeletal-muscle-specific knockdown of *tid1* can be achieved by crossing a mouse where loxP sites surround a portion of the *tid1* gene with a mouse that transcribes Cre under the control of a truly skeletal-muscle specific promoter, such as the one for *mef2c* (Heidt and Black, 2005). Prior “skeletal muscle”-specific promoters, such as those for *muscle creatine kinase (MCK)* and *myosin light chain* have been problematic, in that they have also expressed Cre in cardiac and smooth muscle and they have not expressed Cre in both fast and slow-twitch fibers. If *tid1* is indeed necessary for AChR cluster formation, then the phenotype of its knockout mouse should be similar to those observed for MuSK and rapsyn. Namely, it should lack AChR clusters entirely. Given that *tid1* is likely mediating signaling just downstream of MuSK and that it may also be mediating ErbB-linked regulation of subsynaptic-specific transcription of NMJ proteins, a skeletal-muscle specific knockout of *tid1* should appear more like the MuSK knockout than the rapsyn knockout mouse. For instance, it would be reasonable to expect that clustering of other NMJ-specific proteins, such as utrophin, is disrupted and that the transcription of these proteins is uniform throughout muscle fibers.

A similar approach could be used to further confirm the proposition that *tid1* regulates the maintenance of AChR clusters at the NMJ. The strongest evidence for this notion comes from the current electroporation studies of shRNA-mediated knockdown of *tid1* in adult mice. Knocking down *tid1* in the adult mouse results in severe disruptions in the structure and function of the NMJ. Recently, Hesser et al. (2006) conditionally knocked out MuSK postnatally. They did this by utilizing a loxP/Cre system in which expression of Cre recombinase increases during postnatal development. In their system, Cre recombinase is under the control of the MCK promoter, which controls MCK expression such that it reaches a maximal level at postnatal day 10. This level of protein expression is then sustained throughout life. Hesser and colleagues found that postnatal inactivation of MuSK results in the disappearance of AChR clusters and a disruption of NMJ structure, similar to what was observed in the electroporation studies detailed above. The same system could be used to knock out *tid1* postnatally. It would be expected that the phenotype of this mouse would be similar to that observed for shRNA-mediated knock down of *tid1*, with disrupted NMJ structure and function.

Further studies need to be undertaken to clarify the mechanism of action of *tid1*. For instance, Figure 31 outlines a number of different pathways through which *tid1* could be acting at the NMJ. It is important to determine which one(s) of these are relevant. For instance, experiments need to be performed to determine whether *tid1* binds to APC and/or RasGAP at the NMJ. This could be accomplished by co-immunoprecipitation studies and/or immunostaining experiments, as were done to demonstrate that *tid1* binds to MuSK and that *tid1* colocalizes with AChRs at the NMJ. Other *tid1*-interactors could be identified by running a 2 dimensional gel of anti-*tid1*-immunoprecipitated myotube or skeletal muscle extracts, followed by mass spectrophotometric analyses of resulting proteins. Biochemical studies need to be carried out to

determine whether the RhoA/Cdc42/Rac1 small GTPases are activated downstream of tid and whether they are activated by p190 and/or dbl. Additionally, it needs to be determined whether downstream effectors of Trk and ErbB are stimulated by tid1. An example experiment could be transfecting C2C12 myotubes with the N-terminal half of tid1 and seeing whether the small GTPases and/or Trk and ErbB pathways are activated. If they are stimulated, then studies could be done to determine whether the activation is blocked by co-expression of the H121Q mutant, which could serve as a dominant negative tid1 construct. Additionally, inhibitors of the various pathways could be tested to determine whether they disrupt the increases in AChR clustering and expression that are induced by the transfection of the N-terminal half of tid1 into C2C12 myotubes.

One of the ultimate goals of this research is to make medically relevant discoveries. For instance, in the case of MuSK, there are patients with myasthenia gravis that make autoantibodies against MuSK (Hoch et al., 2001). For rapsyn and Dok-7, there are patients with congenital myasthenic syndromes that have mutations in these proteins (Ohno et al., 2000; Beeson et al., 2006; Muller et al., 2006). There are also patient populations with congenital muscular dystrophy that have defects in the glycosylation of α -dystroglycan (Matsumoto et al., 2005). It would be interesting and relevant to study whether mutations in tid1 underlie previously uncharacterized congenital myasthenic syndromes. Furthermore, it would be imperative to determine whether the discovery of tid1 at the NMJ has any therapeutic relevance. For instance, “mini-agrin” has been used to successfully stabilize the muscle cell membrane and to relieve symptoms in a mouse model of congenital muscular dystrophy (Moll et al., 2001; Bentzinger et al., 2005). Could the N-terminal half of tid1 relieve NMJ dysfunction caused by autoantibodies targeted towards MuSK or by one of the many congenital muscular dystrophy

disorders? By exploring such possibilities, tid1 may become the latest example of a hsp-like protein that is targeted as a therapy for a neurological condition (Soti et al., 2005).

BIBLIOGRAPHY

- Apel, E. D., Roberds, S. L., Campbell, K. P., and Merlie, J. P. (1995). Rapsyn may function as a link between the acetylcholine receptor and the agrin-binding dystrophin-associated glycoprotein complex. *Neuron* 15, 115-126.
- Apel, E. D., Glass, D. J., Moscoso, L. M., Yancopoulos, G. D., and Sanes, J. R. (1997). Rapsyn is required for MuSK signaling and recruits synaptic components to a MuSK-containing scaffold. *Neuron* 18, 623-635.
- Arrowsmith, J. E. (2007). The neuromuscular junction. *Surgery (Oxford)* 25(3), 105-111.
- Bai, L., Swayne, L. A., and Braun, J. E. (2007). The CSPalpha/G protein complex in PC12 cells. *Biochem Biophys Res Commun* 352, 123-129.
- Beeson, D., Higuchi, O., Palace, J., Cossins, J., Spearman, H., Maxwell, S., Newsom-Davis, J., Burke, G., Fawcett, P., Motomura, M., Muller, J. S., Lochmuller, H., Slater, C., Vincent, A., Yamanashi, Y. (2006). Dok-7 mutations underlie a neuromuscular junction synaptopathy. *Science* 313, 1975-1978.
- Bentzinger, C. F., Barzaghi, P., Lin, S., and Ruegg, M. A. (2005). Overexpression of mini-agrin in skeletal muscle increases muscle integrity and regenerative capacity in laminin-alpha2-deficient mice. *Faseb J* 19, 934-942.
- Brandon, E. P., Lin, W., D'Amour, K. A., Pizzo, D. P., Dominguez, B., Sugiura, Y., Thode, S., Ko, C. P., Thal, L. J., Gage, F. H., and Lee, K. F. (2003). Aberrant patterning of neuromuscular synapses in choline acetyltransferase-deficient mice. *J Neurosci* 23, 539-549.
- Bronk, P., Nie, Z., Klose, M. K., Dawson-Scully, K., Zhang, J., Robertson, R. M., Atwood, H. L., and Zinsmaier, K. E. (2005). The multiple functions of cysteine-string protein analyzed at *Drosophila* nerve terminals. *J Neurosci* 25, 2204-2214.
- Burden, S. (2002). Building the vertebrate neuromuscular synapse. *J. Neurobiol.* 53, 501-511.

- Calabrese, V., Boyd-Kimball, D., Scapagnini, G., and Butterfield, D. A. (2004). Nitric oxide and cellular stress response in brain aging and neurodegenerative disorders: the role of vitagenes. *In Vivo* 18, 245-267.
- Carraway, K. L., 3rd, and Burden, S. J. (1995). Neuregulins and their receptors. *Curr Opin Neurobiol* 5, 606-612.
- Chamberlain, L. H., Graham, M. E., Kane, S., Jackson, J. L., Maier, V. H., Burgoyne, R. D., and Gould, G. W. (2001). The synaptic vesicle protein, cysteine-string protein, is associated with the plasma membrane in 3T3-L1 adipocytes and interacts with syntaxin 4. *J Cell Sci* 114, 445-455.
- Changeux, J.-P., Edelman, S. J. (2005). *Nicotinic Acetylcholine Receptors; From Molecular Biology to Cognition* (New York: Odile Jacob Publishing Corporation).
- Cheetham, M. E., and Caplan, A. J. (1998). Structure, function and evolution of DnaJ: conservation and adaptation of chaperone function. *Cell Stress Chaperones* 3, 28-36.
- Christian, C. N., Daniels, M. P., Sugiyama, H., Vogel, Z., Jacques, L., and Nelson, P. G. (1978). A factor from neurons increases the number of acetylcholine receptor aggregates on cultured muscle cells. *Proceedings of the National Academy of Sciences of the United States of America* 75, 4011-4015.
- DeChiara, T. M., Bowen, D. C., Valenzuela, D. M., Simmons, M. V., Poueymirou, W. T., Thomas, S., Kinetz, E., Compton, D. L., Rojas, E., Park, J. S., et al. (1996). The receptor tyrosine kinase MuSK is required for neuromuscular junction formation in vivo. *Cell* 85, 501-512.
- Denzer, A. J., Brandenberger, R., Gesemann, M., Chiquet, M., and Rugg, M. A. (1997). Agrin binds to the nerve-muscle basal lamina via laminin. *J Cell Biol* 137, 671-683.
- Drachman, D. B. (1981). The biology of myasthenia gravis. *Annu Rev Neurosci* 4, 195-225.
- Driever, W., Stemple, D., Schier, A., and Solnica-Krezel, L. (1994). Zebrafish: genetic tools for studying vertebrate development. *Trends Genet* 10, 152-159.
- Dutton, E. K., Uhm, C. S., Samuelsson, S. J., Schaffner, A. E., Fitzgerald, S. C., and Daniels, M. P. (1995). Acetylcholine receptor aggregation at nerve-muscle contacts in mammalian cultures: induction by ventral spinal cord neurons is specific to axons. *J Neurosci* 15, 7401-7416.
- Escher, P., Lacazette, E., Courtet, M., Blindenbacher, A., Landmann, L., Bezakova, G., Lloyd, K. C., Mueller, U., Brenner, H. R. (2005). Synapses form in skeletal muscles lacking neuregulin receptor. *Science* 308(5730), 1920-1923.

- Fallon, J. R., and Hall, Z. W. (1994). Building synapses: agrin and dystroglycan stick together. *Trends Neurosci* 17, 469-473.
- Falls, D. L. (2003). Neuregulins and the neuromuscular system: 10 years of answers and questions. *J. Neurocytol.* 32(5-8), 619-647.
- Ferns, M., Hoch, W., Campanelli, J. T., Rupp, F., Hall, Z. W., and Scheller, R. H. (1992). RNA splicing regulates agrin-mediated acetylcholine receptor clustering activity on cultured myotubes. *Neuron* 8, 1079-1086.
- Ferns, M. J., Campanelli, J. T., Hoch, W., Scheller, R. H., and Hall, Z. (1993). The ability of agrin to cluster AChRs depends on alternative splicing and on cell surface proteoglycans. *Neuron* 11, 491-502.
- Ferns, M., Deiner, M., Hall, Z. (1996). Agrin-induced acetylcholine receptor clustering in mammalian muscle requires tyrosine phosphorylation. *J. Cell Biol.* 132(5), 937-944.
- Ferns, M., and Carbonetto, S. (2001). Challenging the neurocentric view of neuromuscular synapse formation. *Neuron* 30, 311-314.
- Finn, A. J., Feng, G., Pendergast, A. M. (2003). Postsynaptic requirement for Abl kinases in assembly of the neuromuscular junction. *Nature Neuroscience* 6(7), 717-723.
- Flanagan-Steet, H., Fox, M. A., Meyer, D., and Sanes, J. R. (2005). Neuromuscular synapses can form in vivo by incorporation of initially aneural postsynaptic specializations. *Development* 132, 4471-4481.
- Forsayeth, J. R., Garcia, P. D. (1994). Adenovirus-mediated transfection of cultured cells. *Biotechniques* 17(2), 354-356.
- Frail, D. E., McLaughlin, L. L., Mudd, J., and Merlie, J. P. (1988). Identification of the mouse muscle 43,000-dalton acetylcholine receptor-associated protein (RAPsyn) by cDNA cloning. *J Biol Chem* 263, 15602-15607.
- Frank, E., Gautvik, K., Sommerschild, H. (1976). Persistence of junctional acetylcholine receptors following denervation. *Cold Spring Harb. Symp. Quant. Biol.* 40, 275-281.
- Fuhrer, C., Sugiyama, J. E., Taylor, R. G., and Hall, Z. W. (1997). Association of muscle-specific kinase MuSK with the acetylcholine receptor in mammalian muscle. *EMBO J* 16, 4951-4960.
- Gaestel, M. (2006). Molecular chaperones in signal transduction. *Handb. Exp. Pharmacol.* 172, 93-109.
- Gateff, E. (1978). Malignant neoplasms of genetic origin in *Drosophila melanogaster*. *Science* 200, 1448-1459.

- Gateff, E., and Mechler, B. M. (1989). Tumor-suppressor genes of *Drosophila melanogaster*. *Crit Rev Oncog 1*, 221-245.
- Gautam, M., Noakes, P. G., Mudd, J., Nichol, M., Chu, G. C., Sanes, J. R., and Merlie, J. P. (1995). Failure of postsynaptic specialization to develop at neuromuscular junctions of rapsyn-deficient mice. *Nature 377*, 232-236.
- Gautam, M., Noakes, P. G., Moscoso, L., Rupp, F., Scheller, R. H., Merlie, J. P., and Sanes, J. R. (1996). Defective neuromuscular synaptogenesis in agrin-deficient mutant mice. *Cell 85*, 525-535.
- Glass, D. J., Bowen, D. C., Stitt, T. N., Radziejewski, C., Bruno, J., Ryan, T. E., Gies, D. R., Shah, S., Mattsson, K., Burden, S. J., DiStefano, P. S., Valenzuela, D. M., DeChiara, T. M., Yancopoulos, G. D. (1996). Agrin acts via a MuSK receptor complex. *Cell 85*, 513-523.
- Gonzalez, M., Ruggiero, F. P., Chang, Q., Shi, Y.-J., Rich, M. M., Kraner, S., and Balice-Gordon, R. J. (1999). Disruption of TrkB-mediated signaling induces disassembly of postsynaptic receptor clusters at neuromuscular junctions. *Neuron 24*, 567-583.
- Hayashi, M., Imanaka-Yoshida, K., Yoshida, T., Wood, M., Fearn, C., Tatake, R. J., and Lee, J. D. (2006). A crucial role of mitochondrial Hsp40 in preventing dilated cardiomyopathy. *Nat Med 12*, 128-132.
- Heffner, R. R., Jr., Balos, L. L. (2006). Skeletal Muscle. In *Histology for pathologists*, S. E. Mills, ed. (Lippincott, Williams and Wilkins), pp. 195-216.
- Heidt, A. B., and Black, B. L. (2005). Transgenic mice that express Cre recombinase under control of a skeletal muscle-specific promoter from *mef2c*. *Genesis 42*, 28-32.
- Henry, M. D., and Campbell, K. P. (1996). Dystroglycan: an extracellular matrix receptor linked to the cytoskeleton. *Curr Opin Cell Biol 8*, 625-631.
- Herbst, R., Burden, S. (2000). The juxtamembrane region of MuSK has a critical role in agrin-mediated signaling. *EMBO 19(1)*, 67-77.
- Hesser, B. A., Henschel, O., and Witzemann, V. (2006). Synapse disassembly and formation of new synapses in postnatal muscle upon conditional inactivation of MuSK. *Mol Cell Neurosci 31*, 470-480.
- Hoch, W., Ferns, M., Campanelli, J. T., Hall, Z. W., and Scheller, R. H. (1993). Developmental regulation of highly active alternatively spliced forms of agrin. *Neuron 11*, 479-490.

- Hoch, W., McConville, J., Helms, S., Newsom-Davis, J., Melms, A., and Vincent, A. (2001). Auto-antibodies to the receptor tyrosine kinase MuSK in patients with myasthenia gravis without acetylcholine receptor antibodies. *Nat Med* 7, 365-368.
- Hopkins, L. C. (1994). Clinical features of myasthenia gravis. *Neurol Clin* 12, 243-261.
- Hsu, C. H., Wen, Z. H., Lin, C. S., and Chakraborty, C. (2007). The zebrafish model: use in studying cellular mechanisms for a spectrum of clinical disease entities. *Curr Neurovasc Res* 4, 111-120.
- Jacobson, C., Montanaro, F., Lindenbaum, M., Carbonetto, S., Ferns, M. (1998). Alpha-dystroglycan functions in acetylcholine receptor aggregation but is not a coreceptor for agrin-MuSK signaling. *J. Neurosci.* 18(16), 6340-6348.
- Jacobson, C., Cote, P. D., Rossi, S. G., Rotundo, R. L., Carbonetto, S. (2001). The dystroglycan complex is necessary for stabilization of acetylcholine receptor clusters at neuromuscular junctions and formation of the synaptic basement membrane. *J. Cell Biology* 152(3), 435-450.
- Jaworski, A., Burden, S. J. (2006). Neuromuscular synapse formation in mice lacking motor neuron- and skeletal muscle-derived Neuregulin-1. *J. Neurosci.* 26(2), 655-661.
- Jo, S. A., Zhu, X., Marchionni, M. A., Burden, S. J. (1995). Neuregulins are concentrated at nerve-muscle synapses and activate ACh-receptor gene expression. *Nature* 373(6510), 158-161.
- Joung, J., Ramm, E., Pabo, C. (2000). A bacterial two-hybrid system for studying protein-DNA and protein-protein interactions. *PNAS* 97(13), 7382-7387.
- Kauppinen, K., Duan, F., Wels, J., Manor, D. (2005). Regulation of the Dbl proto-oncogene by heat shock cognate protein 70 (Hsc70). *J. Biol. Chem.* 280(22), 21638-21644.
- Kim, S.-W., Chao, T. H., Xiang, R., Lo, J. F., Campbell, M. J., Fearn, C., Lee, J.-D. (2004). Tid1, the human homologue of a Drosophila tumor suppressor, reduces the malignant activity of ErbB-2 in carcinoma cells. *Cancer Research* 64(21), 7732-7739.
- Kim, S. W., Hayashi, M., Lo, J. F., Fearn, C., Xiang, R., Lazennec, G., Yang, Y., and Lee, J. D. (2005). Tid1 negatively regulates the migratory potential of cancer cells by inhibiting the production of interleukin-8. *Cancer Res* 65, 8784-8791.
- Kong, X. C., Barzaghi, P., Ruegg, M. (2004). Inhibition of synapse assembly in mammalian muscle in vivo by RNA interference. *EMBO Reports* 5(2), 183-188.
- Kummer, T. T., Misgeld, T., Lichtman, J. W., and Sanes, J. R. (2004). Nerve-independent formation of a topologically complex postsynaptic apparatus. *J Cell Biol* 164, 1077-1087.

- Kurzik-Dumke, U., Phannavong, B., Gundacker, D., and Gateff, E. (1992). Genetic, cytogenetic and developmental analysis of the *Drosophila melanogaster* tumor suppressor gene lethal(2)tumorous imaginal discs (l(2)tid). *Differentiation* 51, 91-104.
- Kurzik-Dumke, U., Gundacker, D., Renthrop, M., and Gateff, E. (1995). Tumor suppression in *Drosophila* is causally related to the function of the lethal(2) tumorous imaginal discs gene, a DnaJ homolog. *Dev Genet* 16, 64-76.
- Landowne, David. (2006). Synapses. In *Cell Physiology*, (United States: McGraw-Hill Medical Publishing Division), pp. 95-97.
- Liang, P., MacRae, T. H. (1997). Molecular chaperones and the cytoskeleton. *J. Cell Science* 110, 1431-1440.
- Lin, W., Burgess, R. W., Dominguez, B., Pfaff, S. L., Sanes, J. R., Lee, K. F. (2001). Distinct roles of nerve and muscle in postsynaptic differentiation of the neuromuscular synapse. *Nature* 410, 1057-1064.
- Lindstrom, J. M., Engel, A. G., Seybold, M. E., Lennon, V. A., and Lambert, E. H. (1976). Pathological mechanisms in experimental autoimmune myasthenia gravis. II. Passive transfer of experimental autoimmune myasthenia gravis in rats with anti-acetylcholine receptor antibodies. *J Exp Med* 144, 739-753.
- Liu, H.-Y., MacDonald, J. I. S., Hryciw, T., Li, C., Meakin, S. O. (2005). Human tumorous imaginal disc 1 (TID1) associates with Trk receptor tyrosine kinases and regulates neurite outgrowth in nnr5-TrkA cells. *J. Biol. Chem.* 280(20), 19461-19471.
- Lo, J. F., Hayashi, M., Woo-Kim, S., Tian, B., Huang, J. F., Fearn, C., Takayama, S., Zapata, J. M., Yang, Y., Lee, J.D. (2004). Tid1, a cochaperone of the heat shock 70 protein and the mammalian counterpart of the *Drosophila* tumor suppressor l(2)tid, is critical for early embryonic development and cell survival. *Mol. Cell. Biol.* 24(6), 2226-2236.
- Lu, B., Garrido, N., Spelbrink, J. N., Suzuki, C. K. (2006). Tid1 isoforms are mitochondrial DnaJ-like chaperones with unique carboxyl termini that determine cytosolic fate. *J. Biol. Chem.* 281(19), 13150-13158.
- Luo, Z. G., Wang, Q., Zhou, J. Z., Wang, J., Luo, Z., Liu, M., He, X., Wynshaw-Boris, A., Xiong, W. C., Lu, B., Mei, L. (2002). Regulation of AChR clustering by Dishevelled interacting with MuSK and PAK1. *Neuron* 35, 489-505.
- Luo, Z. G., Wang, Q., Dobbins, G. C., Levy, S., Xiong, W. C., Mei, L. (2003). Signaling complexes for postsynaptic differentiation. *J. Neurocyt.* 32, 697-708.

- Luo, Z. G., Je, H.-S., Wang, Q., Yang, F., Dobbins, G. C., Yang, Z.-H., Xiong, W. C., Lu, B., Mei, L. (2003). Implication of geranylgeranyltransferase I in synapse formation. *Neuron* 40, 703-717.
- Mastrogiacomo, A., Parsons, S. M., Zampighi, G. A., Jenden, D. J., Umbach, J. A., and Gundersen, C. B. (1994). Cysteine string proteins: a potential link between synaptic vesicles and presynaptic Ca²⁺ channels. *Science* 263, 981-982.
- Matsumoto, H., Hayashi, Y. K., Kim, D. S., Ogawa, M., Murakami, T., Noguchi, S., Nonaka, I., Nakazawa, T., Matsuo, T., Futagami, S., et al. (2005). Congenital muscular dystrophy with glycosylation defects of alpha-dystroglycan in Japan. *Neuromuscul Disord* 15, 342-348.
- McMahan, U. J., and Slater, C. R. (1984). The influence of basal lamina on the accumulation of acetylcholine receptors at synaptic sites in regenerating muscle. *J Cell Biol* 98, 1453-1473.
- McMahan, U. J. (1990). The agrin hypothesis. *Cold Spring Harb Symp Quant Biol* 55, 407-418.
- Meyer, G., and Wallace, B. G. (1998). Recruitment of a nicotinic acetylcholine receptor mutant lacking cytoplasmic tyrosine residues in its beta subunit into agrin-induced aggregates. *Mol Cell Neurosci* 11, 324-333.
- Misgeld, T., Burgess, R. W., Lewis, R. M., Cunningham, J. M., Lichtman, J. W., and Sanes, J. R. (2002). Roles of neurotransmitter in synapse formation: development of neuromuscular junctions lacking choline acetyltransferase. *Neuron* 36, 635-648.
- Mittaud, P., Marangi, P. A., Erb-Vogtli, S., Fuhrer, C. (2001). Agrin-induced activation of acetylcholine receptor-bound Src family kinases requires rapsyn and correlates with acetylcholine receptor clustering. *J. Biol. Chem.* 276, 14505-14513.
- Mittaud, P., Camilleri, A. A., Willmann, R., Erb-Vogtli, S., Burden, S. J., and Fuhrer, C. (2004). A single pulse of agrin triggers a pathway that acts to cluster acetylcholine receptors. *Mol Cell Biol* 24, 7841-7854.
- Mohamed, A. S., and Swope, S. L. (1999). Phosphorylation and cytoskeletal anchoring of the acetylcholine receptor by Src class protein-tyrosine kinases. Activation by rapsyn. *J Biol Chem* 274, 20529-20539.
- Moll, J., Barzaghi, P., Lin, S., Bezakova, G., Lochmuller, H., Engvall, E., Muller, U., and Ruegg, M. A. (2001). An agrin minigene rescues dystrophic symptoms in a mouse model for congenital muscular dystrophy. *Nature* 413, 302-307.

- Muller, J. S., Baumeister, S. K., Rasic, V. M., Krause, S., Todorovic, S., Kugler, K., Muller-Felber, W., Abicht, A., and Lochmuller, H. (2006). Impaired receptor clustering in congenital myasthenic syndrome with novel RAPSN mutations. *Neurology* 67, 1159-1164.
- Nasevicius, A., and Ekker, S. C. (2000). Effective targeted gene 'knockdown' in zebrafish. *Nat Genet* 26, 216-220.
- Neubig, R. R., Krodel, E. K., Boyd, N. D., and Cohen, J. B. (1979). Acetylcholine and local anesthetic binding to Torpedo nicotinic postsynaptic membranes after removal of nonreceptor peptides. *Proc Natl Acad Sci U S A* 76, 690-694.
- Noakes, P. G., Phillips, W. D., Hanley, T. A., Sanes, J. R., and Merlie, J. P. (1993). 43K protein and acetylcholine receptors colocalize during the initial stages of neuromuscular synapse formation in vivo. *Dev Biol* 155, 275-280.
- Ohno, K., Engel, A. G., Shen, X. M., Selcen, D., Brengman, J., Harper, C. M., Tsujino, A., and Milone, M. (2002). Rapsyn mutations in humans cause endplate acetylcholine-receptor deficiency and myasthenic syndrome. *Am J Hum Genet* 70, 875-885.
- Ohtsuka, K., and Suzuki, T. (2000). Roles of molecular chaperones in the nervous system. *Brain Res Bull* 53, 141-146.
- Okada, K., Inoue, A., Okada, M., Murata, Y., Kakuta, S., Jigami, T., Kubo, S., Shiraishi, H., Eguchi, K., Motomura, M., Akiyama, T., Iwakura, Y., Higuchi, O., Yamanashi, Y. (2006). The muscle protein Dok-7 is essential for neuromuscular synaptogenesis. *Science* 312, 1802-1805.
- Panzer, J. A., Gibbs, S. M., Song, Y., Dosch, R., Granato, M., Mullins, M., Wagner, D., Balice-Gordon, R. J. (2004). Temporal dynamics and role of activity in neuromuscular synaptogenesis in wildtype and mutant zebrafish, 6th International Conference on Zebrafish Development and Genetics, Madison WI: 479, 2004.
- Panzer, J. A., Gibbs, S. M., Dosch, R., Wagner, D., Mullins, M. C., Granato, M., and Balice-Gordon, R. J. (2005). Neuromuscular synaptogenesis in wild-type and mutant zebrafish. *Dev Biol* 285, 340-357.
- Panzer, J. A., Song, Y., and Balice-Gordon, R. J. (2006). In vivo imaging of preferential motor axon outgrowth to and synaptogenesis at prepatterned acetylcholine receptor clusters in embryonic zebrafish skeletal muscle. *J Neurosci* 26, 934-947.
- Polakis, P. (1997). The adenomatous polyposis coli (APC) tumor suppressor. *Biochimica et Biophysica Acta* 1332, F127-F147.
- Ruegg, M. A., Tsim, K. W., Horton, S. E., Kroger, S., Escher, G., Gensch, E. M., and McMahan, U. J. (1992). The agrin gene codes for a family of basal lamina proteins that differ in function and distribution. *Neuron* 8, 691-699.

- Rupp, F., Payan, D. G., Magill-Solc, C., Cowan, D. M., and Scheller, R. H. (1991). Structure and expression of a rat agrin. *Neuron* 6, 811-823.
- Sadasivam, G., Willmann, R., Lin, S., Erb-Vogtil, S., Kong, X. C., Ruegg, M. A., Fuhrer, C. (2005). Src-family kinases stabilize the neuromuscular synapse in vivo via protein interactions, phosphorylation, and cytoskeletal linkage of acetylcholine receptors. *J. Neurosci.* 25(45), 10479-10493.
- Saito, F., Masaki, T., Saito, Y., Nakamura, A., Takeda, S., Shimizu, T., Toda, T., and Matsumura, K. (2007). Defective peripheral nerve myelination and neuromuscular junction formation in fukutin-deficient chimeric mice. *J Neurochem* 101, 1712-1722.
- Sarkar, S., Pollack, B. P., Lin, K. T., Kotenko, S. V., Cook, J. R., Lewis, A., Pestka, S. (2001). HTid-1, a human DnaJ protein, modulates the interferon signaling pathway. *Biol. Chem.* 276(52), 49034-49042.
- Schilling, B., De-Medina, T., Syken, J., Vidal, M., and Munger, K. (1998). A novel human DnaJ protein, hTid-1, a homolog of the *Drosophila* tumor suppressor protein Tid56, can interact with the human papillomavirus type 16 E7 oncoprotein. *Virology* 247, 74-85.
- Settleman, J., Narasimhan, V., Foster, L. C., Weinberg, R. A. (1992). Molecular cloning of cDNAs encoding the GAP-associated protein p190: implications for a signaling pathway from ras to the nucleus. *Cell* 69(3), 539-549.
- Smith, C. L., Mittraud, P., Prescott, E. D., Fuhrer, C., and Burden, S. J. (2001). Src, Fyn, and Yes are not required for neuromuscular synapse formation but are necessary for stabilization of agrin-induced clusters of acetylcholine receptors. *J Neurosci* 21, 3151-3160.
- Sobel, A., Weber, M., and Changeux, J. P. (1977). Large-scale purification of the acetylcholine-receptor protein in its membrane-bound and detergent-extracted forms from *Torpedo marmorata* electric organ. *Eur J Biochem* 80, 215-224.
- Soti, C., Nagy, E., Giricz, Z., Vigh, L., Csermely, P., and Ferdinandy, P. (2005). Heat shock proteins as emerging therapeutic targets. *Br J Pharmacol* 146, 769-780.
- Strochlic, L., Cartaud, A., Labas, V., Hoch, W., Rossier, J., Cartaud, J. (2001). MAGI-1c: A synaptic MAGUK interacting with MuSK at the vertebrate neuromuscular junction. *J. Cell Biology* 153, 1127-1132.
- Strochlic, S., Cartaud, A., Cartaud, J. (2005). The synaptic, muscle-specific kinase complex: new partners, new functions. *BioEssays* 27, 1129-1135.

- Sugiyama, J. E., Glass, D. J., Yancopoulos, G. D., and Hall, Z. W. (1997). Laminin-induced acetylcholine receptor clustering: an alternative pathway. *J Cell Biol* 139, 181-191.
- Syken, J., De-Medina, T., Münger, K. (1999). TID1, a human homolog of the *Drosophila* tumor suppressor *l(2)tid*, encodes two mitochondrial modulators of apoptosis with opposing functions. *PNAS* 96(15), 8499-504.
- Tarunina, M., Alger, L., Chu, G., Munger, K., Gudkov, A., and Jat, P. S. (2004). Functional genetic screen for genes involved in senescence: role of *Tid1*, a homologue of the *Drosophila* tumor suppressor *l(2)tid*, in senescence and cell survival. *Mol Cell Biol* 24, 10792-10801.
- Toyka, K. V., Brachman, D. B., Pestronk, A., and Kao, I. (1975). Myasthenia gravis: passive transfer from man to mouse. *Science* 190, 397-399.
- Trentin, G. A., Yin, X., Tahir, S., Lhotak, S., Farhang-Fallah, J., Li, Y., Rozakis-Adcock M. (2001). A mouse homologue of the *Drosophila* tumor suppressor *l(2)tid* gene defines a novel Ras GTPase-activating protein (RasGAP)-binding protein. *J. Biol. Chem.* 276(16), 13087-13095.
- Trentin, G. A., He, Y., Wu, D. C., Tang, D., and Rozakis-Adcock, M. (2004). Identification of a *hTid-1* mutation which sensitizes gliomas to apoptosis. *FEBS Lett* 578, 323-330.
- Urbanics, R. (2002). Heat shock proteins in stroke and neurodegenerative diseases. *Curr Opin Investig Drugs* 3, 1718-1719.
- Valenzuela, D. M., Stitt, T. N., DiStefano, P. S., Rojas, E., Mattsson, K., Compton, D. L., Nunez, L., Park, J. S., Stark, J. L., Gies, D. R., Thomas, S., Le Beau, M. M., Fernald, A. A., Copeland, N. G., Jenkins, N. A., Burden, S. J., Glass, D. J., Yancopoulos, G. D. (1995). Receptor tyrosine kinase specific for the skeletal muscle lineage: expression in embryonic muscle, at the neuromuscular junction, and after injury. *Neuron* 15, 573-584.
- Wallace, B. G. (1989). Agrin-induced specializations contain cytoplasmic, membrane, and extracellular matrix-associated components of the postsynaptic apparatus. *J Neurosci* 9, 1294-1302.
- Wallace, B. G., Qu, Z., and Haganir, R. L. (1991). Agrin induces phosphorylation of the nicotinic acetylcholine receptor. *Neuron* 6, 869-878.
- Wang, J., Jing, Z., Zhang, L., Zhou, G., Braun, J., Yao, Y., Wang, Z. Z. (2003). Regulation of acetylcholine receptor clustering by the tumor suppressor APC. *Nature Neuroscience* 6(10), 1017-1018.
- Watty, A., Neubauer, G., Dreger, M., Zimmer, M., Wilm, M., Burden, S. J. (2000). The in vitro and in vivo phosphotyrosine map of activated MuSK. *PNAS* 97(9), 4585-4590.

- Witzemann, V. (2006). Development of the neuromuscular junction. *Cell Tissue Res* 326, 263-271.
- Weston, C., Yee, B., Hod, E., Prives, J. (2000). Agrin-induced acetylcholine receptor clustering is mediated by the small guanosine triphosphatases Rac and Cdc42. *J. Cell Biol.* 150(1), 205-212.
- Weston, C., Gordon, C., Teressa, G., Hod, E., Ren, X.-D., Prives, J. (2003). Cooperative regulation by Rac and Rho of agrin-induced acetylcholine receptor clustering in muscle cells. *J. Biol. Chem.* 278(8), 6450-6455.
- Wu, J. S., Hogan, G. R., Morris, J. D. (1985). Modified methods for preparation of cryostat sections of skeletal muscle. *Muscle Nerve* 8(8), 664-666.
- Yamanashi, Y., and Baltimore, D. (1997). Identification of the Abl- and rasGAP-associated 62 kDa protein as a docking protein, Dok. *Cell* 88, 205-211.
- Yang, X., Li, W., Prescott, E. D., Burden, S. J., and Wang, J. C. (2000). DNA topoisomerase IIbeta and neural development. *Science* 287, 131-134.
- Yang, X., Arber, S., William, C., Li, L., Tanabe, Y., Jessell, T. M., Birchmeier, C., and Burden, S. J. (2001). Patterning of muscle acetylcholine receptor gene expression in the absence of motor innervation. *Neuron* 30, 399-410.